

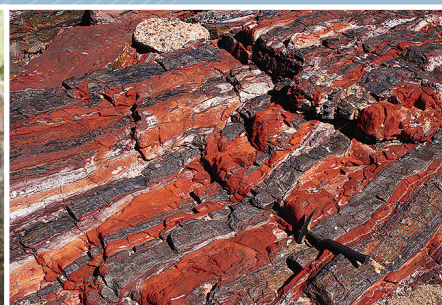


Government of **Western Australia**
Department of **Mines and Petroleum**

RECORD 2015/6

GSWA KIMBERLEY WORKSHOP 2014: EXTENDED ABSTRACTS

compiled by
DW Maidment



Geological Survey
of Western Australia



Government of **Western Australia**
Department of **Mines and Petroleum**

Record 2015/6

GSWA KIMBERLEY WORKSHOP 2014: EXTENDED ABSTRACTS

**compiled by
DW Maidment**

Perth 2015



**Geological Survey of
Western Australia**

MINISTER FOR MINES AND PETROLEUM
Hon. Bill Marmion MLA

DIRECTOR GENERAL, DEPARTMENT OF MINES AND PETROLEUM
Richard Sellers

EXECUTIVE DIRECTOR, GEOLOGICAL SURVEY OF WESTERN AUSTRALIA
Rick Rogerson

REFERENCE

The recommended reference for this publication is:

(a) For reference to an individual contribution:

Morris, PA 2015, Bedrock–regolith relationships: examples from the Balangarra area, north Kimberley, *in* GSWA Kimberley workshop 2014: extended abstracts *compiled by* DW Maidment: Geological Survey of Western Australia, Record 2015/6, p. 50–51.

(b) For reference to the publication:

Maidment, DW (compiler) 2015, GSWA Kimberley workshop 2014: extended abstracts: Geological Survey of Western Australia, Record 2015/6, 56p.

National Library of Australia Card Number and ISBN 978-1-74168-649-4

Grid references in this publication refer to the Geocentric Datum of Australia 1994 (GDA94). Locations mentioned in the text are referenced using Map Grid Australia (MGA) coordinates, Zones 51 and 52. All locations are quoted to at least the nearest 100 m.

About this publication

This Record presents the results of studies carried out by GSWA staff and researchers from external organizations. External authors are responsible for the scientific content, interpretations and drafting of figures in their abstracts. No significant editing was undertaken by GSWA.

Disclaimer

This product was produced using information from various sources. The Department of Mines and Petroleum (DMP) and the State cannot guarantee the accuracy, currency or completeness of the information. DMP and the State accept no responsibility and disclaim all liability for any loss, damage or costs incurred as a result of any use of or reliance whether wholly or in part upon the information provided in this publication or incorporated into it by reference.

Published 2015 by Geological Survey of Western Australia

This Record is published in digital format (PDF) and is available online at <www.dmp.wa.gov.au/GSWApublications>.

Further details of geological products and maps produced by the Geological Survey of Western Australia are available from:

Information Centre
Department of Mines and Petroleum
100 Plain Street
EAST PERTH WESTERN AUSTRALIA 6004
Telephone: +61 8 9222 3459 Facsimile: +61 8 9222 3444
www.dmp.wa.gov.au/GSWApublications

Contents

Geology of the Kimberley Craton, Halls Creek and King Leopold Orogens	1
<i>by JA Hollis, IM Tyler, and CL Kirkland</i>	
Evolution of the Speewah and Kimberley Basins	6
<i>by C Phillips</i>	
A geophysical investigation of the east Kimberley	11
<i>by M Lindsay, SA Occhipinti, ARA Aitken, V Metelka, MC Dentith, J Miller, JA Hollis, and IM Tyler</i>	
Preliminary outcomes from mineral systems analysis for the Halls Creek Orogen	15
<i>by SA Occhipinti, V Metelka, MD Lindsay, J Hollis, ARA Aitken, S Sheppard, K Orth, IM Tyler, T Beardsmore, M Hutchison, and JM Miller</i>	
Constraints on Paleoproterozoic crust–mantle evolution from the Hf, Nd and O isotope record of igneous rocks in the Lamboo Province of the Halls Creek and King Leopold Orogens	18
<i>by AIS Kemp, S Sheppard, IM Tyler, and S Bodorkos</i>	
Volcanology of the Carson Volcanics: outpouring of a 1.79 Ga Large Igneous Province	20
<i>by K Orth</i>	
The textural and geochemical architecture of the Hart Dolerite at Speewah Dome	25
<i>by A Eves, RR Ramsay, ML Fiorentini, L Gwalani, W Maier, and K Rogers</i>	
Characterization and timing of events in the richly mineralized Speewah area of the East Kimberley, Western Australia: Palaeoproterozoic sedimentation, intrusion of the Hart Dolerite and fault-hosted alteration and vein systems	29
<i>by RR Ramsay, A Eves, MTD Wingate, M Fiorentini, G Batt, S Denyszyn, and K Rogers</i>	
The deep structure of the Kimberley from magnetotelluric (MT) data	32
<i>by J Spratt, MC Dentith, S Evans, ARA Aitken, MD Lindsay, JA Hollis, IM Tyler, A Joly, and J Shragge</i>	
3D crustal structure of the Kimberley region from joint magnetic/gravity inversion	35
<i>by ARA Aitken, MD Lindsay, L Griss, and C Altinay</i>	
Lithospheric structure of the western Kimberley margin: implications for marginal basin development.....	43
<i>by K Czarnota, and N White</i>	
Regolith landforms of the west Kimberley: distribution and composition.....	45
<i>by N de Souza Kovacs</i>	
Bedrock–regolith relationships: examples from the Balangarra area, north Kimberley	50
<i>by PA Morris</i>	
Overview of the REE mineralization in the East Kimberley – West Tanami region	52
<i>by S Morin-Ka and T Beardsmore</i>	
The regolith sampling program in the Kimberley: an overview	54
<i>by AJ Scheib, PA Morris, and N de Souza Kovacs</i>	

Geology of the Kimberley Craton, Halls Creek and King Leopold Orogens

by

JA Hollis, IM Tyler, and CL Kirkland

The geological evolution of the Kimberley region (Fig. 1) spans almost two billion years and charts the development of a Paleo- to Neoproterozoic active margin through to intraplate tectonism. This work summarises the geological evolution of the Kimberley Craton, Halls Creek Orogen, and King Leopold Orogen. Subsequent Proterozoic and Paleozoic basin formation in the Kimberley is not addressed in this contribution and the interested reader should consult Phillips et al. (this volume).

The Kimberley Craton is entirely covered by the Speewah and Kimberley Basins. Nonetheless, despite the lack of exposure, two important conclusions can be drawn on the nature of the Kimberley Craton. One is that the Kimberley Craton comprises northeast-trending accreted basement terranes, based on modelling of magnetic and gravity data (Gunn and Meixner, 1998; Fig. 2). The second conclusion is that these terranes probably comprise both Archean and Paleoproterozoic crust, underlain by Archean mantle lithosphere. This is based on four lines of evidence: 1) Archean and Paleoproterozoic ages dominate the detrital zircon spectra of the c. 1870 Ma turbiditic Marboo Formation, which is inferred to have been derived from the Kimberley Craton (Tyler et al., 1999). 2) Sm-Nd whole rock (Griffin et al., 2000) and zircon Lu-Hf isotopes of granites in the Paperbark Supersuite (Kemp, this volume) and of xenoliths from the Aries Kimberlite (Downes et al., 2007) are consistent with their formation by melting of Neoproterozoic crust. 3) Re-Os whole rock and mineral isotopic data for the Argyle Lamproite and Seppelt and Maude Creek kimberlites are consistent with the presence of Archean lithospheric mantle beneath the Kimberley (Graham et al., 1999). 4) seismic velocity data for the Kimberley Craton is characterised by high wave speeds and a 1D seismic velocity structure similar to the Archean Pilbara and Yilgarn Cratons (Collins et al., 2003; Saygin and Kennett, 2012).

The Halls Creek and King Leopold Orogens appear to wrap the Kimberley Craton on its southern and eastern margin (Fig. 1). These orogens record the tectonic evolution of the Kimberley Craton margin in the period 1910–1810 Ma, including the 1865–1850 Ma Hooper Orogeny and the 1835–1810 Ma Halls Creek Orogeny.

The Halls Creek Orogen is a northeast-trending orogenic belt divided into three tectonostratigraphic terranes – the western, central and eastern zones (Fig. 1; Tyler et al., 1995). These terranes are separated by major sinistral fault systems that have been reactivated through the Proterozoic and Paleozoic (e.g. Thorne and Tyler, 1996).

The western zone is correlated with the King Leopold orogenic belt (Fig. 1; Tyler et al., 1995; Griffin et al., 2000). The western zone comprises low to high grade metasedimentary rocks of the Marboo Formation, thought to represent rifting marginal to the Kimberley Craton following accretion of earlier Paleoproterozoic terranes (Griffin et al., 1993; Tyler et al., 1999; Griffin et al., 2000). These were intruded by the Ruins Dolerite and then deformed and metamorphosed during the Hooper Orogeny (Tyler and Griffin, 1993; Griffin et al., 1993). During orogenesis the felsic Whitewater Volcanics were extruded and granites and gabbros of the cogenetic Paperbark Supersuite were emplaced during extension of the Kimberley margin (Fig. 3; Griffin et al., 2000; Page and Hoatson, 2000; Page et al., 2001). Meanwhile, outboard of the margin, southeast directed subduction produced the Tickalara oceanic arc, an interpretation based on the geochemistry and isotopic character of mafic rocks (Sheppard et al., 1999; Griffin et al., 2000).

The oceanic arc is represented by the central zone, dominated by medium to high grade turbiditic metasedimentary and mafic volcanic rocks of the Tickalara Metamorphics. The central zone is thought to have accreted to the western zone by 1850 Ma, based on the timing of deformation affecting both zones, which pre-dates intrusion of the Dougalls Suite (Thorne et al., 1999; Bodorkos et al., 1999; Blake et al., 2000; Bodorkos et al., 2000b; Page et al., 2001; Tyler, 2005). Subsequently, mafic and felsic volcanic rocks of the Koongie Park Formation were deposited in the central zone at 1845–1840 Ma, possibly during rifting of the arc (Page et al., 1994; Tyler, 2005), and during emplacement of layered mafic and ultramafic intrusions (Page and Hoatson, 2000; Kemp, this volume).

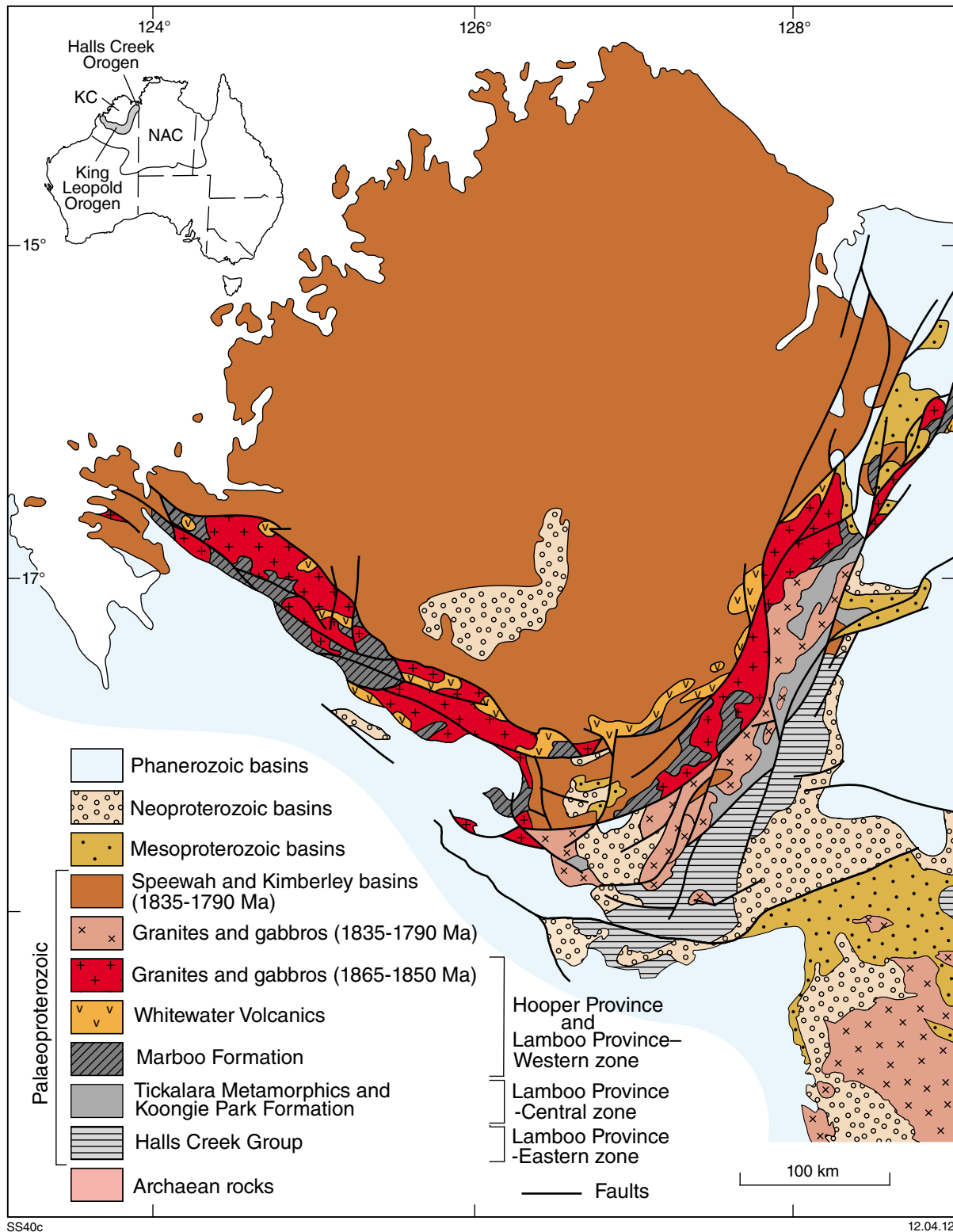


Figure 1. Palaeoproterozoic geology of the Kimberley region. The inset shows the locations of the North Australian Craton (NAC) and the Kimberley Craton (KC) (from Griffin et al., 2000).

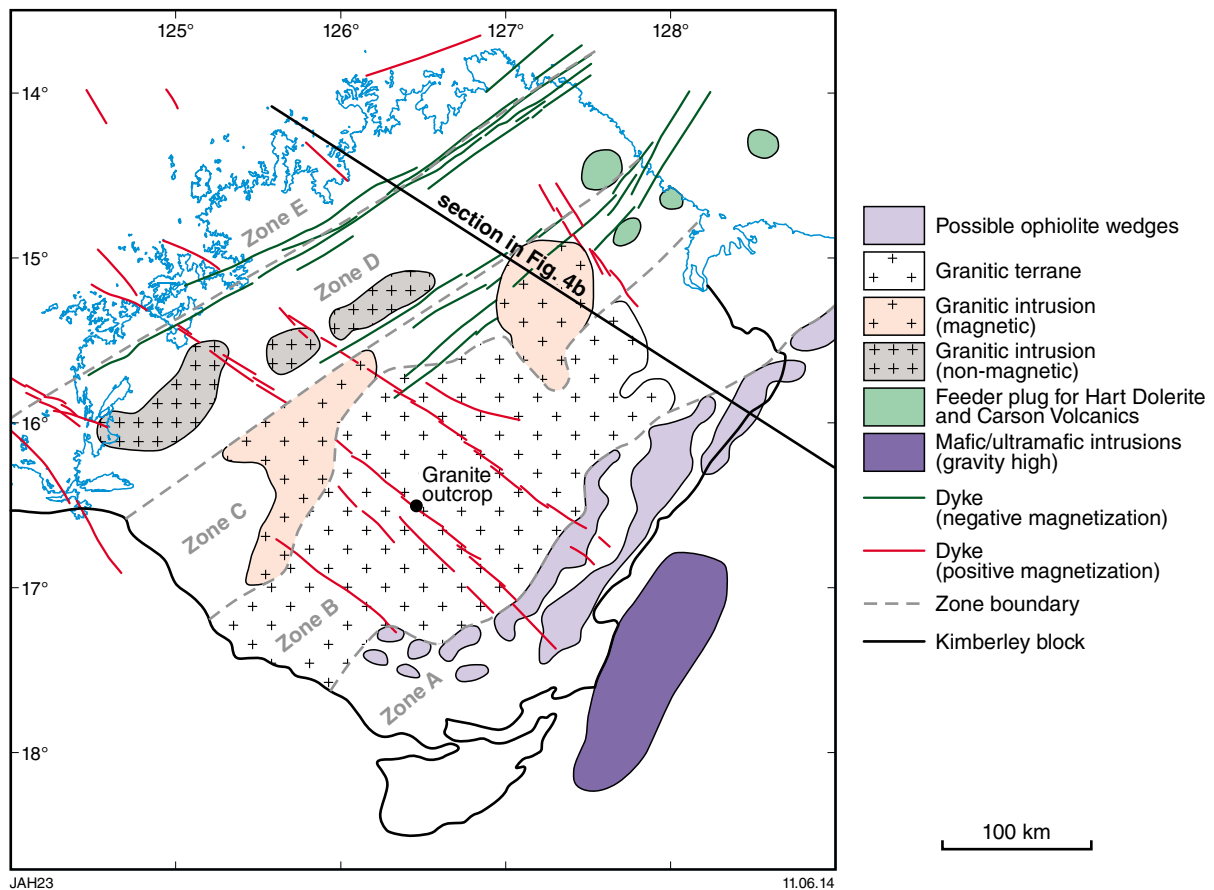


Figure 2. Interpreted basement geology of the Kimberley Craton redrawn from (Gunn and Meixner, 1998) and based on magnetic and gravity data.

The eastern zone is interpreted as the passive margin of the North Australian Craton, which began to encroach on the Kimberley Craton when subduction switched toward the northwest after cessation of the Hooper Orogeny (Tyler, 2005; Fig. 3). The eastern zone comprises 1910 Ma granitic and volcanic basement of the Ding Dong Downs Volcanics, overlain by the 1880–1835 Ma Halls Creek Group (Tyler et al., 1998). The Halls Creek Group comprises braided river sandstones of the Saunders Creek Formation overlain by shallow marine carbonates and mafic volcanics of the 1880 Ma Biscay Formation, both with dominantly Neo- to Paleoarchean detrital sources. These are overlain by stacked deeper water turbidite fans of the Olympio Formation that records a transition from passive to active margin deposition in an evolving foreland basin. The Olympio Formation contains 1857 Ma and 1848 Ma alkaline volcanics with intraplate geochemical affinities (Hancock, 1991; Tyler et al., 1995; Blake et al., 1999; Blake et al., 2000; Tyler, 2005; Phillips et al., this volume).

The western, central and eastern zones were deformed and metamorphosed during the 1835–1810 Ma Halls Creek Orogeny, which records the collision of the Kimberley Craton and North Australian Craton (Blake et al., 2000; Tyler, 2005). During and after orogenesis the three zones were stitched by granites and gabbros of the relatively

juvenile Sally Downs Supersuite (Bodorkos et al., 2000a; Page et al., 2001; Kemp, this volume). During the Halls Creek Orogeny the 1835 Ma Speewah Basin was deposited and then the c. 1800 Ma Kimberley Basin.

The subsequent Proterozoic history of the Kimberley involves intraplate tectonic reactivation along the orogenic belts and the margins of the overlying basins. The first of these events is the Neoproterozoic Yampi Orogeny, which produced northeast-facing folds and north-directed thrusts in the Speewah and Kimberley Basins on the Yampi Peninsula (Tyler and Griffin, 1990, 1993; Griffin et al., 1993). These thrusts can be traced into northwest-trending ductile shear zones in the King Leopold Orogen. The Yampi Orogeny also produced north-northeast- and east-northeast-trending strike-slip faults in the Halls Creek Orogen (White and Muir, 1989; Tyler et al., 1995; Thorne and Tyler, 1996). The age of the Yampi Orogeny is poorly constrained to 1475–1000 Ma, based on K-Ar dating of shear zones (Shaw et al., 1992). However, this was questioned by (Bodorkos and Reddy, 2004), who suggested unsupported excess Ar influenced this result. (Bodorkos and Reddy, 2004) argued for an age of 1000–800 Ma based on Ar-Ar plateau step heating results and the relative timing of strike-slip faults in the Halls Creek Orogen.

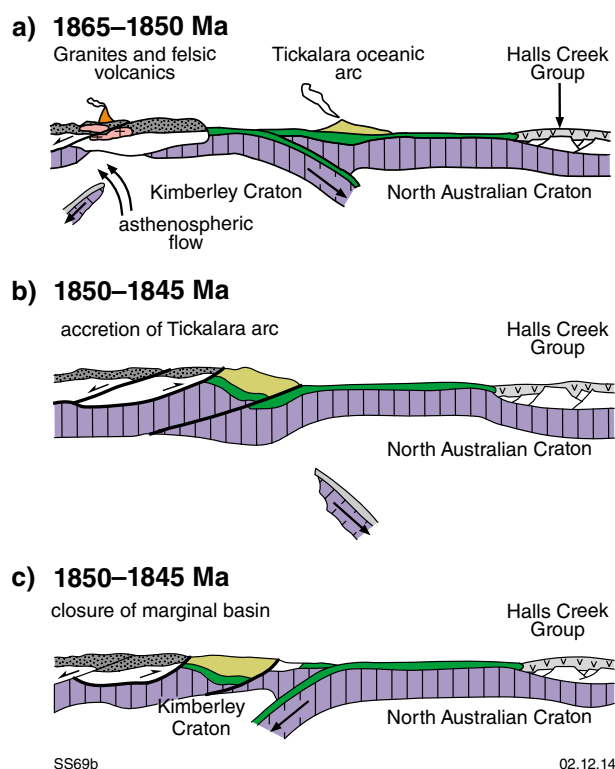


Figure 3. Plate tectonic reconstruction of the Kimberley during the Hooper to Halls Creek Orogenies (from Griffin et al., (2000).

The last Proterozoic orogenic event is the King Leopold Orogeny, which produced west-northwest-trending folds and south-directed thrusts in the King Leopold Ranges (Precipice Fold Belt) along the southwest margin of the Kimberley Basin and reactivation of shear zones in the King Leopold Orogen and sinistral strike-slip faulting in the Halls Creek Orogen (Tyler and Griffin, 1990, 1993; Shaw et al., 1992). It also resulted in uplift and erosion producing the unconformity at the base of the Ord and Bonaparte Basins, marked by the 510 Ma Kalkarindji continental flood basalt province. The age of the King Leopold Orogeny is constrained to 560–500 Ma based on K-Ar dating of shear zones in the King Leopold Orogen (Shaw et al., 1992), consistent with deformation of the c. 670 Ma Mount House Group and the undeformed, cross-cutting 510 Ma Milliwindi Dolerite (Hanley and Wingate, 2000).

References

- Blake, DH, Tyler, IM, Griffin, TJ, Sheppard, S, Thorne, AM and Warren, RG 1999, *Geology of the Halls Creek 1:100 000 Sheet area (4461)*, Western Australia: Australian Geological Survey Organisation, Explanatory Notes, 36p.
- Blake, DH, Tyler, IM and Page, RW 2000, Regional Geology of the Halls Creek Orogen, *in* *Geology and economic potential of the Palaeoproterozoic layered mafic-ultramafic intrusions in the East Kimberley*, Western Australia *edited by* DM Hoatson and DH Blake: Australian Geological Survey Organisation, Bulletin 246, p. 35–62.
- Bodorkos, S, Cawood, PA and Oliver, NHS 2000a, Timing and duration of synmagmatic deformation in the Mabel Downs Tonalite, northern Australia: *Journal of Structural Geology*, v. 22, p. 1181–1198.
- Bodorkos, S, Cawood, PA, Oliver, NHS and Nemchin, AA 2000b, Rapidity of orogenesis in the Paleoproterozoic Halls Creek Orogen, northern Australia: evidence from SHRIMP zircon data, CL zircon images, and mixture modeling studies: *American Journal of Science*, v. 300, no. 1, p. 60–82.
- Bodorkos, S, Oliver, NHS and Cawood, PA 1999, Thermal evolution of the central Halls Creek Orogen, northern Australia: *Australian Journal of Earth Sciences*, v. 46, p. 453–465.
- Bodorkos, S and Reddy, SM 2004, Proterozoic cooling and exhumation of the northern central Halls Creek Orogen, Western Australia: constraints from a reconnaissance $^{40}\text{Ar}/^{39}\text{Ar}$ study: *Australian Journal of Earth Sciences*, v. 51, no. 4, p. 561–609.
- Collins, CDN, Drummond, BJ and Nicoll, MG 2003, Crustal thickness patterns in the Australian continent: *Geological Society of America Special Papers*, v. 372, p. 121–128.
- Downes, PP, Griffin, BJ and Griffin, WL 2007, Mineral chemistry and zircon geochronology of xenocrysts and altered mantle and crustal xenoliths from the Aries micaceous kimberlite: Constraints on the composition and age of the central Kimberley Craton, Western Australia: *Lithos*, v. 93, p. 175–198.
- Graham, S, Lambert, DD, Shee, SR, Smith, CB and Reeves, S 1999, Re-Os isotopic evidence for Archaean lithospheric mantle beneath the Kimberley block, Western Australia: *Geology*, v. 27, no. 5, p. 431–434.
- Griffin, TJ, Page, RW, Sheppard, S and Tyler, IM 2000, Tectonic implications of Palaeoproterozoic post-collisional, high-K felsic igneous rocks from the Kimberley region of northwestern Australia: *Precambrian Research*, v. 101, p. 1–23.
- Griffin, TJ, Tyler, IM and Playford, PE 1993, Explanatory notes on the Lennard River 1:250 000 geological sheet SE/51-8, Western Australia (3rd edition): *Geological Survey of Western Australia, Record 1992/5*, 85p.
- Gunn, PJ and Meixner, AJ 1998, The nature of the basement to the Kimberley Block, northwestern Australia: *Exploration Geophysics*, v. 29, p. 506–511.
- Hancock, SL 1991, Tectonic development of the Lower Proterozoic basement in the Kimberley district of northwestern Western Australia: University of Adelaide, Adelaide, South Australia, PhD thesis (unpublished).
- Hanley, LM and Wingate, MTD 2000, SHRIMP zircon age for an Early Cambrian dolerite dyke: an intrusive phase of the Antrim Plateau Volcanics of northern Australia: *Australian Journal of Earth Sciences*, v. 47, p. 1029–1040.
- Page, RW, Blake, DH, Sun, S-S, Tyler, IM, Griffin, TJ and Thorne, AM 1994, New geological and geochronological constraints on volcanogenic massive sulphide prospectivity near Halls Creek (WA): *AGSO Research Newsletter*, v. 20, p. 5–7.
- Page, RW, Griffin, TJ, Tyler, IM and Sheppard, S 2001, Geochronological constraints on tectonic models for Australian Palaeoproterozoic high-K granites: *Journal of the Geological Society*, v. 158, p. 535–545.
- Page, RW and Hoatson, DM 2000, Geochronology of the mafic-ultramafic intrusions, *in* *Geology and economic potential of the Palaeoproterozoic layered mafic-ultramafic intrusions in the East Kimberley*, Western Australia *edited by* DM Hoatson and DH Blake: Australian Geological Survey Organisation, Bulletin 246, p. 163–172.
- Saygin, E and Kennett, BLN 2012, Crustal structure of Australia from ambient seismic noise tomography: *Journal of Geophysical Research: Solid Earth*, v. 117, no. B01304, 15p., doi:10.1029/2011JB008403.

- Shaw, RD, Tyler, IM, Griffin, TJ and Webb, A 1992, New K–Ar constraints on the onset of subsidence in the Canning Basin, Western Australia: *BMR Journal of Australian Geology and Geophysics*, v. 13, p. 31–35.
- Sheppard, S, Tyler, IM, Griffin, TJ and Taylor, RW 1999, Palaeoproterozoic subduction-related and passive margin basalts in the Halls Creek Orogen, northwest Australia: *Australian Journal of Earth Sciences*, v. 46, p. 679–690.
- Thorne, AM, Sheppard, S and Tyler, IM 1999, Lissadell, Western Australia (2nd edition): Geological Survey of Western Australia, 1:250 000 Geological Series Explanatory Notes, 68p.
- Thorne, AM and Tyler, IM 1996, Mesoproterozoic and Phanerozoic sedimentary basins in the northern Halls Creek Orogen: constraints on the timing of strike-slip movement on the Halls Creek Fault system, *in Annual Review 1995–96: Geological Survey of Western Australia*, p. 156–168.
- Tyler, IM 2005, Australia — Proterozoic, in *Encyclopedia of Geology* edited by RC Selley, LRM Cocks and IR Plimer: Elsevier Academic, Amsterdam, The Netherlands, p. 201–211.
- Tyler, IM and Griffin, TJ 1993, Yampi, Western Australia (2nd edition): Geological Survey of Western Australia, 1:250 000 Geological Series Explanatory Notes, 32p.
- Tyler, IM, Griffin, TJ, Page, RW and Shaw, RD 1995, Are there terranes within the Lamboo Complex of the Halls Creek Orogen?, *in Annual Review 1993–94: Geological Survey of Western Australia*, p. 37–46.
- Tyler, IM, Griffin, TJ and Sheppard, S 1998, Geology of the Dockrell 1:100 000 sheet: Geological Survey of Western Australia, 1:100 000 Geological Series Explanatory Notes, 24p.
- Tyler, IM and Griffin, WL 1990, Structural development of the King Leopold Orogen, Kimberley region, Western Australia: *Journal of Structural Geology*, v. 12, p. 703–714.
- Tyler, IM, Page, RW and Griffin, TJ 1999, Depositional age and provenance of the Marboo Formation from SHRIMP U–Pb zircon geochronology: Implications for the early Palaeoproterozoic tectonic evolution of the Kimberley region, Western Australia: *Precambrian Research*, v. 95, no. 3, p. 225–243.
- White, SH and Muir, MD 1989, Multiple reactivation of coupled orthogonal fault systems: An example from the Kimberley region in north Western Australia: *Geology*, v. 17, p. 618–621.

Evolution of the Speewah and Kimberley Basins

by

C Phillips

The >1835 to <1740 Ma Speewah and Kimberley Basins dominate the exposed geology in the Kimberley region of northern Western Australia (Fig. 1). Both basins are filled with siliciclastic sedimentary rocks and lesser volcanic rocks unconformable on older Paleoproterozoic meta-igneous and metasedimentary rocks of the Lamboo Province (Tyler et al., 1995; Tyler et al., 2012). Fieldwork and geochronological studies of the Speewah and lower Kimberley Basins have demonstrated that sedimentology, paleocurrent data, and zircon detrital age populations are inconsistent with many of the current tectonic and depositional models.

The Speewah Basin is filled by the Speewah Group deposited during a transgressive-regressive cycle from fluvial to shallow marine settings with subsequent shoreline progradation and a return to a fluvial setting (Fig. 2). A retro-arc foreland basin model has been proposed to explain the distribution of the Speewah Group, which does not crop out east of the Greenvale and Dunham Faults in the east Kimberley, and the purported thickening of fluvial conglomerates in the basal O'Donnell Formation towards these structures (Gellatly et al., 1970; Thorne et al., 1999). Contrary to these observations, the results of this study indicate that these conglomerates are equally thick away from the Greenvale and Dunham Faults along the edges of the exposed basin in the west Kimberley. Furthermore, the Speewah Group is ubiquitously quartzofeldspathic with paleocurrent data from all formations recording a dominant source from the northeast (Gellatly et al., 1970; this study). Sedimentation in a retro-arc basin should compositionally varied, texturally and mineralogically immature, with a significant component of lithic fragments sourced from the adjacent (recycled) orogen (e.g. Dickinson and Suczek, 1979; Jordan, 1995). These features are not seen. Above the O'Donnell conglomerates the Speewah Group is dominated by well-sorted, very fine- to medium-grained subarkose and arkose with subangular to subrounded grains. These features indicate that these grains were transported from a probable granitic province to the northeast, rather than the developing Halls Creek Orogen to the immediate east. Detrital zircon populations from Speewah Group sandstones show dominant peaks at 1880–1850 Ma (Hollis et al., 2014). These peaks are similar in age to underlying

1865–1850 Ma Paperbark Supersuite granitic rocks of the Western Zone of the Lamboo Province and also share similar Hf compositions (Griffin et al., 2000; Sheppard et al., 2001; Hollis et al., 2014). However, grain size, sorting, angularity, and lack of granitic lithic fragments suggest that the Speewah Group was not sourced from its underlying and adjacent basement. The source was probably an extrabasinal, similarly aged granitic suite to the northeast, as indicated by ubiquitous paleocurrent data. The 1886–1850 Ma Nimbuwah Complex in the Pine Creek Orogen, northeast of the Halls Creek Orogen and Speewah Basin, contain sources of appropriate age and composition and are a possible source. These data refute the Speewah retro-arc foreland basin model. Instead, a broad continental interior basin is proposed, formed by crustal extension over the inferred Kimberley Craton during the onset of the c. 1835–1810 Ma Halls Creek Orogeny.

The Speewah Basin is unconformably or disconformably overlain by the Kimberley Basin which is filled by siliciclastic sedimentary rocks and lesser mafic volcanic rocks of the Kimberley Group deposited during a series of basin-wide transgressive-regressive cycles in a shallow marine setting (Fig. 2). In the east Kimberley the Speewah Group disconformably underlies the King Leopold Sandstone of the lower Kimberley Group. The disconformable surface is marked a laterally extensive conglomerate 30–100 cm thick (Fig. 3a). Conglomerates are clast-supported and dominantly monomictic consisting of subrounded to rounded, granule- to cobble-sized quartz clasts. These rocks have previously been interpreted as glacial deposits with the disconformable surface marked by frost fissures, nye channels (sub-glacial melt-water channels), and purported striations indicating ice movement from the east (Williams, 2005; Schmidt and Williams, 2008). This study refutes a glacial event during deposition of the lower Kimberley Group at c. 1.8 Ga. Purported frost fissures and nye channels are reinterpreted as conglomerate lags infilling steep troughs of straight-crest ripples (Fig. 3b). Previously interpreted east-west orientated striations are tectonic fractures widened by weathering. Fractures are not only orientated east–west but also trend northeast–southwest and northwest–southeast (Fig. 3c). Such a fracture pattern is ubiquitous in the King

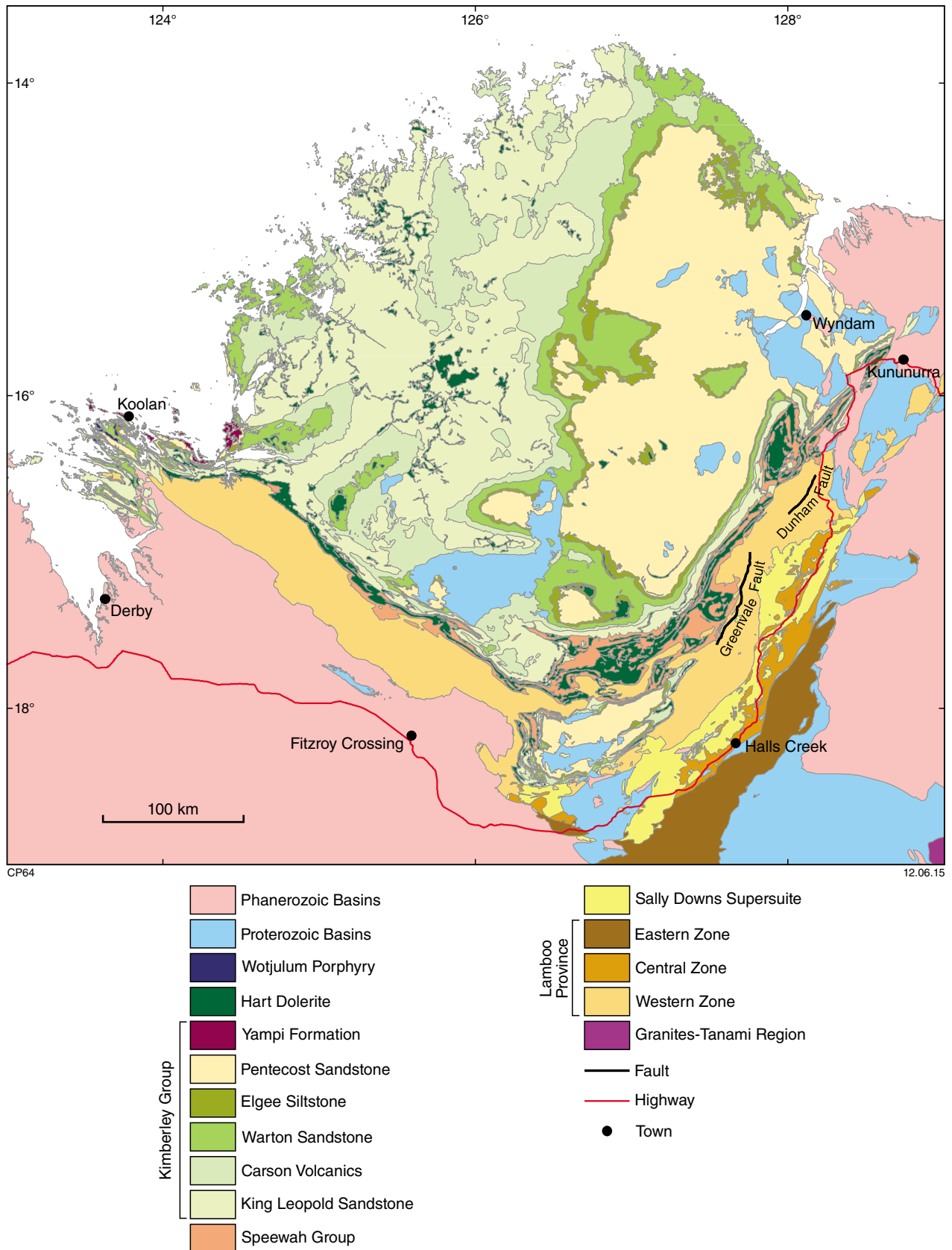
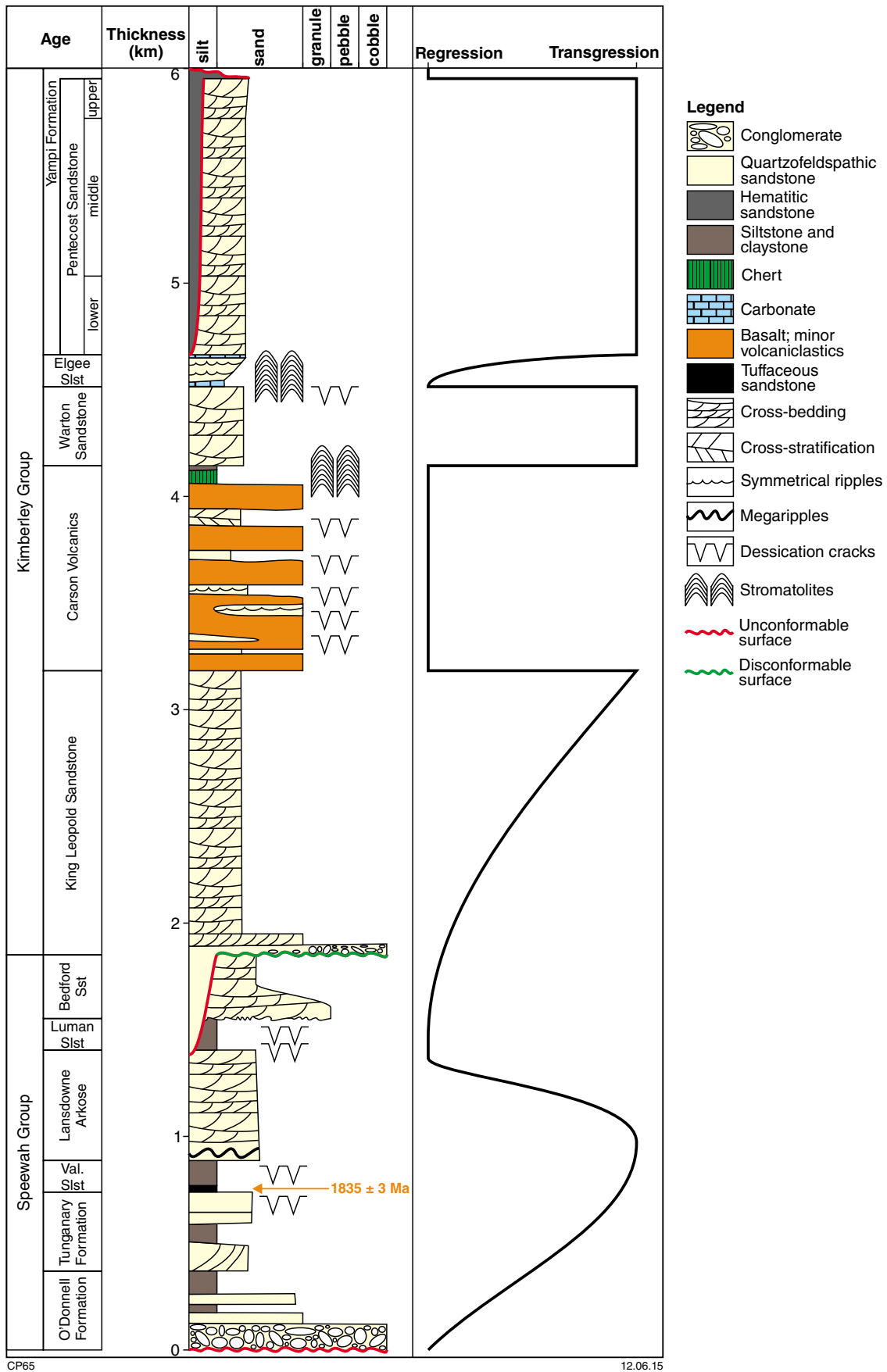


Figure 1. Location map and generalised geology of the Kimberley region showing the Kimberley and Speewah Basins, positions of the Greenvale and Dunham Faults, and divisions of the Lamboo Province of Tyler et al. (1995).



CP65

12.06.15

Figure 2. A generalized log through the Speewah and Kimberley Groups. The transgressive-regressive curve indicates changes in relative sea level during deposition of the groups. The 1835 ± 3 Ma age was obtained from a rhyolitic tuff at the base of the Valentine Siltstone (Page and Sun, 1994; Sheppard et al., 2012).

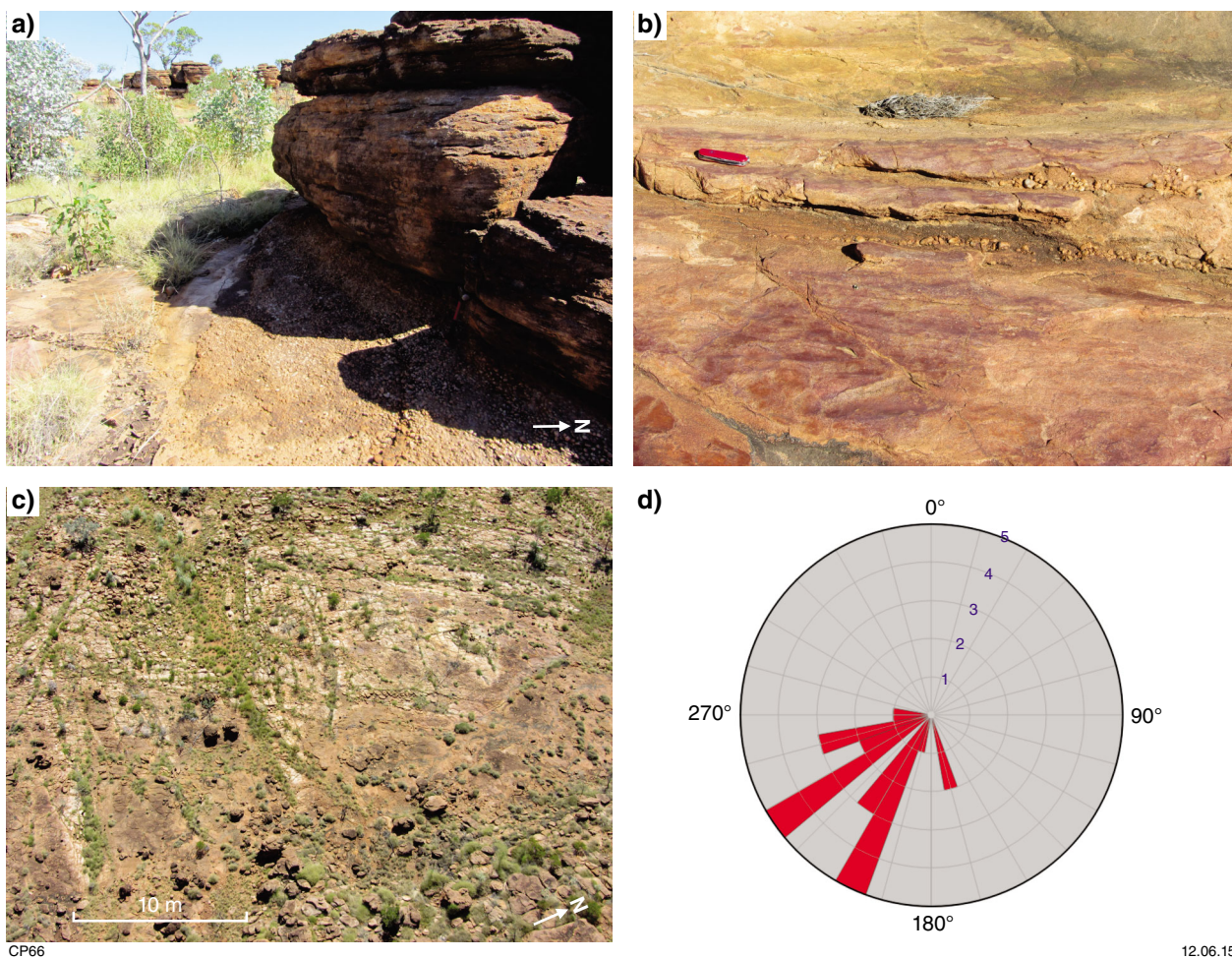


Figure 3. Field images and paleocurrent data from the King Leopold Sandstone in the east Kimberley, north of the Springvale-Lansdowne track: a) The disconformable surface between the Speewah Group and King Leopold Sandstone (UTM 52K 268602E 8057707N), approximately 4 km east of the pavement outcrop shown in Fig. 3c. The uppermost surface of the Bedford Sandstone (foreground, left) is disconformable under a 30 cm thick, clast-supported, monomictic quartz pebble conglomerate and thick-bedded, coarse-grained quartz arenite at the base of the King Leopold Sandstone. Hammer for scale; b) Clast-supported, granule and pebble quartz conglomerate filling steep, straight-crested ripple troughs. UTM 52K 264716E 8058136N; c) An aerial view of the purported glacial pavement visited by Williams (2005). Tectonic fractures exploited by weathering rather than glacial striations; not only in an east-west orientation but also trend northeast-southwest and northwest-southeast. UTM 52K 264716E 8058136N; d) Rose diagram showing paleocurrent data on the purported glacial surface featured in Fig. 2c. The dominant flow direction is from the northeast.

Leopold Sandstone as well as other Kimberley Group and Speewah Group formations. The King Leopold Sandstone is demonstrably quartz-dominated. Glaciers originating from the east (i.e. the Halls Creek Orogen) should have entrained large volumes of Speewah Group lithofacies and possibly metasedimentary and metavolcanic basement rocks from the Lamboo Province, yet these lithologies are absent. Paleocurrents from cross-beds and asymmetrical ripples recorded immediately above and below the disconformable surface are dominated by flow from the northeast (Fig. 3d; Gellatly et al., 1970; this study). This would suggest that lower Kimberley Group rocks share a similar provenance to the underlying Speewah Group. Detrital zircons populations within the King Leopold

Sandstone contain significant peaks in the 1880–1850 Ma range similar to Speewah Group sandstones but with an additional 2525–2480 Ma Neoproterozoic source (Hollis et al., 2014). The metasedimentary Marboo Formation in the underlying Western Zone of the Lamboo Province contains grains with significant c. 2.5 Ga peaks (Tyler et al., 1999). However, grain size, angularity, lack of lithic clasts, and paleocurrent data do not support a reworked metasedimentary source, or glacial source, in the adjacent Halls Creek Orogen. The basal conglomeratic lithofacies of the King Leopold Sandstone is not glacial unit but is reinterpreted as a high current energy fluvial deposit transgressed and reworked by overlying shallow marine lithofacies.

References

- Dickinson, WR and Suczek, CA 1979, Plate tectonics and sandstone compositions: American Association of Petroleum Geologists Bulletin, v. 63, p. 2164–2182.
- Gellatly, DC, Derrick, GM and Plumb, KA 1970, Proterozoic palaeocurrent directions in the Kimberley region, northwestern Australia: Geological Magazine, v. 107, p. 249–257.
- Griffin, TJ, Page, RW, Sheppard, S and Tyler, IM 2000, Tectonic implications of Palaeoproterozoic post-collisional, high-K felsic igneous rocks from the Kimberley region of northwestern Australia: Precambrian Research, v. 101, p. 1–23.
- Hollis, JA, Kemp, AIS, Tyler, IM, Kirkland, CL, Wingate, MTD, Phillips, C, Sheppard, S, Belousova, E and Greau, Y 2014, Basin formation by orogenic collapse: zircon U–Pb and Lu–Hf isotope evidence from the Kimberley and Speewah Groups, northern Australia: Geological Survey of Western Australia, Report 137, 46p.
- Jordan, TE 1995, Retroarc foreland and related basins, in Tectonics of sedimentary basins edited by CJ Busby and RV Ingersoll: Blackwell Science, Massachusetts, USA, p. 331–362.
- Page, RW and Sun, S-S 1994, Evolution of the Kimberley Region, W.A. and adjacent Proterozoic inliers — new geochronological constraints: Geological Society of Australia; Geoscience Australia — 1994 and Beyond, Abstracts v. 37, p. 332–333.
- Schmidt, PW and Williams, GE 2008, Palaeomagnetism of red beds from the Kimberley Group, Western Australia: implications for the palaeogeography of the 1.8 Ga King Leopold Glaciation: Precambrian Research, v. 167, p. 267–280.
- Sheppard, S, Griffin, TJ, Tyler, IM and Page, RW 2001, High- and low-K granites and adakites at a Palaeoproterozoic plate boundary in northwestern Australia: Journal of the Geological Society, v. 158, p. 547–560.
- Sheppard, S, Page, RW, Griffin, TJ, Rasmussen, B, Fletcher, IR, Tyler, IM, Kirkland, CL, Wingate, MTD, Hollis, J and Thorne, AM 2012, Geochronological and isotopic constraints on the tectonic setting of the c. 1800 Ma Hart Dolerite and the Kimberley and Speewah Basins, northern Western Australia: Geological Survey of Western Australia, Record 2012/7, 28p.
- Thorne, AM, Sheppard, S and Tyler, IM 1999, Lissadell, Western Australia (2nd edition): Geological Survey of Western Australia, 1:250 000 Geological Series Explanatory Notes, 68p.
- Tyler, IM, Griffin, TJ, Page, RW and Shaw, RD 1995, Are there terranes within the Lamboo Complex of the Halls Creek Orogen?, in Annual Review 1993–94: Geological Survey of Western Australia, p. 37–46.
- Tyler, IM, Hocking, RM and Haines, PW 2012, Geological evolution of the Kimberley region of Western Australia: Episodes, v. 35, p. 298–306.
- Tyler, IM, Page, RW and Griffin, TJ 1999, Depositional age and provenance of the Marboo Formation from SHRIMP U–Pb zircon geochronology: Implications for the early Palaeoproterozoic tectonic evolution of the Kimberley region, Western Australia: Precambrian Research, v. 95, no. 3, p. 225–243.
- Williams, GE 2005, Subglacial meltwater channels and fluvio-glacial deposits in the Kimberley Basin, WA: 1.8 Ga low-latitude glaciation coeval with continental assembly: Journal of the Geological Society of London, v. 162, p. 111–124.

A geophysical investigation of the east Kimberley

by

**MD Lindsay^{1*}, SA Occhipinti¹, ARA Aitken¹, V Metelka¹, MC Dentith¹,
JM Miller¹, JA Hollis, and IM Tyler**

The 550 by 220 km study area in the east Kimberley, northern Western Australia strikes north-northeast to south-southwest and includes the eastern part of Kimberley Basin and the Halls Creek Orogen (Fig. 1a). The Lamboo Province, which includes the Halls Creek Orogen, is separated into three zones by (Tyler et al., 1995) based on different tectonostratigraphic characteristics. The two billion year geological evolution of the region is punctuated by four major tectonic events: the 1865–1850 Ma Hooper Orogeny; the 1835–1810 Ma Halls Creek Orogeny; the 1000–800 Ma Yampi Orogeny and the c.560 Ma King Leopold Orogeny. Magmatic and deformation events accompany these orogenies and intervening periods resulting in a geologically complex region.

Finding a link between the geology and mineralisation is the primary focus of this study, and the outcomes are used in a companion mineral systems analysis performed by Occhipinti et al. (this volume). Critical to the success of mineral systems analysis is the identification of deep crustal-scale features and regions that may feasibly host certain commodities. The crustal architecture of the region is interpreted using magnetic and gravity data in coordination with petrophysical, geological and magnetotelluric (MT) data. The results of this analysis are discussed in context of mineralising systems and reveal new insights into prospective geological features within the east Kimberley.

Geological structure was primarily interpreted from reduced to pole aeromagnetic data and its first vertical and tilt derivatives. Bouguer gravity data was used to identify larger structures and to provide additional insight to regions where magnetic susceptibility contrast was low. Geological information was used to locate some structures, but was principally employed to interpret their tectonic significance. Principal elements of lithospheric architecture have been interpreted and are shown in Figure 1b. Northwest-trending linear gravity anomalies

have been interpreted to be crustal-scale structures that transect the Halls Creek Orogen. These features extend from under the eastern Kimberley Basin and continue across the western, central and eastern zones. Mafic to ultramafic intrusions are coincident with the southernmost feature (Fig. 1d). A north-trending discontinuity has been interpreted primarily from the magnetic data which displays an apparent sinistral offset to the south of Speewah Dome (Fig. 1c – A). A metamorphic map has been compiled from GSWA 1:500 000 and 1:100 000 scale digital maps and petrological data from the WAROX GSWA databases as well as published papers (Bodorkos et al., 1999; Bodorkos et al., 2002). A zone of high metamorphic grade has been delineated in the centre of the region (Fig. 1b). This region is bounded to the north and south by orogen-normal structures, and coincident with a large long wavelength and high-amplitude gravity anomaly. There is a possibility that the orogen-normal structures, gravity anomaly and zone of high metamorphic grade are linked, however the geometry and properties of the gravity anomaly first need to be determined.

Modelling of gravity and magnetic data has attempted to resolve the geological significance of the large gravity anomaly in the centre of the study area (Fig. 2a). One interpretation, proposed by Gunn and Meixner (1998), is that the gravity anomaly represents a mafic intrusion emplaced into the mid-crust (Fig. 2a). Our attempt to model a body such as this requires this body to have a density of 3060 kgm⁻³, a centroid at c. 20 km depth, and dimensions of 17 km thick, 165 km (long axis) and 60 km (short axis) with an estimated volume of 168 300 km³. We propose that a similar process occurred on the eastern boundary to coupling of a west-dipping subducting slab with the overriding plate during the Halls Creek Orogeny may have led to the emplacement of this intrusion (Fig. 3). Exposure of the high-grade metamorphic zone could have occurred during the ‘coupled’ phase through uplift of the overriding plate. Emplacement of mafic magmas could have occurred during the ‘release’ phase when the overriding plate was under extension. The presence of the orogen-normal structures to the north and south could have acted as sidewall fault and facilitated significant vertical movement. This would have partitioned the coupling/release cycle to the central part, and could be one reason

¹ Centre for Exploration Targeting, the University of Western Australia, 35 Stirling Highway, Crawley, 6009 WA

* Corresponding author: mark.lindsay@uwa.edu.au

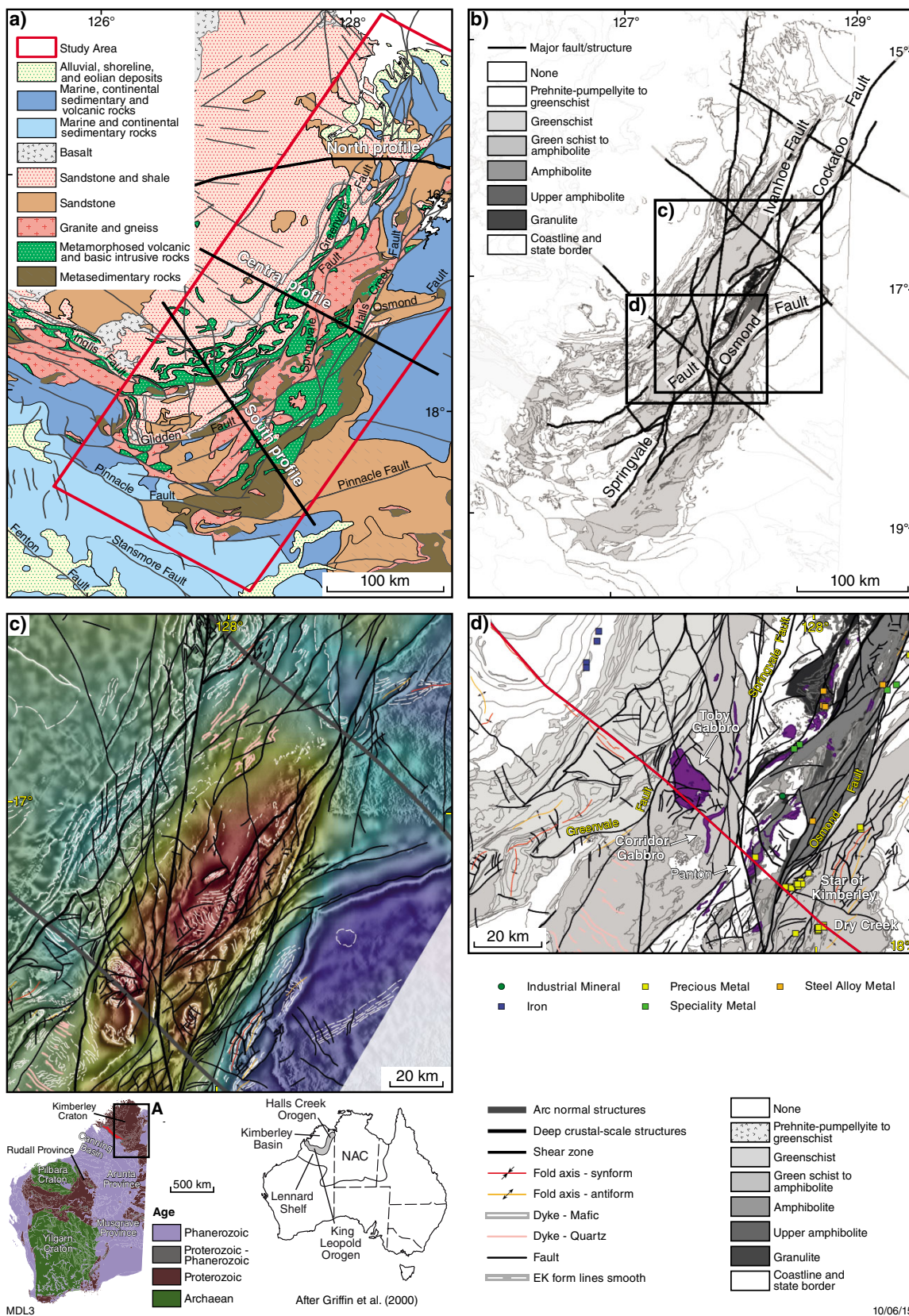


Figure 1. a) Location of the east Kimberley study area showing the major rock units. The thick black lines show the location of forward profiles. We focus on the central profile; b) metamorphic map coded with greyscale (darker greys indicated higher metamorphic grade) overlain by interpreted crustal-scale structures. Inset boxes indicate view extents as indicated; c) inset view of greyscale magnetic data draped over colour scale gravity data. Note the location of the high amplitude gravity anomaly (red region). 'A' indicates apparent sinistral offset on a north-trending structure; d) location of mafic-ultramafic intrusions (purple) coincident with a northwest-trending orogen normal structure (highlighted in red).

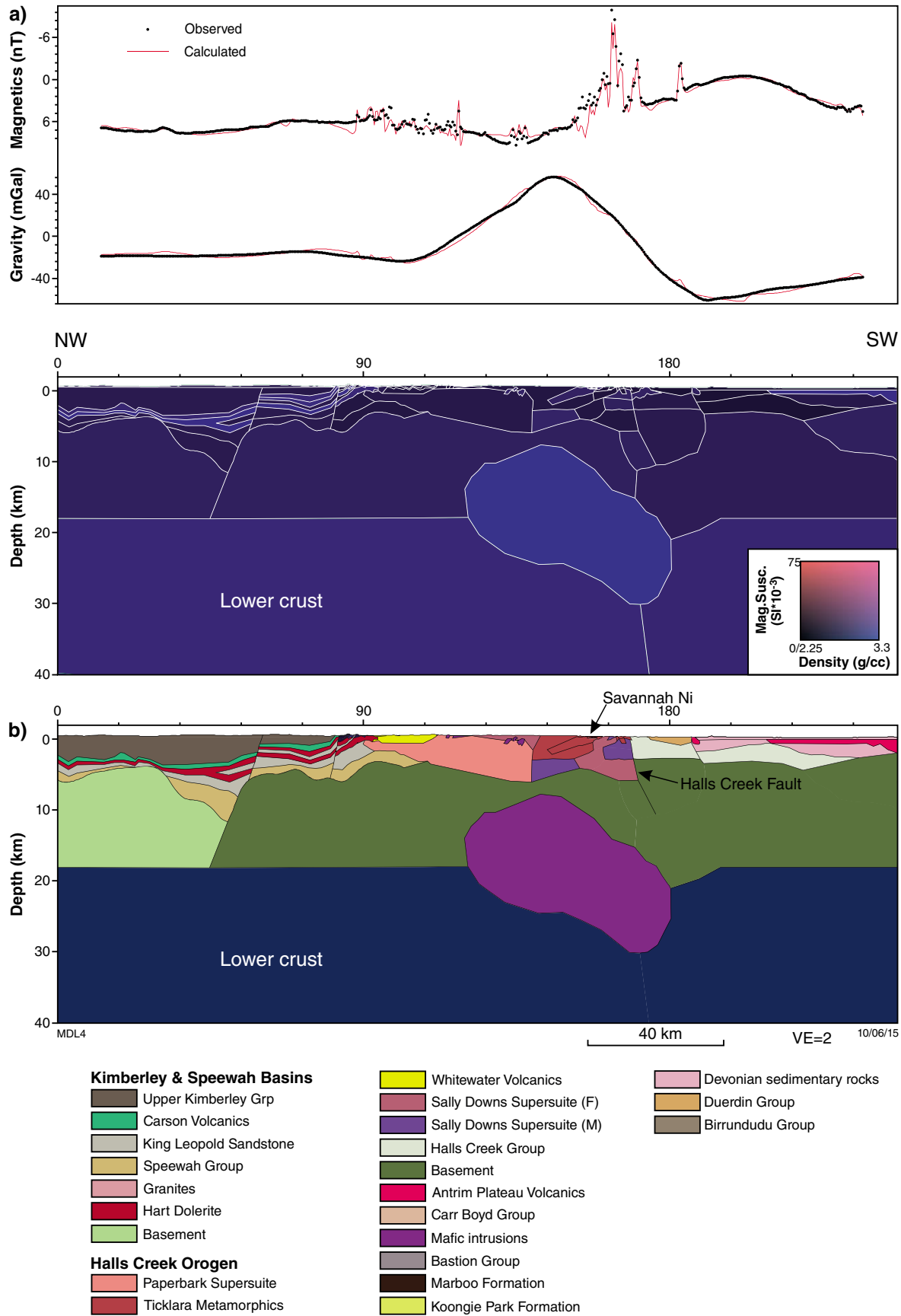


Figure 2. a) Forward model of the central profile (for location refer Figure 1a) showing a dense (3060 kgm^{-3}), c. 20 km thick body that is consistent with the long wavelength, high amplitude gravity signal shown in the top part of the diagram; b) Geological interpretation of the central profile with the geological units shown in the colour-coded legend below.

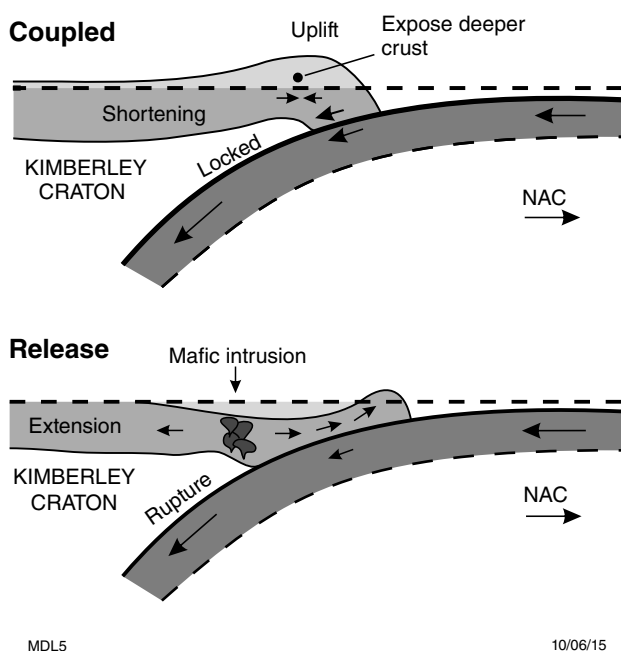


Figure 3. Proposed mechanism for emplacement of a large mafic intrusion and exposure of a high-grade metamorphic zone in the centre of the Halls Creek Orogen. This process is considered to have occurred multiple times during the Halls Creek Orogeny. 'NAC' = North Australian Craton. Modified after Hyndman et al. (1996).

why higher metamorphic grade rocks are not observed along strike to the southwest or northeast. Hyndman et al. (1996) documented coupling of subducting Juan de Fuca plate with the overriding North American Plate, then release, and proposed this has occurred multiple times. As the Tickalara Metamorphics are the high-grade rocks exposed in the central part of the Halls Creek Orogen, this hypothesis requires their accretion prior to at least one cycle of coupling and release.

There are several implications for mineralisation associated with the proposed tectonic model. These deep-penetrating, orogen-normal structures may have acted as side-wall faults throughout the Halls Creek Orogeny and were likely reactivated. Mafic-ultramafic intrusions are coincident with the southern structure (Fig. 1d). If the structure and the intrusions are related, then it is possible that the structure controlled emplacement of these outcropping intrusions. A source of magma for these modelled mafic intrusions may then be the mafic body interpreted from the magnetic and gravity forward models. Fault reactivation, coupled with connectivity to a potentially metal-rich mafic source, suggests these structures and the crust overlying the modelled mafic intrusion are important components in the metallogenic evolution of the east Kimberley.

Acknowledgements

Our work in the east Kimberley has benefitted from fruitful discussion with many working in the region. In particular we would like to thank: Marco Fiorentini, Steve Denyszyn, David Stevenson and Sadie Belica (CET/UWA); Ken Rogers (King River Copper Pty Ltd), John Hicks, Andrew Shaw-Stuart (Panoramic Resources), Karin Orth (University of Tasmania), Trevor Beardsmore, Sidi Morin-Ka, Chris Phillips, John Brett and David Twist (GSWA). The Australian Society of Exploration Geophysicists Research Foundation, Rusty Camille and Jonathon Poh are thanked for their assistance with gathering and analysing petrophysical data.

References

- SA Occhipinti, V Metelka, MD Lindsay, J Hollis, ARA Aitken, S Sheppard, K Orth, IM Tyler, T Beardsmore, M Hutchinson, JM Miller 2015, Preliminary outcomes from Mineral systems analysis for the Halls Creek Orogen, *in* GSWA Kimberley Workshop 2014: extended abstracts: Geological Survey of Western Australia, Record 2015/6.
- Bodorkos, S, Oliver, NHS and Cawood, PA 1999, Thermal evolution of the central Halls Creek Orogen, northern Australia: *Australian Journal of Earth Sciences*, v. 46, p. 453–465.
- Bodorkos, S, Sandiford, M, Oliver, NHS and Cawood, P 2002, High-T, low-P metamorphism in the Palaeoproterozoic Halls Creek Orogen, northern Australia: the middle crustal response to a mantle-related transient thermal pulse: *Journal of Metamorphic Geology*, v. 20, no. 2, p. 217–237.
- Gunn, PJ and Meixner, AJ 1998, The nature of the basement to the Kimberley Block, northwestern Australia: *Exploration Geophysics*, v. 29, p. 506–511.
- Hyndman, RD, Rogers, GC, Dragert, H, Wang, K, Clague, JJ, Adams, J and Bobrowsky, PT 1996, Giant earthquakes beneath Canada's west coast: *Geoscience Canada*, v. 23, no. 2, p. 63–72.
- Tyler, IM, Griffin, TJ, Page, RW and Shaw, RD 1995, Are there terranes within the Lamboo Complex of the Halls Creek Orogen?, *in* Annual Review 1993–94: Geological Survey of Western Australia, Perth, Western Australia, p. 37–46.

Preliminary outcomes from mineral systems analysis for the Halls Creek Orogen

by

SA Occhipinti¹, V Metelka¹, MD Lindsay¹, J Hollis, ARA Aitken¹, S Sheppard², K Orth³, IM Tyler, T Beardsmore, M Hutchison, and JM Miller¹

Mineral systems analysis involves understanding the geodynamic processes that are required to form and preserve ore deposits at a range of scales (Wyborn et al., 1994). In order to complete mineral systems analysis the key controlling processes on the formation and preservation of mineral systems must be understood. These processes include aspects as large scale as the secular evolution of the earth, controlling factors on lithospheric enrichment and the geodynamic drivers in the formation of a mineral system (McCuaig et al., 2010; McCuaig and Hronsky, 2014). Of these processes, lithospheric enrichment and geodynamic drivers can often be directly linked to plate tectonics and therefore the kinematics of plate motion, which have a fundamental link to the formation and breakup of supercontinents (Goldfarb et al., 2001; Begg et al., 2010; Groves et al., 2010; Hayward and Skirrow, 2010). Factors involving the secular evolution of the Earth require the acknowledgement that some styles of ore deposits only formed during certain periods of the Earth's history (Leach et al., 2010), while others (such as those formed in carbonate – evaporate sequences) entail the understanding of plate reconstructions and the determination of paleolatitudes (Cline et al., 2005; Leach et al., 2010). Apart from tectonic and paleoenvironmental drivers, the presence of deep lithospheric scale faults is widely recognised as a fundamental component serving both as a fluid pathway, or an ore trap zone (McCuaig et al., 2010).

The geological evolution of the Kimberley region spans almost two billion years and involves periods of accretion, convergence and rifting, along a margin that was affected by vastly changing tectonic environments through this time (Tyler and Griffin, 1990; Sheppard et al., 1999; Griffin et al., 2000; Tyler et al., 2012; Hollis et al., 2014).

These temporal changes have led to the development of a region in which rock types, and indeed mineralisation formed in different tectonic settings. Contact relationships between different units are varied — they may be tectonically interleaved, conformable, unconformable or intrusive, together metamorphosed to different grades and tectonically juxtaposed. This means that mineralisation that developed early in the history of the region might be overprinted by subsequent events.

Based on the tectonic history recorded in the Halls Creek Orogen several groups of commodities have been targeted at a regional scale through a mineral systems approach. For all of these commodity groups it was noted that a deep crustal scale structure was required to have been operating in the region during a mineralisation event. The groups of commodities considered are thought to have formed in intraplate-extensional or convergent – collisional settings. A knowledge-based fuzzy logic approach has been used for these analyses following a methodology outlined by Bonham-Carter (1994), Joly et al. (2012) and Lindsay et al. (2015).

Commodities such as Ni, Cu, V, Ti and PGEs are thought to occur in both c. 1850 Ma mafic to ultramafic rocks and c. 1800 Ma mafic rocks that intruded as sills into both the western and central domains and western domain – Kimberley Craton margin, respectively. For these rocks, inputs into the prospectivity analysis included, but were not limited to, predictor maps describing the rock type and distance from deep crustal scale structures of different orientations. Predictor maps for diamond targeting included features such as relative thickness of the lithosphere (where thick lithosphere is regarded most prospective), existence of alkaline intrusive bodies, and distance to deep crustal scale structures. The results show that the prospectivity models are largely influenced by mapped rock type and structure. However, it also shows that only some parts of the mafic to ultramafic units preserved in the region are considered prospective for Ni-Cu-PGE-V-Ti, and areas favourable for diamonds are confined mostly to the central zone of the Halls Creek Orogen.

¹ Centre for Exploration Targeting, The University of Western Australia, M006, 35 Stirling Highway, Crawley, WA 6009, Australia.

² Brockman Mining, Level 1, 117 Stirling Hwy, Nedlands, WA 6009, Australia.

³ Centre for Ore Deposit Research and School of Earth Sciences, University of Tasmania, Private Bag 79, Hobart, Tasmania 7001, Australia.

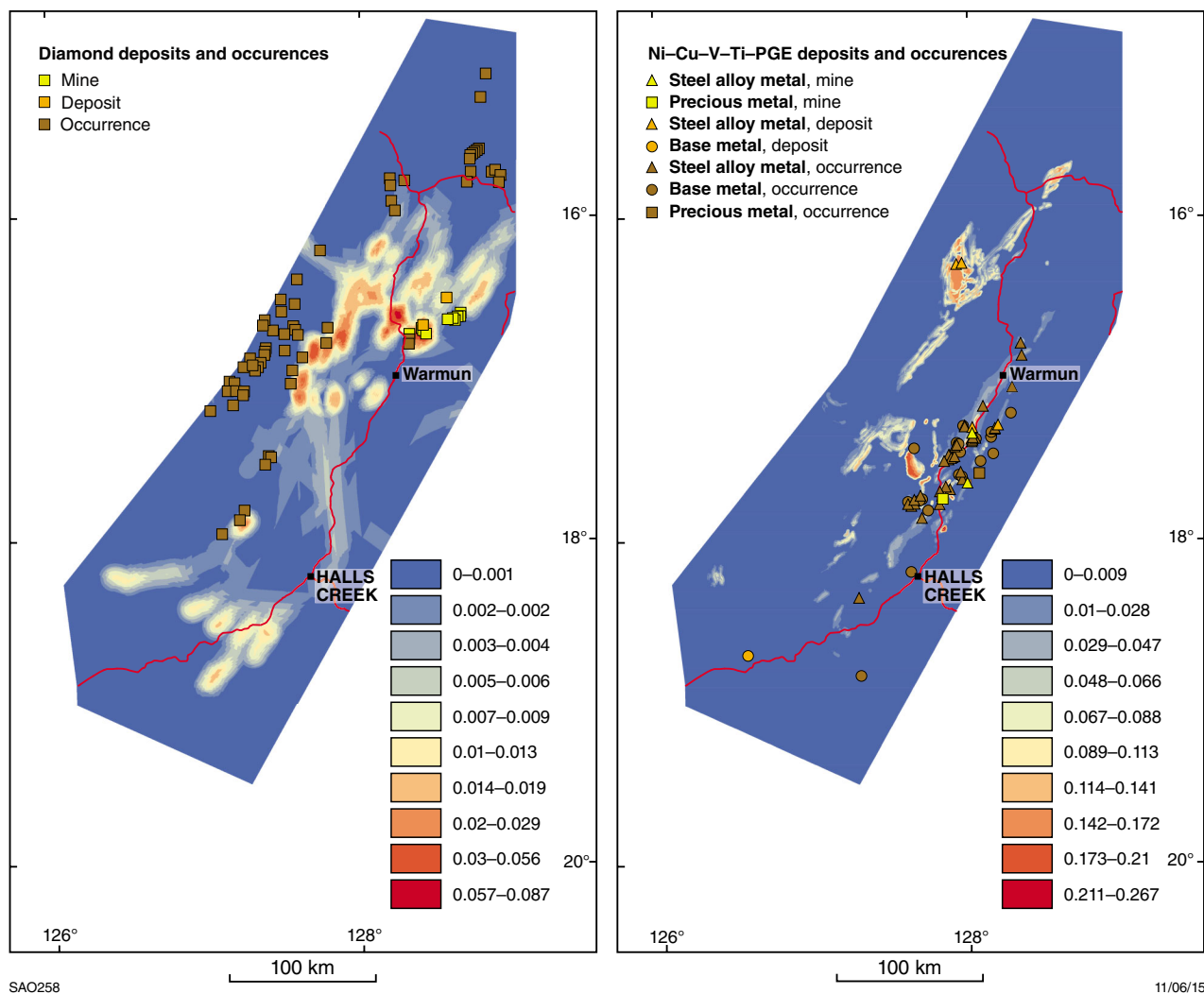


Figure 1. Mineral Prospectivity Analysis for Diamonds and Ni, Cu, PGEs, Ti, and V of the Halls Creek Orogen. Left: diamonds; right: Ni, Cu, V, Ti, PGE

References

- Lindsay, M., Aitken, A.R., Dentiith, M.C., Hollis, J.A. and Tyler, I.M., 2015. Mineral prospectivity of the King Leopold Orogen and Lennard Shelf: potential field analysis in the west Kimberley, Report 142, Geological Survey of Western Australia.
- Begg, GC, Hronsky, JMA, Arndt, NT, Griffin, WL, O'Reilly, S and Hayward, N 2010, Lithospheric, cratonic, and geodynamic setting of Ni-Cu-PGE sulfide deposits: *Economic Geology*, v. 105, p. 1057-1070.
- Bonham-Carter, GF 1994, *Geographic Information Systems for geoscientists: modelling with GIS*: Pergamon Press, Elsevier B.V., Amsterdam, The Netherlands, 416p.
- Cline, JS, Hofstra, AH, Muntean, JL, Tosdal, RM and Hickey, KA 2005, Carlin-type gold deposits in Nevada: critical geologic characteristics and viable models: *Economic Geology 100th Anniversary Volume*, p. 451-484.
- Goldfarb, RJ, Groves, DI and Gardoll, S 2001, Orogenic gold and geologic time: a global synthesis: *Ore Geology Reviews*, v. 18, p. 1-75.
- Griffin, TJ, Page, RW, Sheppard, S and Tyler, IM 2000, Tectonic implications of Palaeoproterozoic post-collisional, high-K felsic igneous rocks from the Kimberley region of northwestern Australia: *Precambrian Research*, v. 101, p. 1-23.
- Groves, DI, Bierlein, FP, Meinert, LD and Hitzman, MW 2010, Iron oxide copper-gold (IOCG) deposits through Earth history: implications for origin, lithospheric setting, and distinction from other epigenetic iron oxide deposits: *Economic Geology*, v. 105, no. 3, p. 641-654.
- Hayward, N and Skirrow, RG 2010, Geodynamic setting and controls on Iron Oxide Cu-Au (+/-U) ore in the Gawler Craton, South Australia, in *Hydrothermal iron oxide copper-gold and related deposits: a global perspective* edited by TM Porter: PGC Publishing, Adelaide, p. 119-145.
- Hollis, JA, Kemp, AIS, Tyler, IM, Kirkland, CL, Wingate, MTD, Phillips, C, Sheppard, S, Belousova, E and Greau, Y 2014, Basin formation by orogenic collapse: zircon U-Pb and Lu-Hf isotope evidence from the Kimberley and Speewah Groups, northern Australia: *Geological Survey of Western Australia, Report 137*, 46p.

- Joly, A, Porwal, A and McCuaig, TC 2012, Exploration targeting for orogenic gold deposits in the Granites–Tanami Orogen: Mineral system analysis, targeting model and prospectivity analysis: *Ore Geology Reviews*, v. 48, p. 349–383.
- Leach, DL, Bradley, DC, Huston, D, Pisarevsky, SA, Taylor, RD and Gardoll, SJ 2010, Sediment-hosted lead–zinc deposits in Earth history: *Economic Geology*, v. 105, no. 3, p. 593–625, doi:10.2113/gsecongeo.105.3.459.
- McCuaig, TC, Beresford, S and Hronsky, J 2010, Translating the mineral systems approach into an effective exploration targeting system: *Ore Geology Reviews*, v. 38, p. 128–138.
- McCuaig, TC and Hronsky, JMA 2014, The mineral system concept: The key to Exploration targeting, in *Building Exploration Capability for the 21st Century* edited by KD Kelley and HC Golden: Society of Economic Geologists, Inc., Special Publication Number 18, p. 153–175.
- Sheppard, S, Tyler, IM, Griffin, TJ and Taylor, RW 1999, Palaeoproterozoic subduction-related and passive margin basalts in the Halls Creek Orogen, northwest Australia: *Australian Journal of Earth Sciences*, v. 46, p. 679–690.
- Tyler, IM and Griffin, WL 1990, Structural development of the King Leopold Orogen, Kimberley region, Western Australia: *Journal of Structural Geology*, v. 12, p. 703–714.
- Tyler, IM, Hocking, RM and Haines, PW 2012, Geological evolution of the Kimberley region of Western Australia: *Episodes*, v. 35, p. 298–306.
- Wyborn, LAI, Heinrich, CA and Jaques, AL 1994, Australian Proterozoic mineral systems: essential ingredients and mappable criteria, in *Australian mining looks north — the challenges and choices* edited by PC Hallenstein: Australian Institute of Mining and Metallurgy; 1994 AusIMM Annual Conference, Darwin, Northern Territory, 5 August 1994, p. 109–115.

Constraints on Paleoproterozoic crust–mantle evolution from the Hf, Nd and O isotope record of igneous rocks in the Lamboo Province of the Halls Creek and King Leopold Orogens

by

AIS Kemp¹, S Sheppard², IM Tyler, and S Bodorkos³

The purpose of this study was to constrain the processes of Paleoproterozoic crust–mantle evolution by investigating the Lu–Hf, Sm–Nd and oxygen isotope systematics of igneous rocks of the Lamboo Province of the Halls Creek and King Leopold Orogens, in the Kimberley region of Western Australia.

The specific objectives were to:

1. Ascertain the nature of the source rocks of the granites, and to test whether granite formation involved the reworking of ancient meta-igneous protoliths in an intra-plate environment or complex crust-mantle interaction processes typical of modern plate tectonic settings.
2. Use data from granite-hosted zircons to quantify the proportion of new crust formed during discrete magmatic events, and to link this with the longer-term record of crustal evolution preserved by detrital zircons.
3. Constrain the tectonic setting of the Lamboo Province, and thus the geodynamic controls on global crustal growth in this key time period.

The study utilised an analytical approach referred to as 'forensic zirconology' (Kemp et al., 2011) — the sequential *in situ* measurement of U–Pb, oxygen and Lu–Hf isotopes from the same micro-domain of zircon crystals. Zircon data were augmented by whole rock Sm–Nd and (for some mafic and metasedimentary rocks) oxygen isotope data from the same samples.

Thirty-two rock samples were collected from across the Lamboo Province in 2008. These encompassed representatives of the major granitic supersuites (e.g. Sheppard et al., 2001), including mafic intrusions and enclaves associated with these supersuites, and Paleoproterozoic metasedimentary units in the Western, Central and Eastern Zones of the province (to assess as

potential melt sources). In addition, zircons of 29 igneous samples were obtained from Geoscience Australia, all having been previously dated by SHRIMP (Griffin et al., 2000; Page et al., 2001).

U–Pb zircon data

New U–Pb (zircon) data (SHRIMP II at Curtin University, Cameca 1270 ion microprobe at the University of Edinburgh) were obtained for 10 igneous rocks across the orogen. The results largely conform to those of prior studies by Page et al. (2001) and Griffin et al. (2000).

Inferred emplacement ages for five granites and gabbros from the Paperbark Supersuite in the Western Zone are indistinguishable at c. 1860 Ma (weighted average ²⁰⁷Pb/²⁰⁶Pb ages, corrected for common lead). A slightly younger age of 1854 ± 4 Ma was obtained from the Toby Gabbro. Significant inheritance was identified in the Topwater Tonalite (cores from 2720 to 2270 Ma), presumably reflecting assimilation of partially melted Marboo Formation metasedimentary rocks, into which this tonalite was emplaced. One older zircon core (c. 2500 Ma) was also identified in the Mount Nyulasy Granite.

Samples from the Central Zone yielded inferred crystallisation ages ranging from c. 1842 Ma (Corridor Gabbro) to c. 1826 Ma (Sally Downs Tonalite). We found no evidence for older, inherited zircon cores in any Central Zone sample, despite a conscious effort to locate such components. Unexpectedly, zircon age groups in both the Dougalls Tonalite and Fletcher Creek Monzogranite suggest igneous crystallisation at c. 1838 Ma, around 10 million years younger than previous estimates based on zircon U–Pb data (Page et al., 2001). In the case of the Dougalls Tonalite, the same apparent age was obtained from two separate analytical sessions. The reason for this discrepancy is unknown, but it suggests that emplacement of the Dougalls Tonalite and Fletcher Creek Monzogranite was synchronous with, or immediately post-dated, high-grade metamorphism in the Central Zone, dated at 1845 ± 4 Ma (Bodorkos et al., 2000). One implication is that early deformation and metamorphic events in the Central Zone are unrelated to those in the Western Zone.

1 Centre for Exploration Targeting, School of Earth and Environment, The University of Western Australia, 35 Stirling Highway, Crawley WA 6009

2 Department of Applied Geology, Curtin University, Bentley WA 6102

3 Resources Division, Geoscience Australia, GPO Box 378, Canberra ACT 2601

Oxygen isotope data

Oxygen isotope data (Cameca 1270 ion microprobe, University of Edinburgh) were obtained from zircons of 11 igneous samples. Zircons from the Dougalls Tonalite and Sally Downs Tonalite yielded mantle-like $\delta^{18}\text{O}$ (4.7 – 6.1 ‰ VSMOW), in accord with their relatively juvenile Sm–Nd isotope composition (Sheppard et al., 2001). Slightly elevated zircon $\delta^{18}\text{O}$ values (6.0 – 6.9 ‰ VSMOW) relative to the mantle range from the Wombarella (c. 1860 Ma), Toby (c. 1854 Ma) and Corridor (c. 1842 Ma) gabbros are consistent with crustal contamination of mafic magmas, as suggested by field and petrographic evidence (e.g., interstitial quartz, and biotite replacing pyroxene). In contrast, the Paperbark Supersuite granites, and cogenetic Whitewater Volcanics samples, yielded strongly elevated zircon $\delta^{18}\text{O}$ values (6.5 – 11‰ VSMOW). Such values indicate extensive reworking of supracrustal source rocks by these high-K magmas.

Hf isotope data

Zircons of 35 igneous samples were analysed for Hf-isotope compositions (LA–MC–ICPMS, James Cook University, Townsville). Overall, these data show limited in-sample variation and correlate closely with the corresponding whole rock Sm–Nd isotope compositions. The Hf–Nd isotope compositions of the granitic samples are bracketed between those of coeval, spatially associated mafic intrusions and regional metasedimentary packages, suggesting that these are the dominant source components. Hf isotope compositions also broadly correlate with zircon $\delta^{18}\text{O}$, such that igneous rocks with the least radiogenic Hf (i.e. those of the Paperbark suite) also have the highest $\delta^{18}\text{O}$. Intriguingly, the c. 1860 Ma igneous samples from the Paperbark Supersuite in the west Kimberley have markedly lower zircon $\delta^{18}\text{O}$ (at similar ϵ_{Hf}) than granites from the supersuite in the east Kimberley, and cannot be part of a simple mixing system between mafic magmas and local metasedimentary basement. This suggests the existence of disparate crustal source domains for these high-K magmas across the Kimberley region.

Conclusions

The main conclusions of this study can be summarised as follows:

1. Paleoproterozoic igneous rocks of the Halls Creek Orogen show large isotope variations, with coherent co-variation between Hf–Nd–O systems indicating the involvement of multiple, contrasting source components
2. Igneous rocks of the c. 1860 Ma Paperbark Supersuite from the Western Zone, through their elevated zircon $\delta^{18}\text{O}$ and low $^{176}\text{Hf}/^{177}\text{Hf}$, record extensive reworking of metasedimentary rocks derived from Archean precursors. This reworking provides an explanation for the high-K signature of these samples, and requires a crustal thickening event prior to 1860 Ma; melting of crystalline Archean basement is not necessary to explain the isotope systematics of these rocks
3. The younger (c. 1840 to 1820 Ma) felsic igneous rocks of the Central Zone incorporate a substantial juvenile component, indicating magmatism remote from older continental sources, possibly reflecting ocean-ward retreat of a west-dipping subduction zone. These younger igneous rocks were evidently emplaced in a tectonic setting conducive to the generation and preservation of new continental crust
4. Collectively, the isotopic diversity, evidence for reworking of metasedimentary rocks, and inflected secular Nd–Hf–O isotope trends are consistent with magma generation in an evolving plate margin setting, as inferred by previous studies (e.g. Sheppard et al., 2001).

References

- Bodorkos, S, Cawood, PA, Oliver, NHS and Nemchin, AA 2000, Rapidity of orogenesis in the Paleoproterozoic Halls Creek Orogen, northern Australia: evidence from SHRIMP zircon data, CL zircon images, and mixture modeling studies: *American Journal of Science*, v. 300, no. 1, p. 60–82.
- Griffin, TJ, Page, RW, Sheppard, S and Tyler, IM 2000, Tectonic implications of Palaeoproterozoic post-collisional, high-K felsic igneous rocks from the Kimberley region of northwestern Australia: *Precambrian Research*, v. 101, p. 1–23.
- Kemp, AIS, Blevin, P, Whitehouse, M and Edinburgh Ion Microprobe Facility 2011, Forensic zirconology: tracing the magmatic and metallogenic evolution of intrusive porphyries of the Macquarie Arc, NSW, Australia: 11th SGA Biennial Meeting, Let's Talk Ore Deposits, 26–29th September, 2011, Antofagasta, Chile, p. 429–431.
- Page, RW, Griffin, TJ, Tyler, IM and Sheppard, S 2001, Geochronological constraints on tectonic models for Australian Palaeoproterozoic high-K granites: *Journal of the Geological Society*, v. 158, p. 535–545.
- Sheppard, S, Griffin, TJ, Tyler, IM and Page, RW 2001, High- and low-K granites and adakites at a Palaeoproterozoic plate boundary in northwestern Australia: *Journal of the Geological Society*, v. 158, p. 547–560.

Volcanology of the Carson Volcanics: outpouring of a 1.79 Ga large igneous province

by

K Orth*

The Carson Volcanics is the only volcanic unit in the Kimberley Basin. Together with the Hart Dolerite they form the Hart-Carson Large Igneous Province (LIP; Tyler et al., 2006). The mean U-Pb crystallization age of zircon obtained from the granophyre in the Hart Dolerite is 1797 ± 11 Ma (Sheppard et al., 2012). The Hart Dolerite intrudes the lower Kimberley Basin (King Leopold Sandstone and Carson Volcanics) and the underlying Speewah Group to a depth of 2–3 km beneath the eruptive surface.

The Carson Volcanics overlie the basal quartz sandstone of the King Leopold Sandstone in the west Kimberley and are overlain by the more feldspathic sandstone of the Warton Sandstone, Elgee Siltstone and the Pentecost Sandstone in the east. A south sloping basin is envisaged at the time of volcanism from paleocurrent data in the King Leopold Sandstone (Gellatly et al., 1970).

The Carson Volcanics are distributed across the Kimberley Basin. They are present in the west on the Yampi Peninsula, form plateaus in the south and west (CHARNLEY, PRINCE REGENT), form the Mitchell Plateau and crop out along the middle of the Kimberley Basin between the coast north of Kalumburu and Bell Creek in the south. The Carson Volcanics also rim the southern and eastern margin of the Kimberley Basin (Fig. 1).

The distribution and thickness of the units across the Kimberley Basin suggest that the Carson Volcanics represent $50\,000\text{ km}^3$ of basaltic magmatism. The Carson Volcanics comprise 17% of the Hart-LIP, the majority represented by the intrusive Hart Dolerite. The volume of the Hart-Carson LIP is around $300\,000\text{ km}^3$, comparable to the volume of the Columbia River Basalts in the Western USA (Reidel et al., 2013). Both these LIPs are an order of magnitude less voluminous than LIPs associated with continental break up, such as the Deccan, Karoo, Parana and Siberian Traps. The Deccan, for example, has a volume of 8.6 million km^3 .

Many features evident in the Carson Volcanics are comparable to the volcanic rocks in LIPs elsewhere around the world. Typical is the tabular appearance of many basalt units to form layer cake stratigraphy. Although these are only up to 40 m thick, they cover extensive areas (250×200 km). The internal features of many lavas are consistent with basalt described from the Columbia River Basalts (Hooper, 1997; Reidel et al., 2013; Vye-Brown et al., 2013) with up to one third of the flow formed by amygdaloidal crust that was inflated (Self et al., 1996). The lavas erupt along fissure vent systems hundreds of kilometres long. Fluidal, pahoehoe lavas issuing from these vents form lobes that coalesce into large tabular bodies. Pahoehoe features evident in the Carson Volcanics include ropy flow tops and bases (Fig. 2a), basal pipe vesicles (Fig. 2b) and lobe toes.

The internal stratigraphy of the Carson Volcanics includes six or more basalt lava units, with more lava flows on the edge of the Yampi Peninsula (Fig. 3). In the north, the Carson Volcanics are up to 180 m thick, but in the south the Carson Volcanics are at least 250 m thick at Mornington and possibly up to 800 m thick near the Yampi Peninsula.

Mappable units of sedimentary rocks, intercalated with the basalt, are 30 m thick and traceable for up to 40 km along strike. The exceptions are up to 200-m thick packages of sandstone, matrix-supported granule to cobble conglomerate and breccia with intervening siltstone on the Yampi Peninsula. Most intercalated sandstone and siltstone display cross-bedding, asymmetrical ripples, and desiccation cracks (Fig. 2c), consistent with fluvial to shallow and emergent marine environments. Near the top of the Carson Volcanics are fine-grained sandstone, siltstone and mudstone with restricted stromatolites north and east of Kalumburu (Fig. 2d).

North of Kalumburu, basalt burrowed into a wet unconsolidated substrate, producing peperite. The disturbed basalt and sedimentary rocks are overprinted by hydrothermal alteration in this area. Evidence that the basalt interacted with water are pillow basalt, present on the Yampi Peninsula (Fig. 2e). A previously reported occurrence of pillow basalt near Bell Creek in the south

* CODES, University of Tasmania, in collaboration with Geological Survey of Western Australia

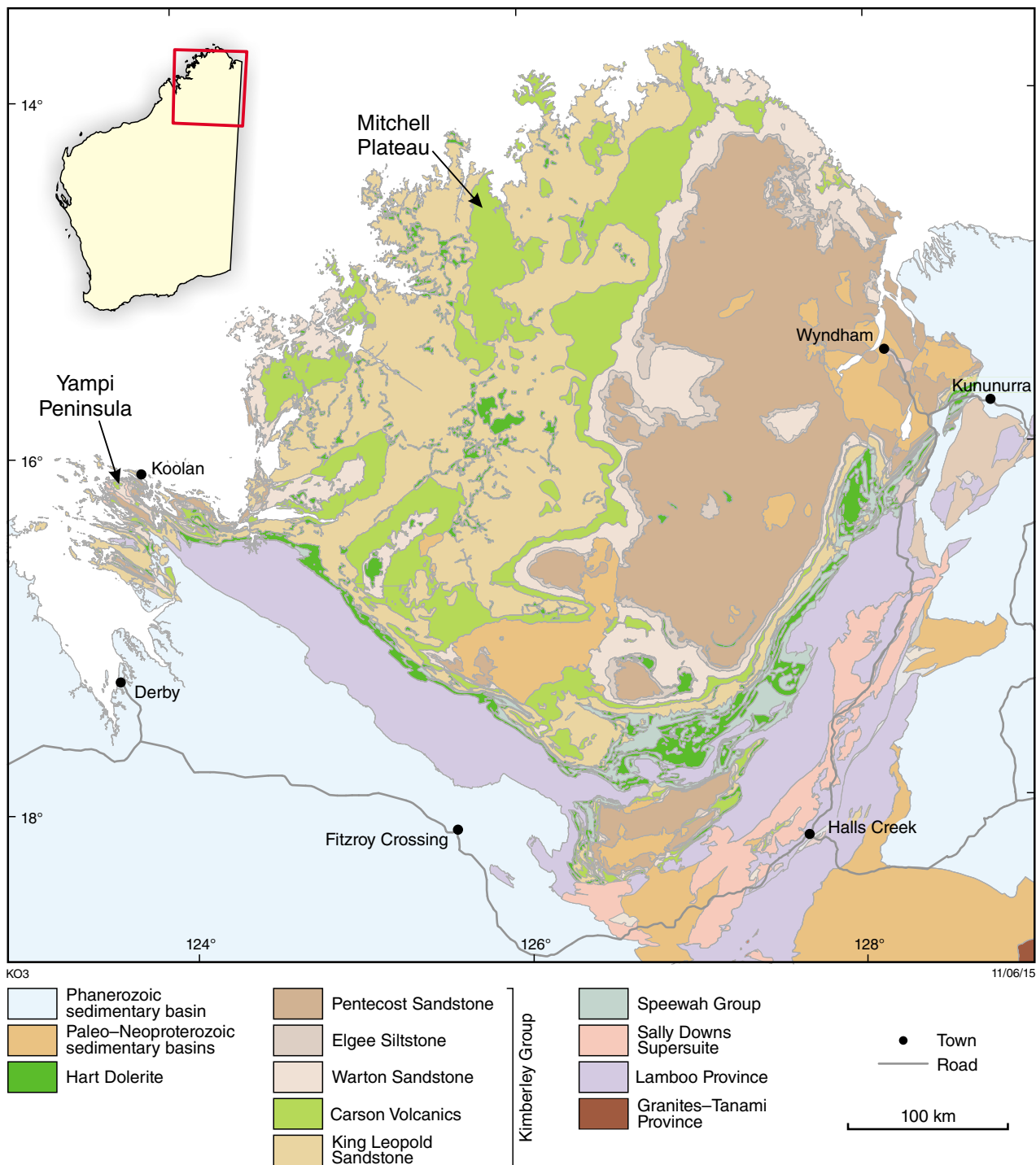


Figure 1. Distribution of the Carson Volcanics in light green and the Hart Dolerite in dark green. The Carson Volcanics crop out in the middle of the Kimberley. Remnants of the Carson Volcanics overlie the King Leopold Sandstone in the west and are overlain by the upper Kimberley Group in the east. Hart Dolerite intrudes the Speewah Group and the lower Kimberley Group, up to the Carson Volcanics around the edges of the main preserved Kimberley Basin. Carson Volcanics are around the margins of the basin between south of Koolan Island to west of Kununurra. Dolerite intruding higher up into the Kimberley Group is not included in the Hart Dolerite in this study.

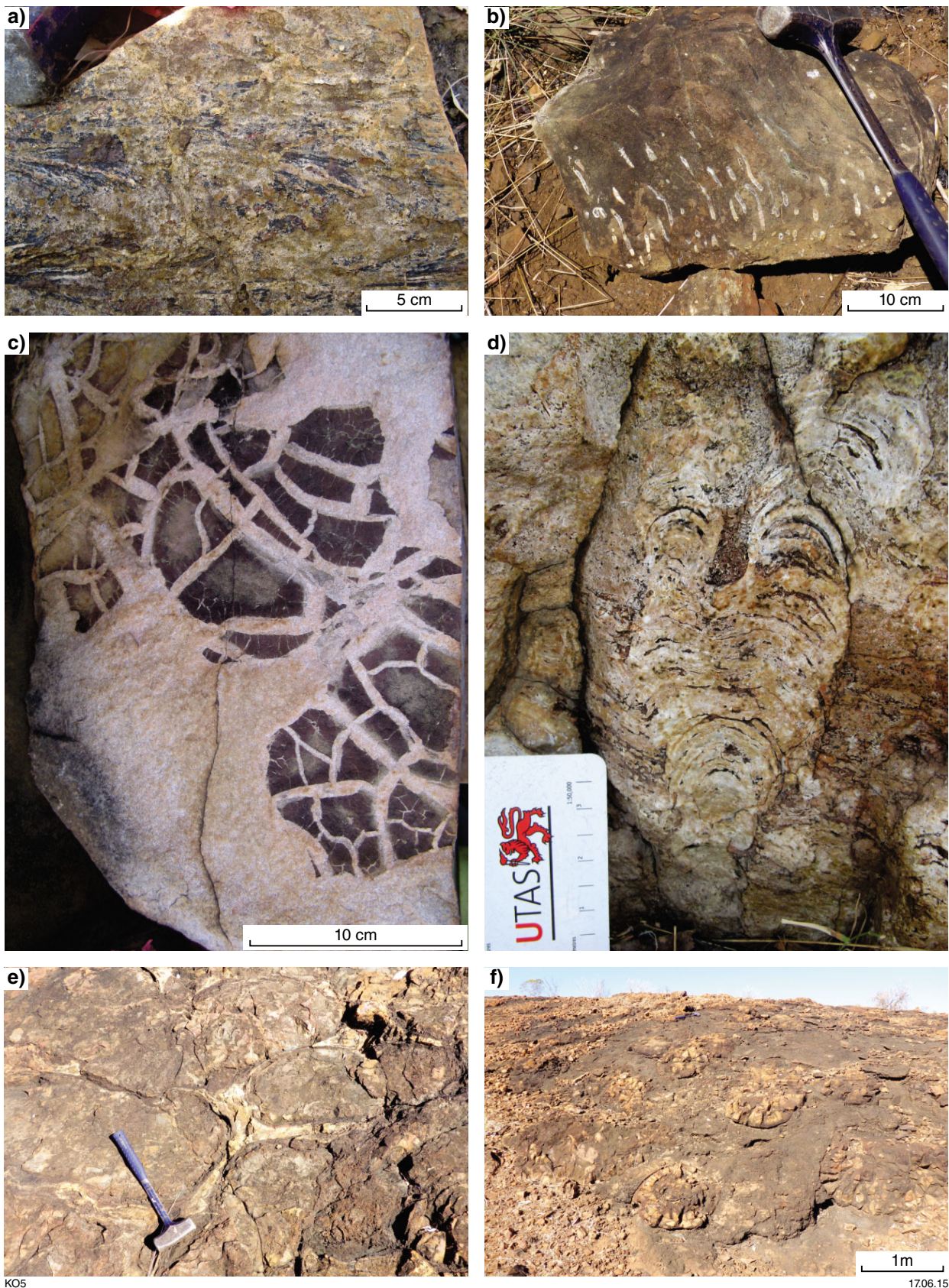


Figure 2. Carson Volcanics A) Ropy texture in basalt flow southeast of Kalumburu. B) Pipe vesicles filled with quartz at the base of a basalt unit on the Mitchell Plateau. Pipe vesicles curve in the direction of flow. C) Desiccation cracks in sandstone unit between basalt flows east of Kalumburu. D) Stromatolites near the top of Carson Volcanics northeast of Kalumburu. E) Pillow basalt on the Yampi Peninsula. F) Pillow-in-breccia facies from the Mt House Track. Many of the pillows are in cross-section and are about 1 m across.

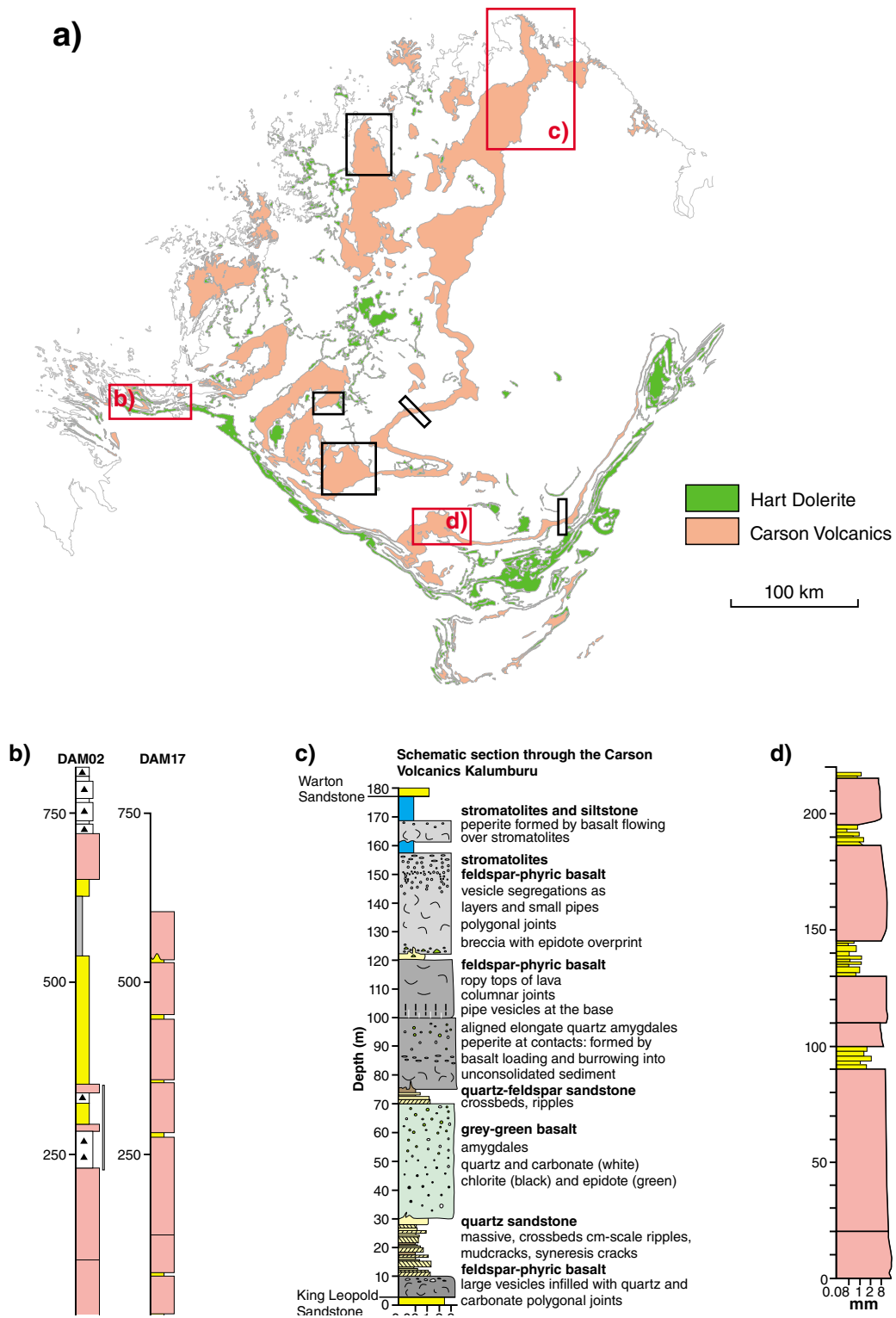


Figure 3. Summary sections of the Carson Volcanics from the Kimberley Basin: c) is a schematic section that summarises the units in the Kalumburu area. Comprising up to six basalt units (in green and grey) the Carson Volcanics reach a maximum thickness of around 180 m. The Mornington summary section (d) is around 200 m thick and it also has six basalt units. In the west, sections are different: more basalt flow units are east of Secure Bay (DAM17, log did not reach the top of the section); and thick sedimentary units on the Yampi Peninsula (DAM02). In b) and d): breccia/conglomerate are filled triangles, sandstone to siltstone dominated units are yellow, chloritic schist and phyllite are grey and basalt is pink.

could not be relocated. A potentially extensive succession of pillow-in-breccia facies is located near the top of the Carson Volcanics on the Mt House Track (Fig. 2f). The pillow-in-breccia facies is an analogue of pillow palagonite basalt units of the Columbia River Basalts, which represent pillow deltas formed as basalt flowed into a standing body of water (Fuller, 1931; Schminke, 1967; Hooper, 1997).

The Carson Volcanics formed on the King Leopold Sandstone on a gentle south-dipping slope. Intervening sedimentary rocks indicate that this was part fluvial to emergent shallow marine during the invasion of the basalt. Recognisable vent facies are lacking throughout the area investigated. South dipping slopes suggest that vents may have lain to the north of the current extent of the Kimberley Basin. The thick succession on the Yampi Peninsula may indicate a steeper slope and deepening of the basin where the basalts flows pooled (Fig. 3). Local stromatolites and fine-grained sedimentary units in the upper portions of the Carson Volcanics, as well as the pillow-in-breccia facies suggest a drowning of the whole basin concomitant with the cessation of volcanism.

Conclusions

The Hart-Carson LIP is comparable to the Columbia River Flood Basalt province in volume. Around 17% is extrusive and comprises the Carson Volcanics. The intrusive equivalent is the Hart Dolerite, which is dated at 1797 ± 11 Ma. Basalts have features consistent with pahoehoe lavas. Up to six units comprise the Carson Volcanics in the Kalumburu area. More basalt units form thicker successions in the south. A gently, south-dipping paleoslope was occupied by fluvial to shallow marine-emergent environments during the invasion of the basalt. Interaction between basalt and wet unconsolidated sediment formed peperite north of Kalumburu. Thick Carson Volcanics, including up to 200 m of matrix-supported breccia, sandstone and siltstone as well as thickened lava and pillow lava units suggest that this may have been a deeper portion of the Kimberley Basin. Fissure vents may lie to the north outside the remnant preserved of the Kimberley Basin.

References

- Fuller, RE 1931, The aqueous chilling of basalt lava on the Columbia River Plateau: *American Journal of Sciences*, v. 21, p. 281–300.
- Gellatly, DC, Derrick, GM and Plumb, KA 1970, Proterozoic palaeocurrent directions in the Kimberley region, northwestern Australia: *Geological Magazine*, v. 107, p. 249–257.
- Hooper, P 1997, The Columbia River Flood Basalt Province: Current status, in *Large Igneous Provinces* edited by JJ Mahoney and MF Coffin: *Geophysical Monograph* 10, p. 1–28.
- Reidel, SP, Camp, VE, Tolan, TL and Martin, BS 2013, The Columbia River Flood Basalt Province: Stratigraphy, areal extent, volume and physical volcanology: *Geological Society of America Special Paper*, v. 497, p. 1–43.
- Schminke, HU 1967, Fused tuffs and pepperite in south-central Washington: *Geological Society of America Bulletin*, v. 78, p. 319–330.
- Self, S, Thordarson, T, Keszthelyi, L, Walker, GPL, Hon, K, Murphy, MT, Long, P and Finnemore, S 1996, A new model for the emplacement of the Columbia River Basalts as inflated pahoehoe lava flow fields: *Geophysical Research Letters*, v. 23, p. 2689–2692.
- Sheppard, S, Page, RW, Griffin, TJ, Rasmussen, B, Fletcher, IR, Tyler, IM, Kirkland, CL, Wingate, MTD, Hollis, J and Thorne, AM 2012, Geochronological and isotopic constraints on the tectonic setting of the c. 1800 Ma Hart Dolerite and the Kimberley and Speewah Basins, northern Western Australia: *Geological Survey of Western Australia, Record* 2012/7, 28p.
- Tyler, IM, Sheppard, S, Pirajno, F and Griffin, TJ 2006, Hart-Carson LIP, Kimberley region, northern Western Australia: *Large Igneous Provinces Commission*, viewed 10 February 2014, <<http://www.largeigneousprovinces.org/06aug>>.
- Vye-Brown, C, Self, S and Barry, TL 2013, Architecture and emplacement of flood basalt flow fields: case studies from the Columbia River Basalt Group, NW USA: *Bulletin of Volcanology*, v. 75, p. 1–21.

The textural and geochemical architecture of the Hart Dolerite at Speewah Dome

by

A Eves¹, RR Ramsay², ML Fiorentini¹, L Gwalani³, W Maier⁴, and K Rogers³

The Hart Dolerite is an extensive system of predominantly massive mafic and lesser felsic granophyre sills and minor dykes intruded at c. 1797 Ma into gently folded and lightly metamorphosed Palaeoproterozoic sediments of the Speewah and Kimberley Basins in the north-western part of the North Australia Craton (Fig 1; cf. Sheppard et al., 2012). Detailed field, mineralogical and geochemical results from this study indicate that rather than a single magma event, the architecture of the Hart Dolerite sill at Speewah Dome (Fig. 1) is complex and reflects the dynamic emplacement of multiple co-genetic but distinct magmatic events.

The Speewah Dome is a regional doubly plunging anticline approximately 20 km in diameter along the eastern margin of the Speewah Basin (Thorne et al., 1999). Eupene (1970) put forward the hypothesis that the Speewah Dome formed in response to the intrusion and differentiation of a lopolithic magmatic edifice. Conversely, (Thorne et al., 1999) interpreted the complex structure as a regional fold on the margin of the Halls Creek Orogen. Our study shows that the mafic and felsic igneous rocks within the Speewah antiform represent a 400 m thick composite sill. Detailed field work has defined an igneous stratigraphy which can be summarized as follows (Fig. 2):

- Above a chilled lower contact, the basal event is a coarse-grained, ophitic-textured, olivine-bearing gabbro which is about 100 m thick and contains traces of blocky to subhedral ilmenite.
- Then above a narrow zone of chloritization, the gabbro is about 150 m of more medium-grained, sub-ophitic textured gabbro with traces of interstitial ilmenite overgrown by titanomagnetite. In the upper 5-10 m, the titanomagnetite forms scattered poikilitic aggregates and this gives the gabbro a distinctive spotted appearance.

- Above a sharp, regionally conformable but locally irregular and metasomatically altered contact the spotted magnetite gabbro is overlain by about 100 m of a medium-grained, sub-ophitic textured gabbro. This intrusive has augite with an abundance of pigeonite exsolution, up to 20% disseminated V-Ti-Fe-oxides (ilmenite and V-rich titanomagnetite) near the base that decreases in abundance upwards and an upwards increase in interstitial potassic granophyre. The disseminated magnetite gabbro is also characterized by a thin PGE reef about 20 m above the basal contact at the point where the magnetite content begins to decrease.
- The last of the mafic events in the sill at Speewah are coarse-grained sub-ophitic textured gabbros emplaced as cross-cutting sills and dykes. The pegmatoidal gabbro has sharp boundaries against the earlier intrusives are up to 50 m thick, contain up to 5% elongate and skeletal Fe-Ti-oxides and the thicker sills and have variable amounts of coarse potassic granophyre segregations.
- Following the mafic events there are two types of potassic granophyre which are emplaced as either 5–20 m thick sills or 1–2 m wide dykes that cut the mafic phases. The early stage mafic granophyre is characterised by an abundance of medium- to fine-grained gabbro xenoliths to 2 cm in diameter that show strong chlorite-epidote alteration. These are supported by a fine- to medium-grained granophyric matrix with scattered plagioclase laths to 2 mm in length. The later stage is a coarse-grained felsic granophyre with traces of euhedral plagioclase laths.

While the early and later mafic rocks in the sill of Hart Dolerite within the Speewah Dome are generally subalkaline and display a broadly co-genetic geochemical affinity, the mineralized disseminated magnetite gabbro appears to be enriched in alkaline content. The disseminated magnetite gabbro also has an abundance of scattered blocky xenoliths up to 30 cm in diameter that are oriented parallel to the lower contact and impart a flow-texture indicating dynamic flow during emplacement. The study shows that both oxygen and sulfur fugacities

1: Centre for Exploration Targeting, School of Earth and Environment, ARC Centre of Excellence for Core to Crust Fluid Systems, University of Western Australia, Australia; 2: Trident Capital Ltd, Perth; 3: King River Copper Ltd, Perth; 4: School of Earth & Ocean Sciences, Cardiff University, UK.

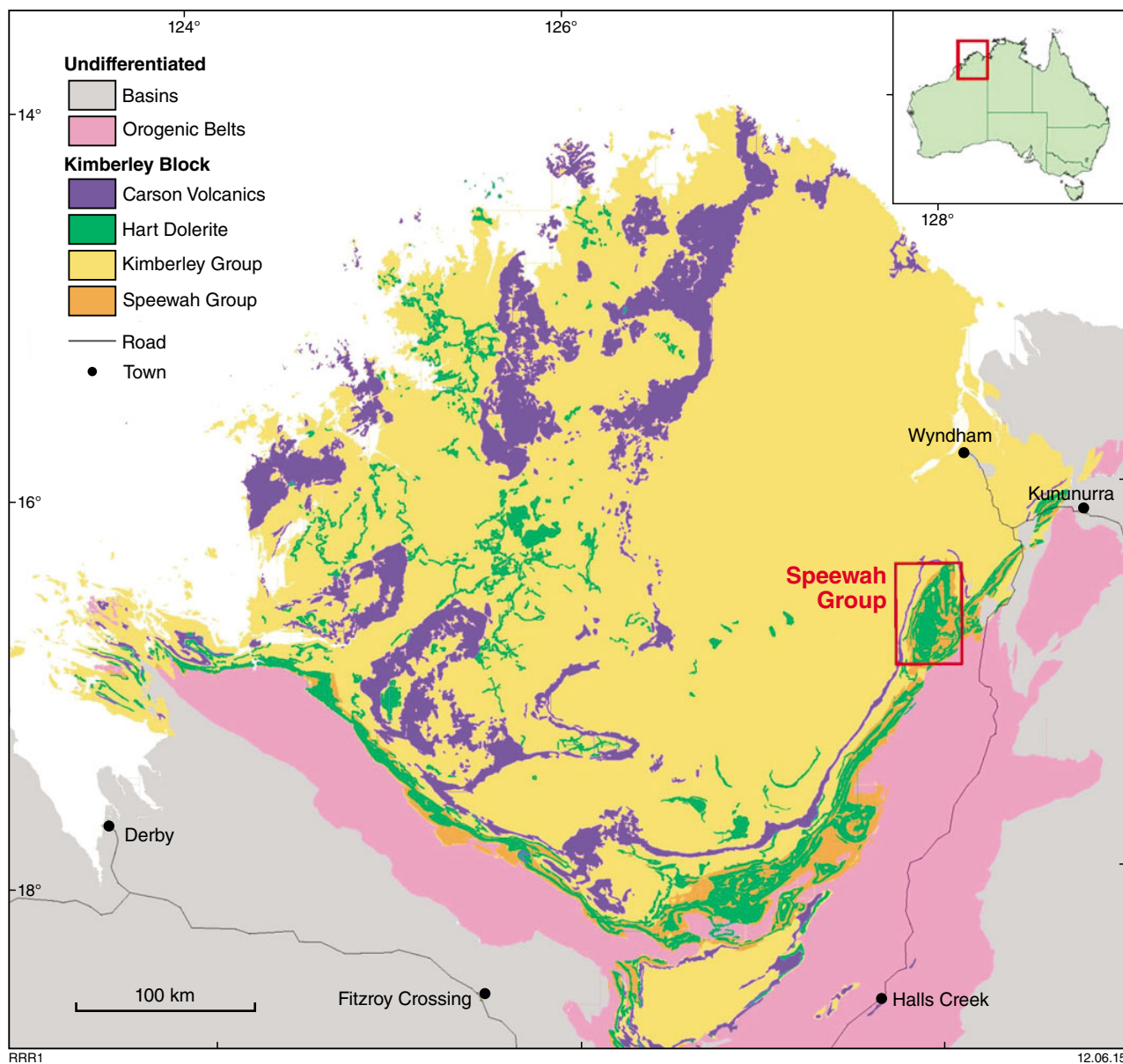


Figure 1. Location of the Speewah Dome within the Kimberley region

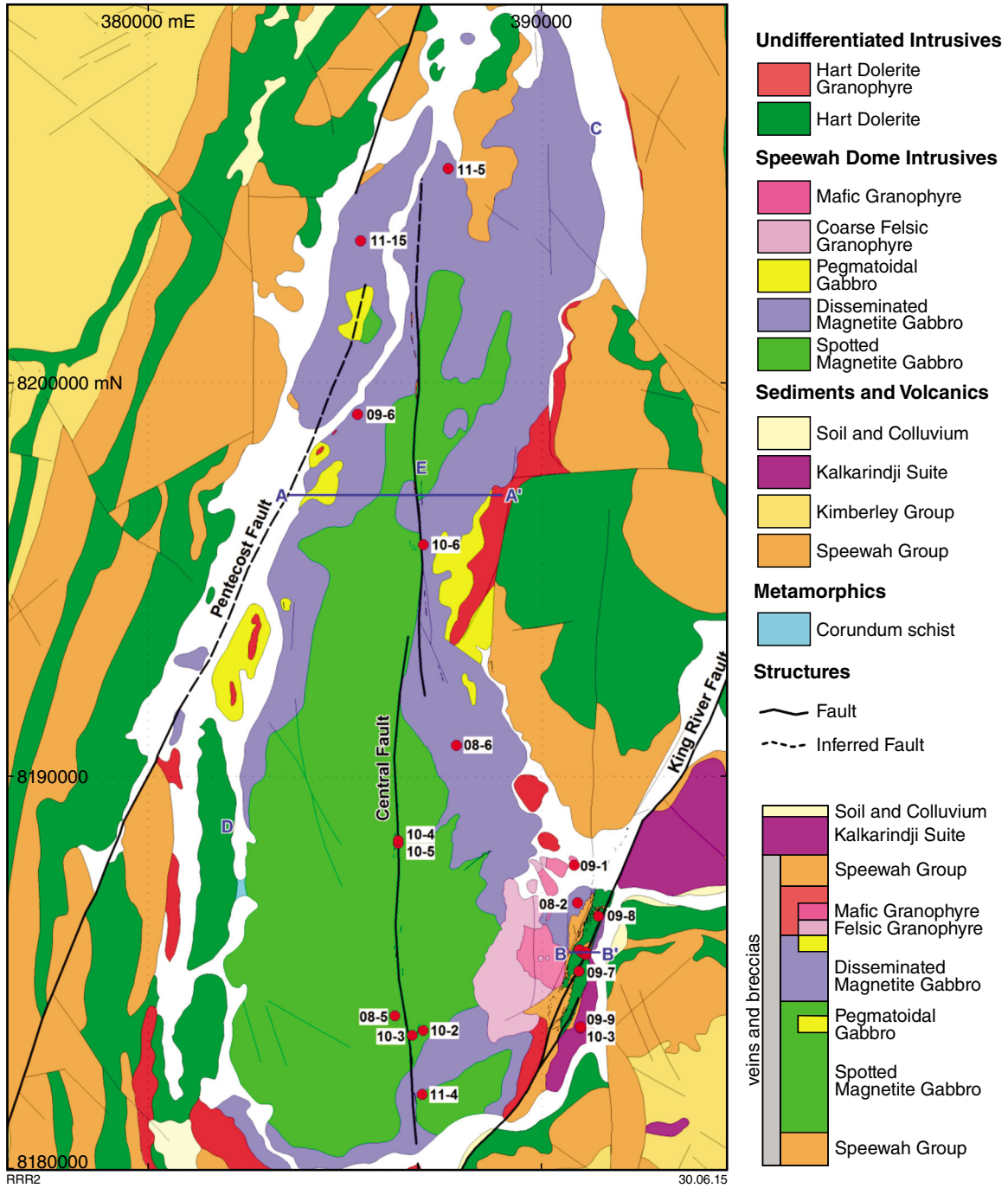


Figure 2. Geology of the Speewah Dome area

have influenced the crystallization of vanadiferous magnetite and the formation of a PGE reef in the lower parts of the unit. Ongoing studies will focus on the relationship between the lithospheric contribution and metal endowment in the Hart Dolerite from the Speewah Dome, with the idea to establish the significance of the disseminated magnetite gabbro.

References

- Eupene, GS 1970, Observations on the petrology of the igneous rocks, Speewah Valley, Western Australia: Geological Survey of Western Australia, Open File Report A060461 (unpublished).
- Sheppard, S, Page, RW, Griffin, TJ, Rasmussen, B, Fletcher, IR, Tyler, IM, Kirkland, CL, Wingate, MTD, Hollis, J and Thorne, AM 2012, Geochronological and isotopic constraints on the tectonic setting of the c. 1800 Ma Hart Dolerite and the Kimberley and Speewah Basins, northern Western Australia: Geological Survey of Western Australia, Record 2012/7, 28p.
- Thorne, AM, Sheppard, S and Tyler, IM 1999, Lissadell, Western Australia (2nd edition): Geological Survey of Western Australia, 1:250 000 Geological Series Explanatory Notes, 68p.

Characterization and timing of events in the richly mineralized Speewah area of the East Kimberley, Western Australia: Palaeoproterozoic sedimentation, intrusion of the Hart Dolerite and fault-hosted alteration and vein systems

by

RR Ramsay¹, A Eves², MTD Wingate, M Fiorentini², G Batt³, S Denyszyn², and K Rogers³

Establishing field relationships between rock-types and precise dating provides a useful approach for identifying the tectonic setting and timing of mineralising events. The Speewah area in the East Kimberley covers a 20 km diameter regional anticline centred around 127.92° E and 16.36° S on the 1:250K Lissadell sheet (Fig. 1; (Thorne et al., 1999). Outcrop in the outer part of the anticline is dominated by shallow-water, siliciclastic sediments of the Speewah Group. Regionally, a volcanoclastic horizon in the Valentine Siltstone contains zircons with a SHRIMP ²⁰⁷Pb/²⁰⁶Pb age of 1834 ± 3 Ma (Page and Sun, 1994). The Speewah Group in the Speewah Basin is then intruded by predominantly mafic and lesser felsic granophyre sills of the Hart Dolerite that outcrop in the core of the anticline (Fig. 1). The dolerite is dated at 1790 ± 4 Ma (Page and Sun, 1994) and locally host large-scale deposits of V-Ti-magnetite and a reef with PGE and Au anomalism. Cutting the Speewah Group and Hart Dolerite are large NE and N-trending faults. In the study area, the faults can be brecciated and veined with quartz, carbonate, K-feldspar, fluorite and barite showing textures typical of high-level epithermal systems. The adjacent wall-rocks can also be replaced with K-feldspar, carbonate and quartz. Then in places, all the rocks are unconformably overlain by outliers of the 522 Ma basalts of the Kalkarindji large igneous province (Glass and Phillips, 2006).

East of the Speewah study area, the Speewah Group unconformably overlies crystalline rocks which record two major tectonothermal events. The older 1870–1850 Ma Hooper Orogeny is widely represented in crystalline rocks around the margin of the Kimberley region (Hassan, 2004). In contrast, the younger 1835–1805 Ma Halls Creek Orogeny is localised along the eastern margin of the region and reflects the suturing of the Kimberley into the North Australian Craton (Blake et al., 2000). To the west of the study area, the Speewah Group is unconformably overlain

by sediments of the Kimberley Basin from which mafic rocks of the Carson Volcanics are correlated with the Hart Dolerite as a large igneous province (Pirajno and Hoatson, 2012).

In the study area, detrital zircons from the Tunganary Formation and Lansdowne Arkose which underlie and overlie the Valentine Siltstone were SHRIMP dated. In the Tunganary Formation, analyses with discordance <5%, have a range of ²⁰⁷Pb/²⁰⁶Pb-ages from c. 2520 to 1803 Ma but with a dominant population at c. 1858 Ma, a smaller population at c. 1813 Ma and a youngest age of 1803 ± 12 Ma (Martin, 2011; Motsoela, 2012). In the Lansdowne, zircons with <5% discordance report ²⁰⁷Pb/²⁰⁶Pb-ages from about 2552–1836 Ma, but with significant populations at 2533, 2470 and 1861 Ma (Martin, 2011; Motsoela, 2012). The results indicated that prior to the volcanoclastic event in the Valentine Siltstone, the Speewah Basin received detritus with zircons that crystallised during the later part of the Halls Creek Orogeny. The younger ages suggest the maximum depositional age is perhaps around c. 1803 Ma or at least more robustly less than c. 1813 Ma. Significantly, at least in the eastern portion of the Speewah Basin, the ages indicate deposition in a post orogenic setting on the North Australian Craton. However, after the volcanoclastic event, it appears that the sediment source contained only detritus with zircons from the Hooper Orogeny.

After deposition the Speewah Group was intruded in the study area at the level of the Valentine Siltstone by a 400 m thick, multiphase mafic and felsic granophyre sill of Hart Dolerite. Amongst the mafic phases which have sharp, thermally eroded contacts, one event has a significant amount of early crystallizing V-Ti-magnetite and a 'reef' with strong PGE and Au anomalism. SHRIMP ages for zircons from the granophyres and baddeleyite from the carbonate-replaced dolerite with interpreted magmatic origins yield ages c. 1799 Ma (Alvin, 1998; Martin, 2011). TIMS dating of the baddeleyite from two mafic phases produced ²⁰⁷Pb/²⁰⁶Pb dates within error at about 1794 Ma and confirms the V-Ti-magnetite bearing intrusive is part of the Hart Dolerite (Motsoela, 2012).

1: Trident Capital Ltd, Perth, Western Australia; 2: Centre for Exploration Targeting, School of Earth and Environment, ARC Centre of Excellence for Core to Crust Fluid Systems, University of Western Australia, Australia; 3: King River Copper Ltd, Perth, Western Australia.

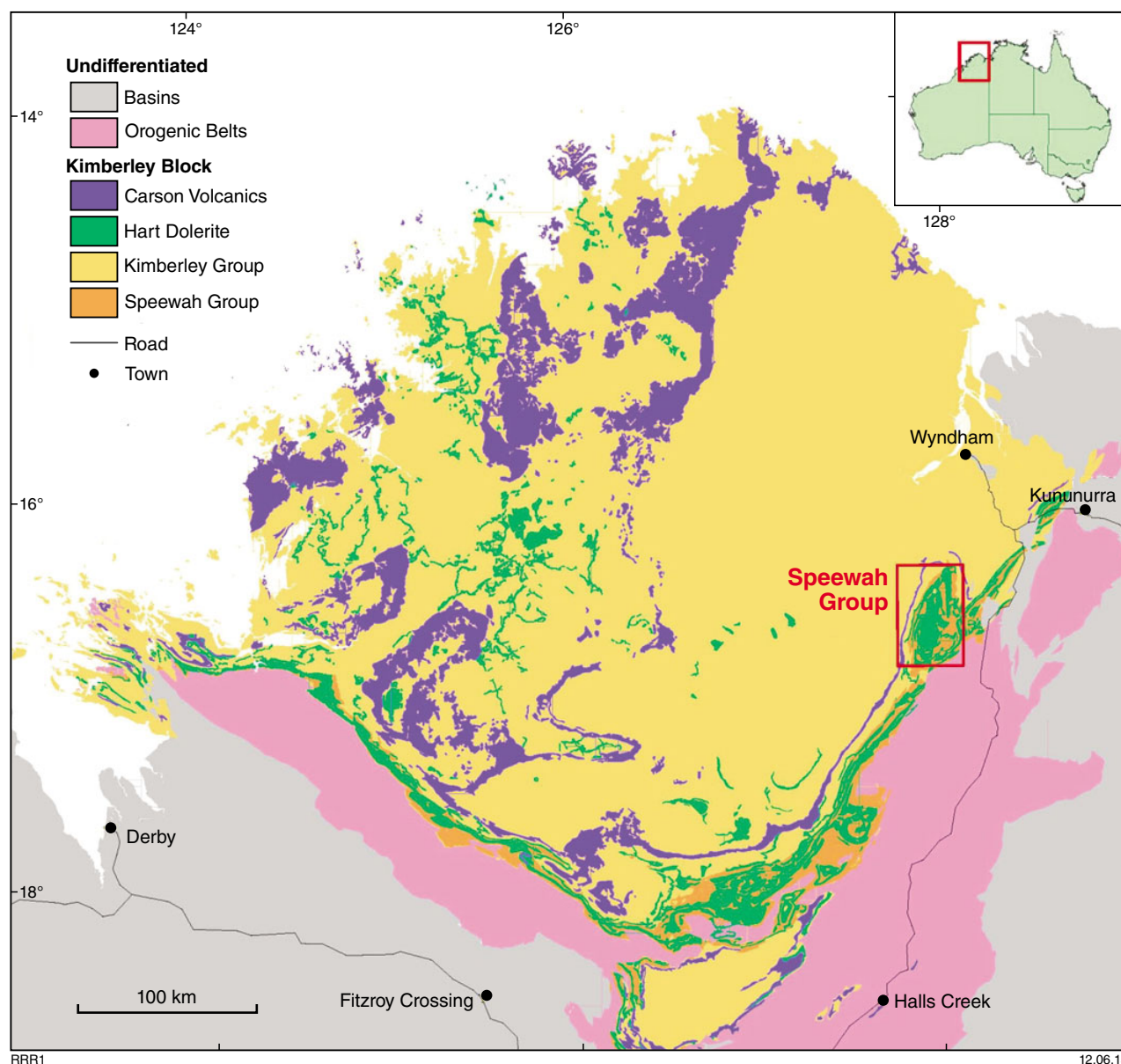


Figure 3. Location of the Speewah Dome within the Kimberley region

In the study area the fault-hosted breccias and epithermal-textured veins show cross-cutting relationships that indicate K-feldspar and carbonate alteration is early stage, while fluorite is later and barite is latest stage. K-Ar and Ar-Ar ages from K-feldspar show a spread of ages from 1050 to 325 Ma (Martin, 2011; Hales, 2014). The most common ages from c. 450–325 Ma indicate that a period associated with the development of the Canning and Bonaparte Basins surrounding the Kimberley region is reflected in crystallization ages along the regional faults in the Speewah area. Further work is required to determine whether the younger K-feldspar ages are co-incident with the large-scale deposition of the fluorite veins which have isotopic signatures suggesting a similar origin to the 325 Ma Mississippi Valley-style Pb–Zn deposits in the basins surrounding the Kimberley region (Czuppon et al., 2014).

In summary, detailed mapping and systematic age-dating in the Speewah area of the East Kimberley is more precisely establishing the timing and setting of geological events. Zircons from the Speewah Group have yielded new SHRIMP ages significantly younger than 1834 Ma and potentially as young as 1803 ± 12 Ma. This indicates that at least parts of the Speewah Basin were forming after the Kimberley region was incorporated into the North Australian Craton. Baddeleyite from the Hart Dolerite has also yielded a precise TIMS age c. 1794 ± 1 Ma which reduces the interval between sedimentation and intrusion. This reduced interval perhaps suggests that the extensional events which allowed sedimentation in the Speewah Basin were generated by a plume associated with the Hart Dolerite magmatism. In addition, K-Ar and Ar-Ar results from K-feldspar alteration, breccia and vein systems hosted by the major regional faults yield ages

from 1050 to 325 Ma. These indicate more localised and recent crystallization events along structures that have been episodically active as intracratonic features since the time of cratonization at c. 1840 Ma.

References

- Alvin, MP 1998, Carbonatite-related epithermal fluorite mineralisation at Speewah, Kimberley Region, with studies of possible analogues in the Pilbara and Gascoyne regions, Western Australia: The University of Western Australia, PhD thesis (unpublished), 416p.
- Blake, DH, Tyler, IM and Page, RW 2000, Regional Geology of the Halls Creek Orogen, *in* Geology and economic potential of the Palaeoproterozoic layered mafic-ultramafic intrusions in the East Kimberley, Western Australia *edited by* DM Hoatson and DH Blake: Australian Geological Survey Organisation, Bulletin 246, p. 35–62.
- Czuppon, G, Ramsay, RR, Özgenc, I, Demény, A, Gwalani, LG, Rogers, K, Eves, A, Papp, L, Palcsu, L, Berkesi, M and Downes, PJ 2014, Stable (H, O, C) and noble-gas (He and Ar) isotopic compositions from calcite and fluorite in the Speewah Dome, Kimberley Region, Western Australia: implications for the conditions of crystallization and evidence for the influence of crustal-mantle fluid mixing: *Mineralogy and Petrology*, v. 108, no. 6, p. 759–775.
- Glass, LM and Phillips, D 2006, The Kalkarindji continental flood basalt province: a new Cambrian large igneous province in Australia with possible links to faunal extinctions: *Geology*, v. 34, no. 6, p. 461–464, doi:10.1130/G22122.1.
- Hales, BJS 2014, ³⁹Ar–⁴⁰Ar study of potassium feldspar-rich rocks of the Speewah Dome, East Kimberley region, Western Australia: The University of Western Australia, B.Sc.(Honours) thesis (unpublished).
- Hassan, LY 2004, Mineral occurrences and exploration potential of the west Kimberley: Geological Survey of Western Australia, Report 88, 88p.
- Martin, S 2011, Geochronological analysis of the Speewah Dome and its implications on the geological evolution of the East Kimberley Province, Western Australia: University of Western Australia, MSc thesis (unpublished).
- Motsoela, G 2012, Applications of SHRIMP and TIMS dating in assessing the geological history of the Speewah Basin, Kimberley Region, Western Australia: The University of Western Australia, MSc thesis (unpublished).
- Page, RW and Sun, S-S 1994, Evolution of the Kimberley Region, W.A. and adjacent Proterozoic inliers — new geochronological constraints: Geological Society of Australia; Geoscience Australia — 1994 and Beyond, Abstracts v. 37, p. 332–333.
- Pirajno, F and Hoatson, DM 2012, A review of Australia's Large Igneous Provinces and associated mineral systems: Implications for mantle dynamics through geological time: *Ore Geology Reviews*, v. 48, p. 2–54.
- Thorne, AM, Sheppard, S and Tyler, IM 1999, Lissadell, Western Australia (2nd edition): Geological Survey of Western Australia, 1:250 000 Geological Series Explanatory Notes, 68p.

The deep structure of the Kimberley from magnetotelluric (MT) data

by

J Spratt¹, MC Dentith², S Evans³, A Aitken², M Lindsay², JA Hollis, IM Tyler, A Joly², J Shragge⁴

A magnetotelluric (MT) survey, a deep penetrating electromagnetic geophysical method, has been completed in the Kimberley region in northern Western Australia (Spratt et al., 2014; Fig.1). The survey was funded by the Kimberley Science and Conservation Strategy and administered by the Geological Survey of Western Australia. The general aim of the survey was to identify and map major structures in the deep crust and upper mantle. The principal reason for the survey was to address a major information gap regarding the concealed basement of the Kimberley Craton, and the geometry of the major tectonic structures within the Craton and the adjacent King Leopold Orogen (KLO) and Halls Creek Orogen (HCO). Information on the geometry of these structures is limited due to a cover of younger rocks.

Broadband and long period MT data, as well as time-domain electromagnetic soundings, were acquired at 155 locations (Fig. 1). Data of excellent quality were acquired at 127 of the 155 sites. Where possible the data were analyzed for static shift by comparing results of time-domain electromagnetic effects at the highest frequencies. Frequency-dependent pseudosections, induction vectors and phase tensors have been analyzed to determine the dimensionality, distortion, and geoelectric-strike direction of the data using the method of Caldwell et al. (2004).

The WinGlinkTM interpretation software package was used to generate two dimensional models along four main regional profiles and four smaller cross profiles. Each inversion included data in the period range of 0.004 to 1000 s, was initiated with a homogeneous half space of 500 ohm-m, and ran for a minimum of 200 iterations. The phases were set with a 5% error floor, and where applicable, the Tipper error was set to an absolute value of 0.02. Initially the apparent resistivities were set with an error floor of 20%, and subsequently reduced to 10%

to assess and account for static shift effects. A uniform grid Laplacian operator and tau value of 3 were applied. Models were generated using different components of the data at differing strike angles in order to assess the change in the observed conductivity structure and resolve features that are robust in the data. The preferred model for each profile shows structure that appears to be robust between various inversions and obtained the lowest overall RMS value. Extensive feature testing was undertaken to determine the reliability and robustness of the imaged structures.

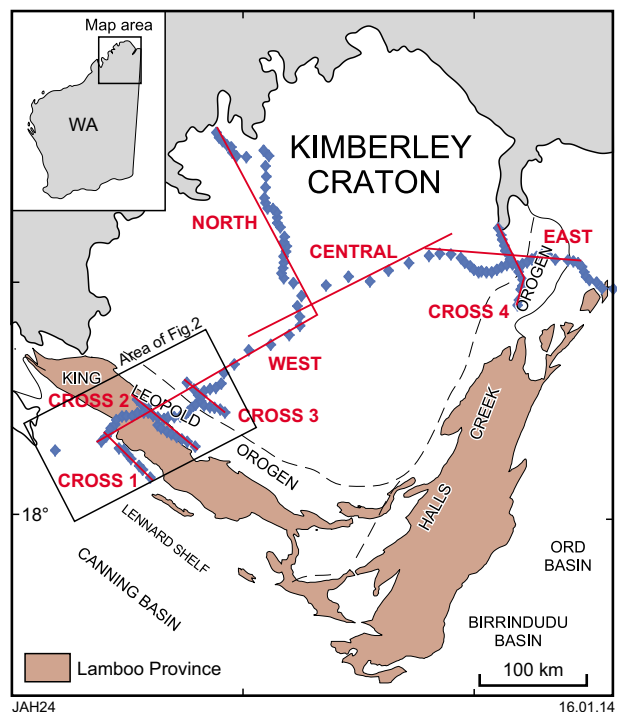


Figure 1. Map of the main geological elements of the Kimberley region in Western Australia. The blue symbols mark the location of the MT stations. The red solid lines show the location of 2D model profiles.

1 Consultant, Wakefield, Quebec, Canada

2 Centre for Exploration Targeting, The University of Western Australia

3 Moombariga Geoscience

4 Centre for Energy Geoscience, The University of Western Australia

The results of 2D modelling of the MT dataset are presented in Spratt et al. (2014). The Kimberley Basin sedimentary and volcanic sequences are revealed as a thin near-surface conductive unit (~200 to 500 ohm-m) with a maximum thickness of 5 km. The upper-to-middle crust is predominantly highly resistive (>10,000 ohm-m) to depths of 15–40 km, consistent with the presence of granitic Archean rocks.

The upper to middle crust is cut by several less resistive, steeply-dipping structures, interpreted as faults. It is unclear if any of these structures penetrate to the mantle. Several upper crustal features are identified that correlate with the location of fractures, or boundaries between crustal terrains that are either mapped at the surface or inferred from gravity and aeromagnetic data (Gunn and Meixner, 1998). Generally, the lower crust is conductive and the depth to its base is in reasonable agreement with seismic Moho depth estimates of 38 – 45 km. A northwest-dipping resistive feature imaged along the eastern margin of the Kimberley Basin to depths of at least 60–100 km is

consistent with the current tectonic models for the survey area that describe the accretion of a crustal fragment at >1900 Ma during west-directed subduction followed by generation of post-collisional granites.

Areas of anomalously low resistivity in the lower crust occur in several locations in the 2D conductivity models. These lie adjacent (to the northwest) of inferred crustal block boundaries, which is suggestive of a tectonic origin. An alternative explanation is large intrusions, some of the responses correlating with subcircular gravity anomalies. Preliminary 3D conductivity models were generated after 95 iterations using the ModEM 3D inversion code (Egbert and Kelbert, 2012) and included data from the full impedance tensor at 19 periods. Data from the KLO are shown in Figure 2. These results are consistent with the 2D modelling but suggest there may be greater continuity of the conductive parts of the lower crust and hence that geological significance should be assigned to these features only with caution (Fig.3).

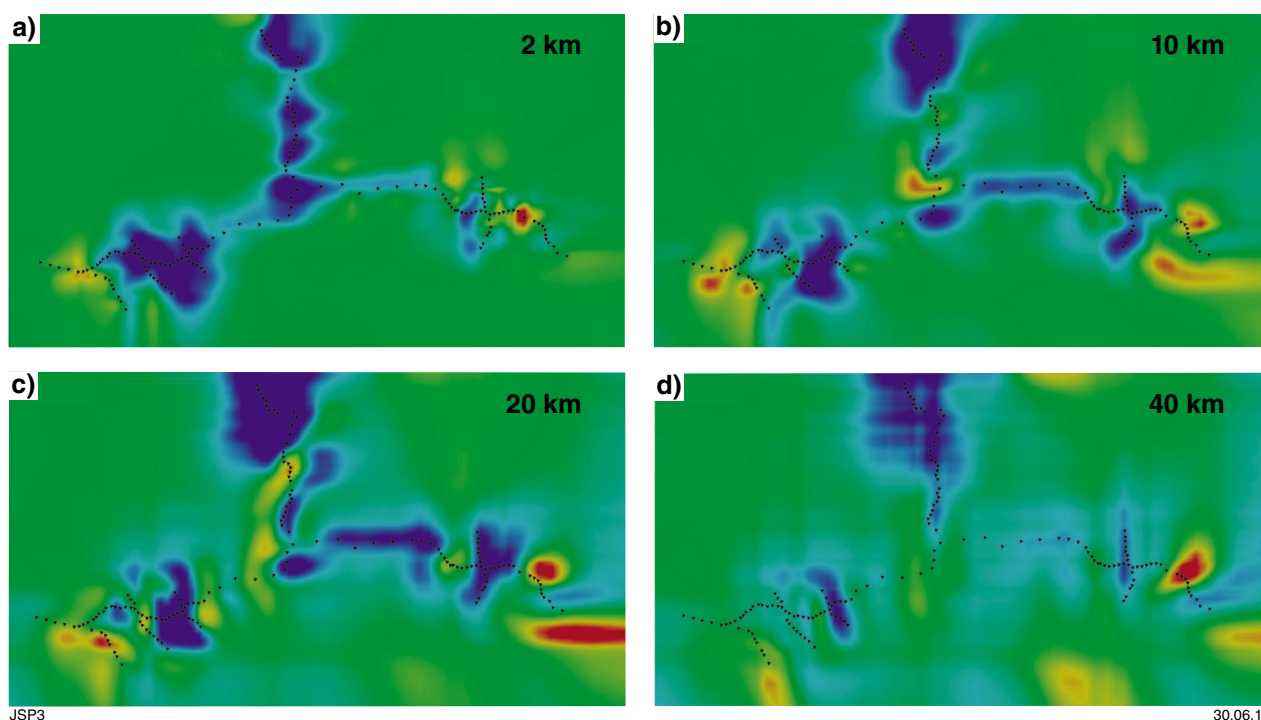


Figure 2. Slices of the 3D inversion results from the KLO for depths of 2, 10, 20, and 40 km. Warm colors represent conductive units and cool colors identify resistors. See Figure 1 for location.

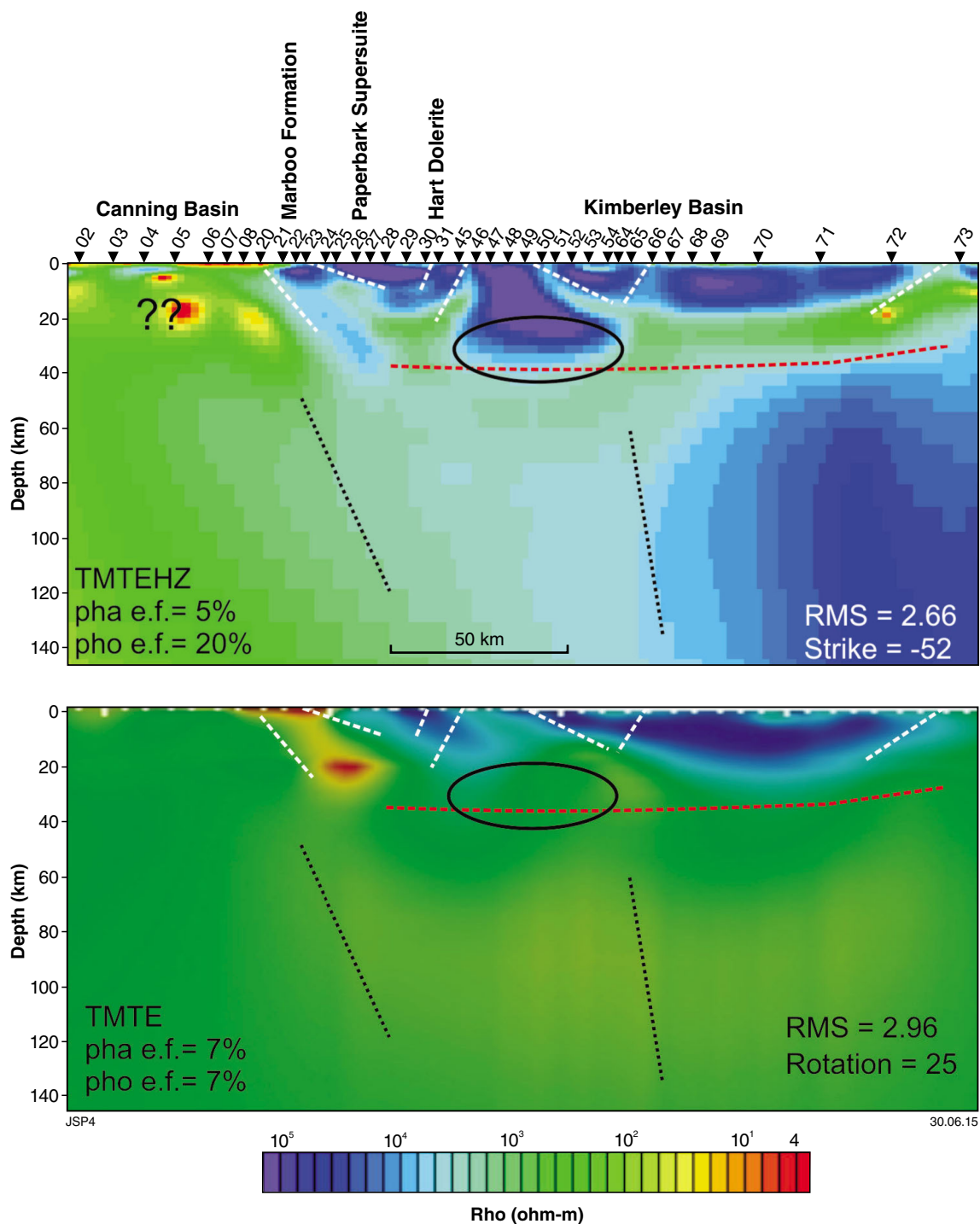


Figure 3. Comparison of the 2D (top) and 3D (bottom) results for the KLO. The white dashed lines mark known faults or terrain boundaries mapped at the surface. The red dashed line marks the estimated depth to the base of the crust. See Figure 1 for location. The 2D profile is the “WEST” traverse.

References

Caldwell, TG, Bibby, HM and Brown, C 2004, The magnetotelluric phase tensor: *Geophysical Journal International*, v. 158, p. 457–469.

Egbert, GD and Kelbert, A 2012, Computational recipes for electromagnetic inverse problems: *Geophysical Journal International*, v. 189, p. 251–267.

Gunn, PJ and Meixner, AJ 1998, The nature of the basement to the Kimberley Block, northwestern Australia: *Exploration Geophysics*, v. 29, p. 506–511.

Spratt, J, Dentith, MC, Evans, S, Aitken, ARA, Lindsay, M, Hollis, JA, Tyler, IM, Joly, A and Shragge, J 2014, A magnetotelluric survey across the Kimberley Craton, northern Western Australia: *Geological Survey of Western Australia, Report 136*, 92p

3D crustal structure of the Kimberley region from joint magnetic/gravity inversion

by

ARA Aitken^{1*}, MD Lindsay¹, L Griss², and C Altinay²

Introduction

Understanding 3D crustal structure is essential to develop a better understanding of the tectonic architecture of regions, and its influence on resource prospectivity, including mineral resources. Fully featured, high resolution models are optimal, however constructing such models is time-consuming and fraught with uncertainty (Lindsay et al., 2012; Wellmann and Regenauer-Lieb, 2012; Lindsay et al., 2013). These problems are amplified considerably at larger scales, especially where geological knowledge is limited. At the opposite end of the scale, geophysical inversions for single properties can be applied relatively rapidly, have repeatable results, and often possess low-variability between models. Unfortunately these tend not to represent crustal structure very well.

The advent of 3D joint magnetic and gravity inversion methods potentially allows a useful approach to understanding regional crustal structure. Of course, both are scalar-fields and are also non-unique, so we cannot expect to correctly define all features from these regional geophysical data. Here we apply this new method to the Kimberley region, with the intent of developing the capability to map the first-order structural and lithological features of this region to gain an impression of their 3D architecture.

Method

Data and model setup

We define the target region for the joint inversion in MGA50 coordinates, from easting 616000 to easting 1128000, from northing 7848000 to northing 8384000

and from the Earth's surface (0) to 40 km depth. Model resolution is 2 km in x and y and 1 km in z. The reference density and susceptibility model is zero.

It is important to recognise that with a zero-reference model, the results cannot be expected to resolve horizontally layered structure to which neither gravity nor magnetic data are very sensitive. Thus the results will represent the deviation from any layered structure present. For example, imagine an extensive flat-lying magnetised mafic sill that is upturned at its edges due to thrusting. In this model, the upturned edges will be detected, but the flat-lying segment will not, except as a regional difference to areas lacking the sill.

Prior to modelling we reduce the gravity data to the terrain-corrected Bouguer anomaly and upward continue the dataset by 4 km to reduce the degree of short-wavelength heterogeneity (Fig. 1a). For the magnetic data we apply differential reduction to pole, and upward continue to 6 km (Fig. 1b). The difference in continuation elevations accounts for the more chaotic nature of the magnetic data and provides a closer match in spectral content.

Finally, the likelihood of intense magnetisation diminishes significantly with depth into the Earth. Curie-depth in the Kimberley region is probably quite deep, with recent analyses returning a base-of-magnetization at about 45 km (Chopping and Kennett, 2013). To control our magnetization distribution we apply a depth weighting to changes in the magnetic susceptibility according to the formula (Altinay et al., 2013):

$$k = \left(\frac{z_0 - z}{l_z} \right)^{\frac{\beta}{2}}$$

In our case we set l_z and Z_0 at 40 km depth, i.e. susceptibility is zero at 40 km depth by definition, and $\beta = 4$, which controls the rate of decay. The maximum weight is at the surface, with values of 75, 50, and 25%, at 5.5, 12, and 20 km respectively.

¹ Centre for Exploration Targeting, the University of Western Australia, Crawley, WA

² School of Earth Sciences, The University of Queensland, St Lucia, Qld

* Corresponding author: alan.aitken@uwa.edu.au

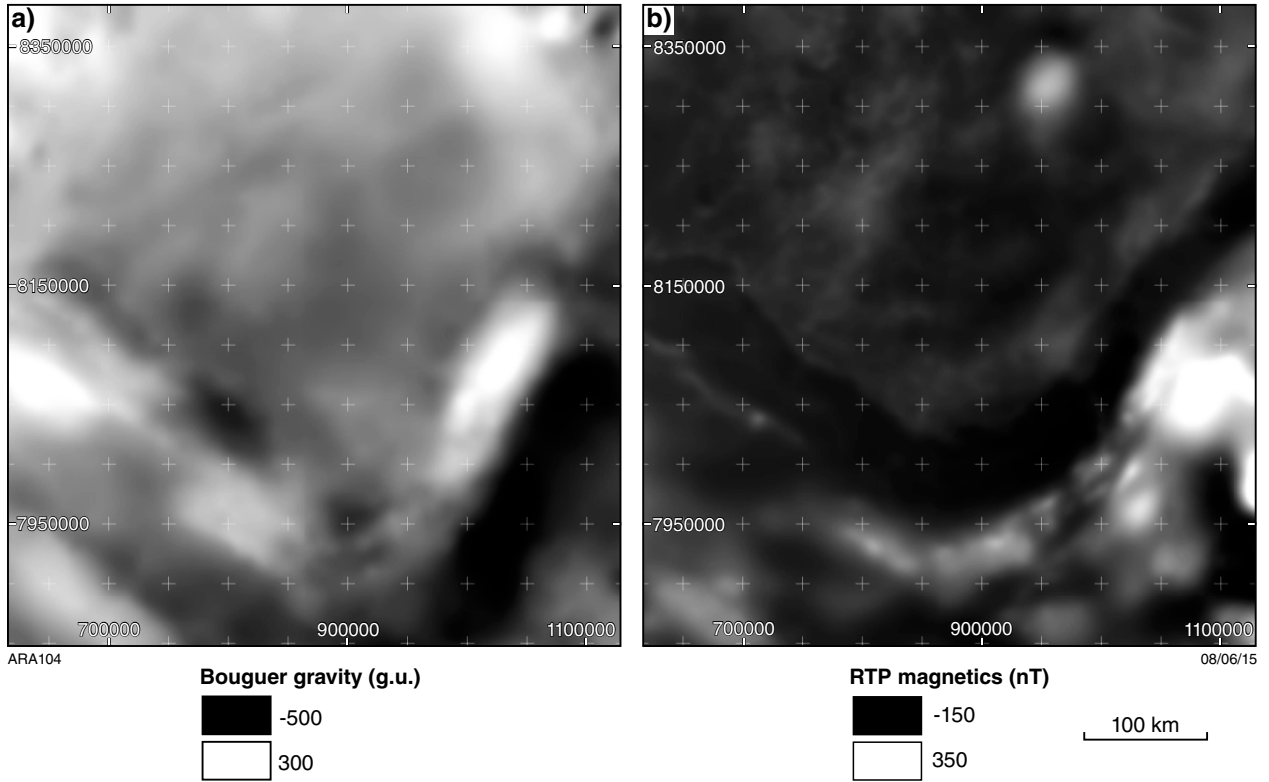


Figure 1. Bouguer Gravity Anomaly (left) and dRTP Magnetic Anomaly (right) data for the Kimberley Region. The former are upward continued by 4 km, the latter 6 km. Both colour stretches are linear between the labelled values, so as to provide the truest possible impression of true anomaly magnitude.

Approach to solution

The *escript* downunder modelling environment

To conduct this investigation we have used the *escript* modelling environment, specifically the *downunder* module that encompasses geophysical inversion tools (Gross et al., 2007; Altinay et al., 2013). The *escript* downunder module poses the inversion problem as a finite element problem, in which the Earth's density and magnetization fields are realised as piecewise define partial differential equations. The governing cost-function that we attempt to minimize is, in very simplified form:

$$J\chi = \mu_g * J_{dg} + \mu_m * J_{dm} + JR$$

This equation has three components, gravity data misfit (J_{dg}), magnetic data misfit (J_{dm}) and regularization (JR). μ_g and μ_m are trade-off parameters that define the relative importance of the three components of the cost function. The regularization term is itself composed of three terms:

$$\begin{aligned} JR = & w_{0g} * (\rho - \rho_0)^2 + w_{1g} * \Delta(\rho - \rho_0) \\ & + w * (\kappa - \kappa_0)^2 + w_{1m} * \Delta(\kappa - \kappa_0) \\ & + w_c * \chi_{cg} \end{aligned}$$

The first term describes the density regularization, which has two parts. Essentially these parts allow the regularization to take the form of minimizing change from the reference model, or to take the form of minimizing the gradients in the derived density distribution, or some combination of these. The weights w_{0g} and w_{1g} control the proportion of each of these sub-terms. The second term in the regularization function is identical in form to the first, although it controls magnetic susceptibility rather than density. The third and final term in the regularization term is the cross-gradient operator, which controls the structural similarity between the density and susceptibility models. Essentially, if the normals to susceptibility and density isosurfaces are closely aligned, this term is minimised. The weighting term w_c controls how important this term is to the overall cost function.

Selecting the optimum parameters

It is clear from the structure of the cost function that we must specify a number of parameters that, along with the data and its influence on the model changes, will define the solution to the model. These are, in order of hierarchy, μ_g and μ_m , and then w_{0g} , w_{1g} , w_{0m} , w_{1m} , w_c . It is not obvious however what these parameters should be, and so we performed a systematic parameter search.

We first performed serial sweeps for μ_g and μ_m , with $w_{0g} = 0$, $w_{1g} = 0$, $w_{0m} = 1$, $w_{1m} = 1$ and $w_c = 0.1$. Due to slight non-linearity we repeat the initial sweep to check that results are not grossly different. It is also necessary to specify some criteria through which to select the "optimum" model response. In this case we seek the value with the best balance of the magnetic and gravity data terms in the cost function, with the proviso that the data-misfits are acceptable (Fig. 2).

From this procedure, the optimum values were $\mu_g = 10$ and $\mu_m = 5$. These values were carried forward into sweeps for w_{0g} , w_{0m} , and w_c . We leave w_{1g} and w_{1m} fixed as reference points for each data type. The optimum values for w_{0g} and w_{0m} were $1 \cdot 10^{-7}$ and $5 \cdot 10^{-7}$ respectively (Fig. 3). The sweep for w_c , performed last, had little influence on the overall fit to the data or the balance within the regularization term. Thus there is no quantitative reason to deviate from our original value of 0.1.

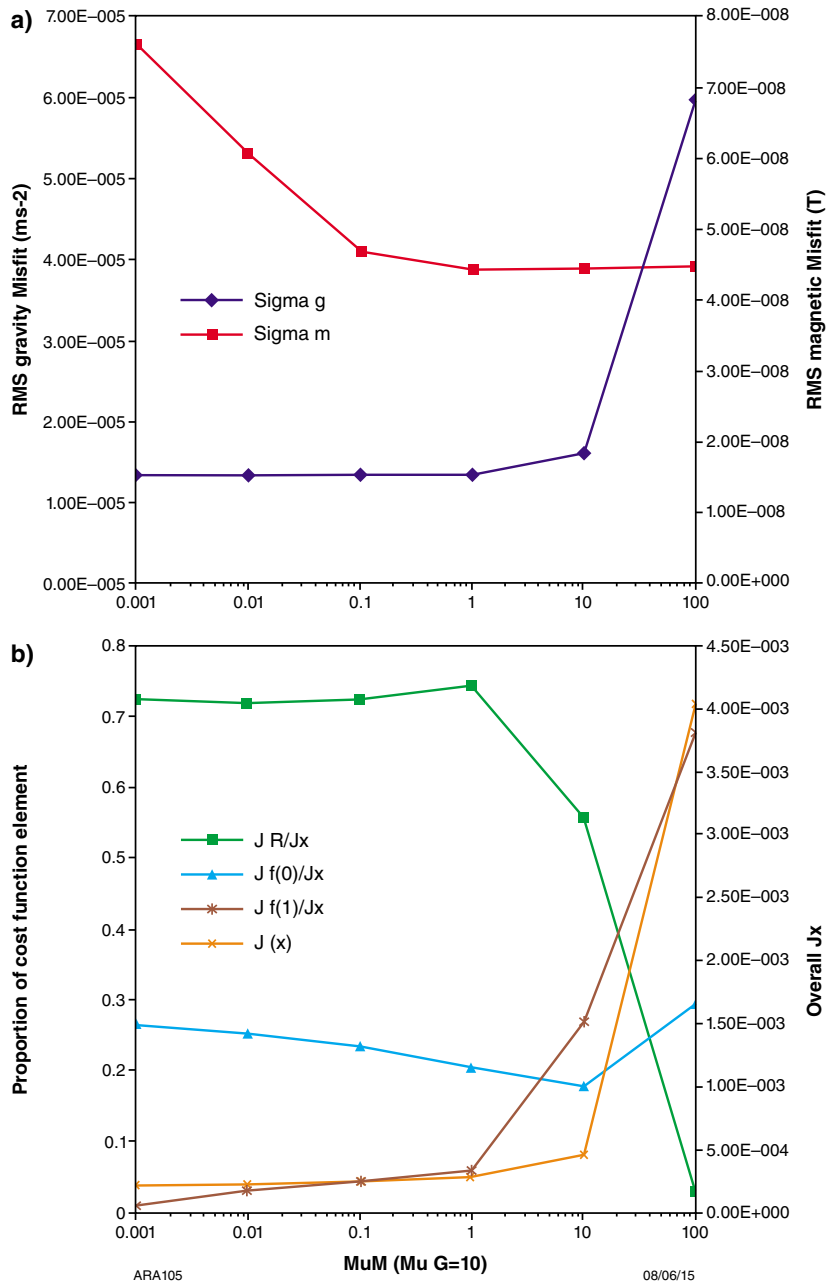


Figure 2. Sample analysis charts for the final μ_m sweep, with $\mu_g = 10$. The top chart shows the misfit reduction with increasing μ , with a final misfit of ~ 44 nT. Note that, except at very high μ , the gravity data misfit remains stable at c. 1.3 mGal. The bottom chart shows the relative magnitude of the components of the cost-function, as well as the magnitude of the overall cost function (J_x). Note that with increasing μ , the size of the magnetic data-fit component (maroon) increases, while the size of the gravity-fit component (cyan) decreases. The crossover is reached at $\mu \approx 5$.

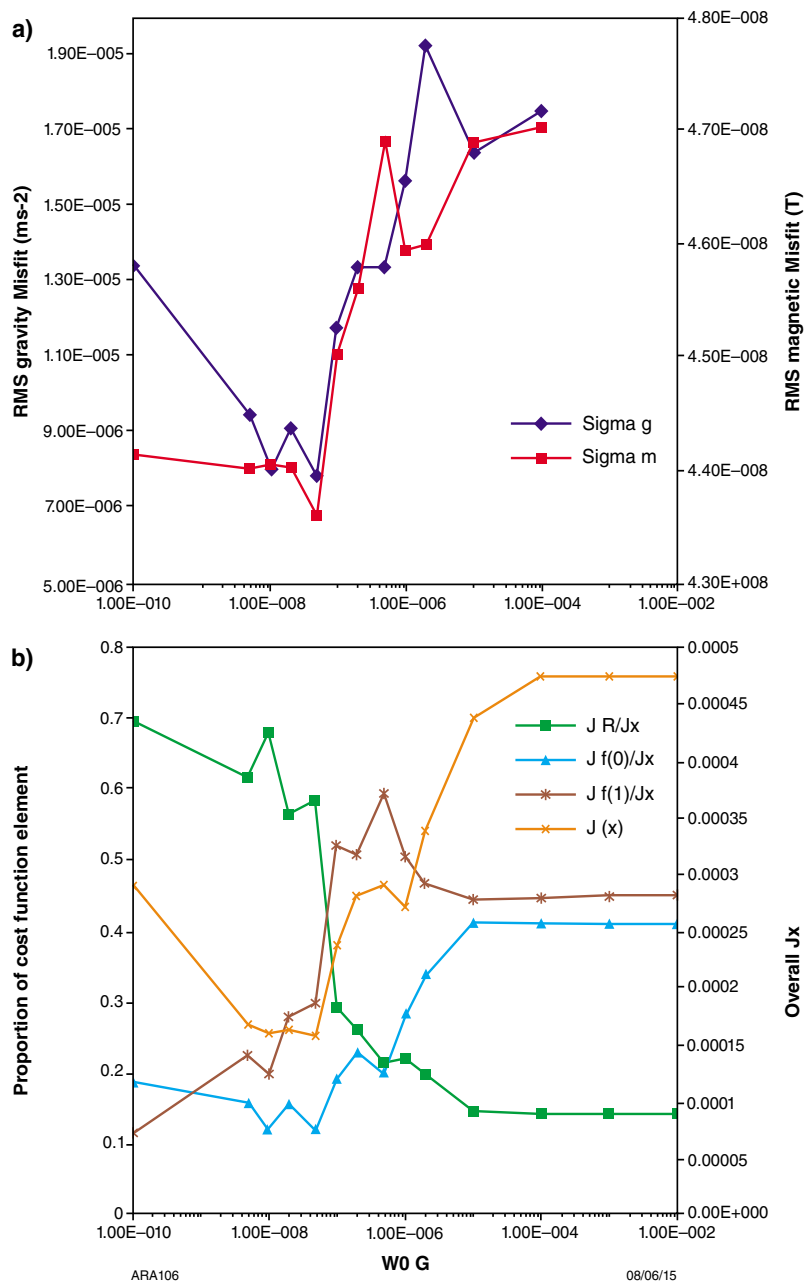


Figure 3. Sample analysis charts for the w_{og} sweep, with $w_{om} = 0$. The top chart shows the misfit reduction with increasing w_{og} . Note that the gravity and magnetic components evolve in parallel. The bottom chart shows the relative magnitude of the components of the cost-function, as well as the magnitude of the overall cost function (Jx). Note that a major threshold is reached at $w_{og} \approx 1 \cdot 10^{-7}$. With w_{og} above this value the gravity and magnetic data-fit components increase markedly relative to the regularization component, and the overall cost function magnitude increase significantly.

Results

The density and susceptibility results of the final selected model are shown in Figure 4. These images show the strong commonality of structural features in both property distributions for many parts of the model. Relative densities range from -45 to $+45 \text{ kgm}^{-3}$, while relative susceptibilities range from -0.0075 to $+0.0075 \text{ SI}$.

Critically, and importantly, we image the dip-direction of major structures, which is typically lacking, or inconsistently defined in single-property inversions. Dip angles likely represent a maximum limit due to the bias in the method, namely, we aim to minimize the gradients in the model result and also the divergence from the

reference model. These will typically be less with a steep structure than with a shallow structure. Despite this bias, we image several structures with moderate dips. This includes the boundaries between the East, West and Central Zones of the Halls Creek Orogen (Tyler et al., 1995) and the Kimberley Craton, as well as many smaller scale lithological boundaries.

Some apparent horizontal boundaries exist at approximately 5–10 km depth, where many magnetic features die out, and also at about 20 km depth (Fig. 4). It is likely that these apparent sub horizontal boundaries are a result of the depth weighting function, rather than being true boundaries.

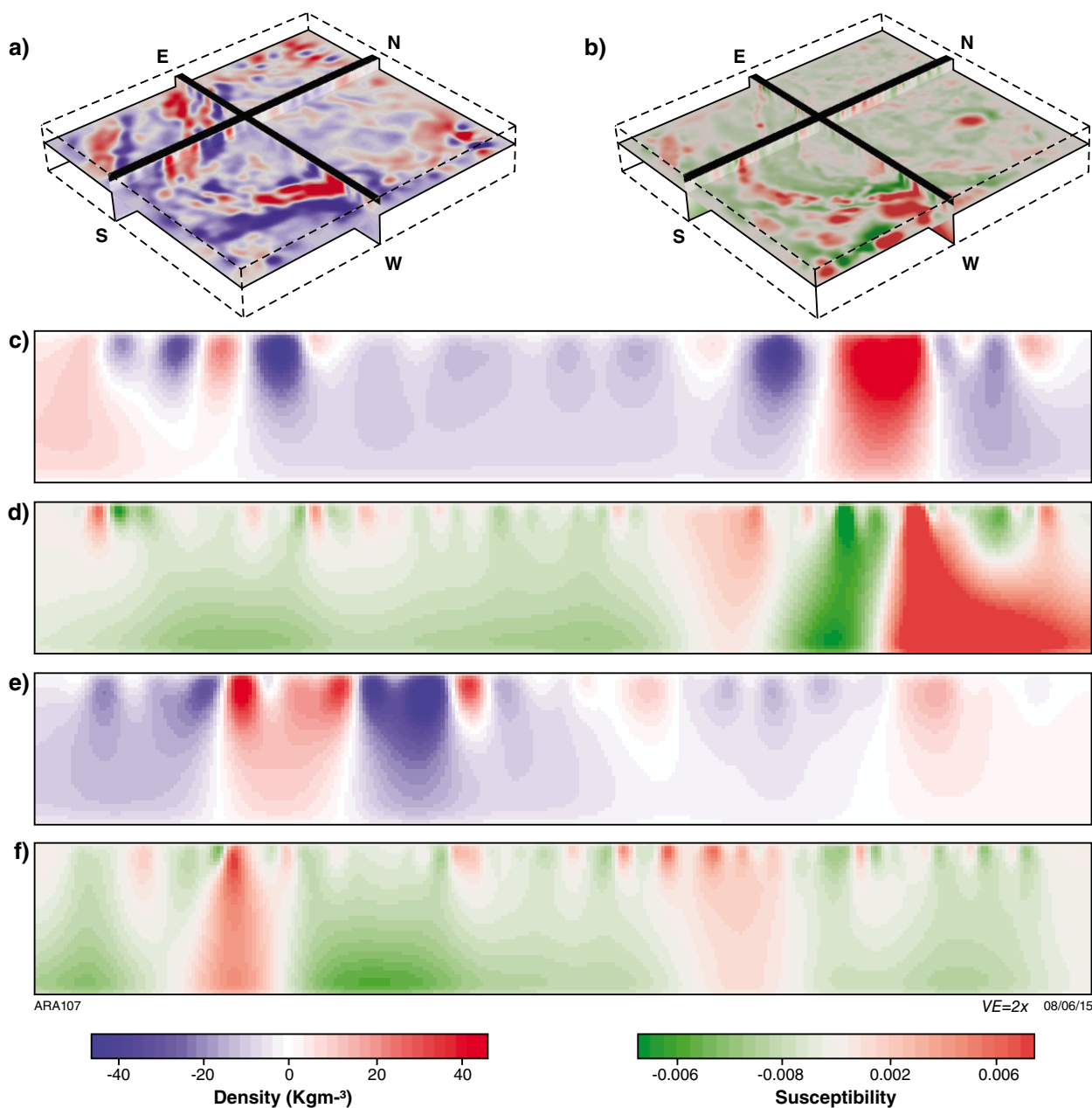


Figure 4. Representative results of the 3D inversion: a) and b) 3D perspective view of the results; c) and d) West to East section along northing 8100000; e) and f) South to North section along easting 800000. Vertical Exaggeration is 2x, depth of modelled sections is 40 km.

Discussion

The usefulness of this model can be qualitatively assessed by considering its ability to define the boundaries of lithological suites, and by proxy, the existence and characteristics of major structures. Comparing property isosurfaces with the plan-view extent of the major lithologies we find the following relationships. The Paperbark Supersuite is well defined by relative densities less than -10 kgm^{-3} and relative susceptibilities less than zero. This is mildly distinctive from the Kimberley Basin Basement, which possesses relative densities of approximately -5 kgm^{-3} and relative susceptibilities close to zero. In contrast the central zone of the Halls Creek Orogen, which is dominated by the Sally Downs Supersuite, is characterised by a highly bimodal susceptibility signature, with susceptibility less than 0.001 SI or greater than 0.005 SI, but characteristically dense, with relative densities of greater than 5 kgm^{-3} . The Eastern Zone basement is highly characteristic, with high relative susceptibility, greater than 0.003 SI, but low density, less than -10 kgm^{-3} . The Kimberley Basin itself is not defined, however, the Hart-Carson LIP is clearly identified with susceptibility greater than 0.001 SI and density greater than 0 kgm^{-3} .

These characteristic differences between the Kimberley Craton, the Paperbark Supersuite dominated Western Zone, the Sally Downs Supersuite dominated Central

Zone, and the Eastern Zone allow some inferences to be made regarding the crustal architecture of the Kimberley Region. The Kimberley Craton appears to be distinct from the Western Zone, with denser basement due to a relative lack of Paperbark Supersuite. This suggests that the influence of the Hooper Orogeny is much less beneath the Kimberley Basin, perhaps suggesting a retro-arc setting. The Lamboo Province is clearly delineated bending around from the East Kimberley to the West Kimberley, but to different extents for each zone. The Western Zone surrounds entirely the Kimberley Craton, whereas the Central Zone extends only to $\sim 750\,000 \text{ mE}$ (MGA94 zone 50) in the west Kimberley and to $8\,130\,000 \text{ mN}$ (MGA94 zone 50) in the East Kimberley. The distinctive magnetised basement of the Eastern Zone does not clearly extend beyond the apex of the bend (c. $950\,000 \text{ mE}$ - MGA94 zone 50). The crust in the South west of the region beneath the Canning Basin possesses different character to the Lamboo Province (Fig. 5)

In addition to lithological boundaries, the model also images the location and dip-direction of major crustal boundaries. In general, crustal structures dip towards the Kimberley Craton, with those on the west Kimberley predominantly dipping North, and those in the east Kimberley dipping west (Figs 6 and 7). These observations support the accretion of crustal domains onto the eastern margin of the Kimberley Craton.

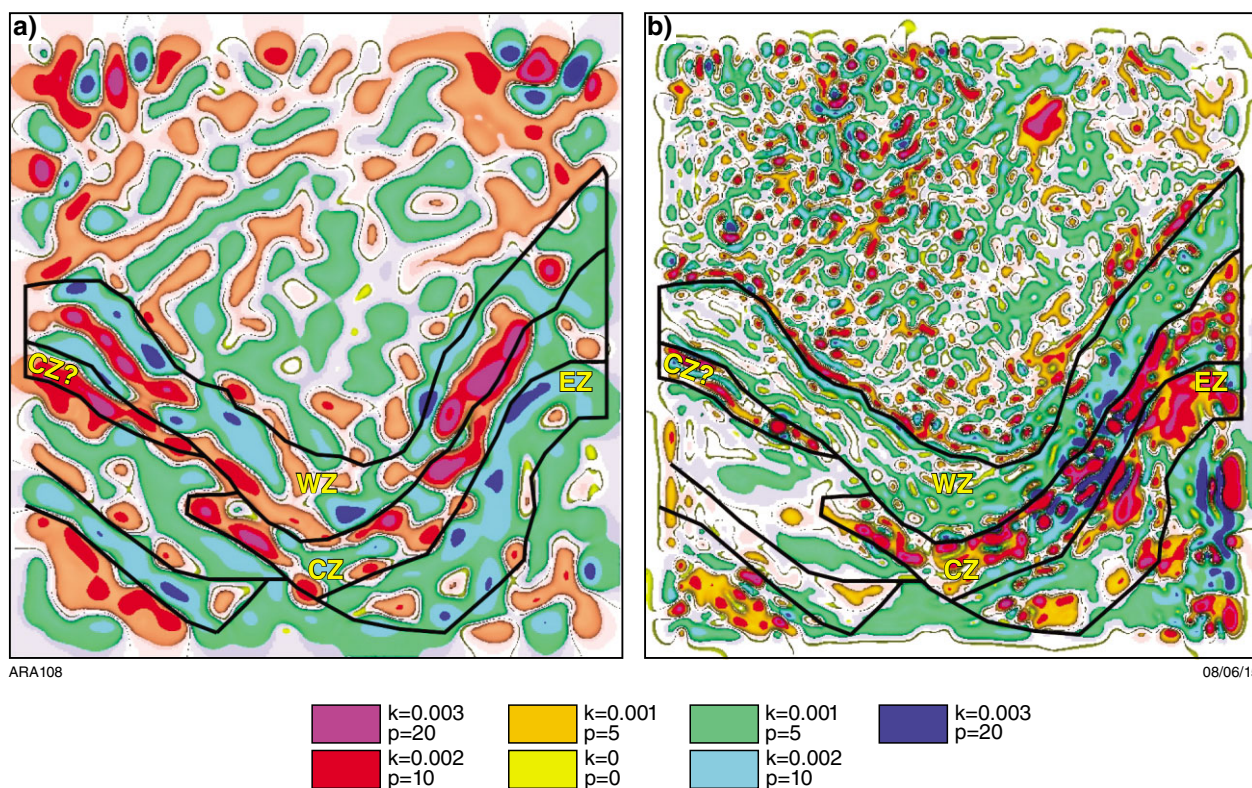


Figure 5. Plan view of the model results at c. 5 km depth: a) density model; b) magnetic susceptibility model. The interpreted boundaries show the major domain boundaries. WZ – Western Zone, CZ – Central Zone, EZ – Eastern Zone. Colours indicate isosurfaces.

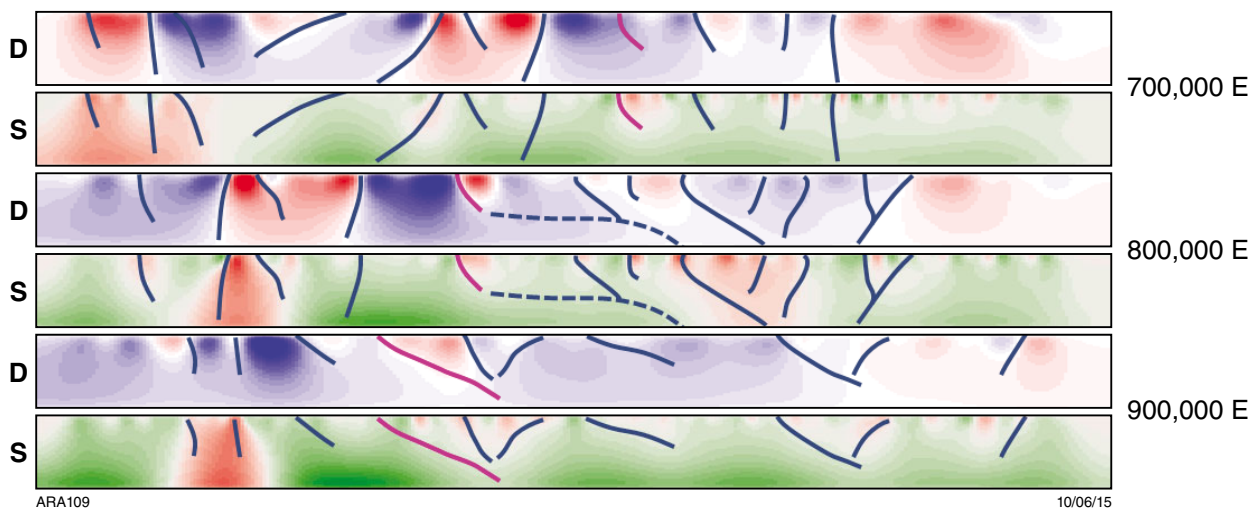


Figure 6. Interpreted south–north cross-sections through the west Kimberley region with no vertical exaggeration. The boundary of the Lamboo Province and Kimberley Basin is highlighted in magenta. Note that most major structures dip north at moderate angles. D – density, S – magnetic susceptibility. Distance along section is 536 km. Colour scale is the same as for Fig. 4.

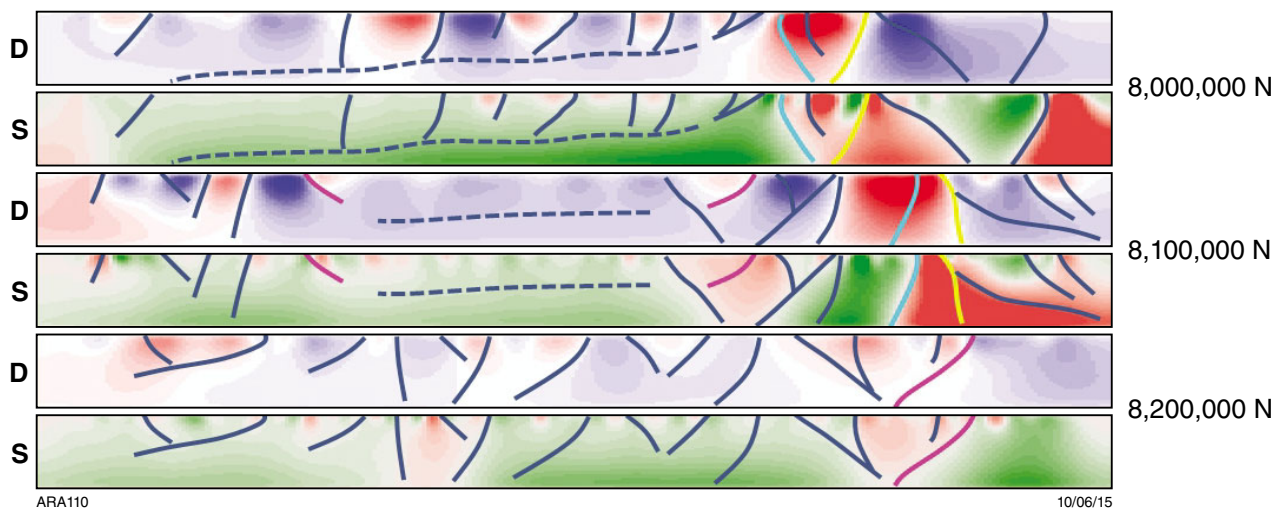


Figure 7. Interpreted west–east cross-sections through the east Kimberley region with no vertical exaggeration. The boundaries between the major zones of the orogeny are delineated in magenta (KC-WZ), cyan (WZ-CZ) and yellow (CZ-EZ). Note that most major structures dip west at moderate angles. Some potential large scale flat lying discontinuities are annotated, but these are not robust features of the model. Distance along section is 512 km. Colour scale is the same as for Fig. 4.

Conclusion

This work applied joint magnetic and gravity inversion to better understand the crustal structure of the Kimberley region with minimal a-priori information. The results should not be interpreted as an image of absolute structure, but rather the deviations from an undetectable “background” structure. Most commonly this is layered in form. Hence, the locations, dip-directions and density/susceptibility contrasts of major lithological boundaries can be defined. Often, and in this case, these will be sufficient to provide some revealing insights into the crustal structure of remote and poorly studied regions

Acknowledgements

This work was achieved through the support of the GSWA’s Exploration Incentive Scheme, funded by the Royalties for Regions Programme. High Performance Computing was supplied by iVEC, using Murdoch University (Epic) and Pawsey Centre (Magnus) Infrastructure.

References

- Altinay, C, Boros, V, Gross, L and Salehi, A 2013, esys.downunder: inversion with escript: The University of Queensland, St Lucia, Queensland, viewed 4 May 2015, 90p. <<http://shake200.esscc.uq.edu.au/esys13/nightly/inversion/inversion.pdf>>.
- Chopping, R and Kennett, BLN 2013, The Curie depth of Australia, and its uncertainty, *in* ASEG Extended Abstracts 2013: CSIRO Publishing; ASEG_PESA 2013 23rd International Geophysical Conference and Exhibition, Melbourne, Australia, 2013, p. 1–3.
- Gross, L, Bourgouin, L, Hale, AJ and Mühlhaus, HB 2007, Interface modelling in incompressible media using level sets in Escript: *Physics of the Earth and Planetary Interiors*, v. 163, no. 1-4, p. 23–34.
- Lindsay, MD, Ailleres, L, Jessell, MW, de Kemp, EA and Betts, PG 2012, Locating and quantifying geological uncertainty in three-dimensional models: Analysis of the Gippsland Basin, southeastern Australia: *Tectonophysics*, v. 546–547, p. 10–27.
- Lindsay, MD, Jessell, MW, Ailleres, L, Perrouty, S, de Kemp, EA and Betts, PG 2013, Geodiversity: Exploration of 3D geological model space: *Tectonophysics*, v. 594, p. 27–37.
- Tyler, IM, Griffin, TJ, Page, RW and Shaw, RD 1995, Are there terranes within the Lamboo Complex of the Halls Creek Orogen?, *in* Geological Survey of Western Australia Annual Review 1993–94: Geological Survey of Western Australia, Perth, Western Australia, p. 37–46.
- Wellmann, JF and Regenauer-Lieb, K 2012, Uncertainties have a meaning: information entropy as a quality measure for 3D geological models: *Tectonophysics*, v. 526–529, p. 207–216.

Lithospheric structure of the western Kimberley margin: implications for marginal basin development

by

K Czarnota^{1,2} and N White²

The stratigraphic record of sedimentary basins acts as a recorder of vertical motions from which changes in lithospheric thickness and density through time can be unravelled. The subsidence histories of most, but not all, basins can be elegantly explained by extension of the lithosphere followed by thermal rethickening of the lithospheric mantle to its pre-rift thickness (McKenzie, 1978; White, 1993). These two phases of basin formation are expressed in the stratigraphic record as syn-rift, fault controlled strata deposition followed by post-rift non-fault sediment deposition. Although this model underpins most basin analysis, it is unclear whether subsidence of rift basins developed over thick lithosphere follows the same trend (Crosby et al., 2010). Here, we examine the subsidence record of the Canning Basin of Western Australia positioned on the western margin of the Kimberley Craton. It can be divided into the, less than 300 km wide and less than 6 km thick, western Canning Basin, and the less than 150 km wide and approximately 15 km thick Fitzroy Trough and Gregory Sub-basin of the eastern Canning Basin.

Recent shear wave tomography models show the basin is situated over lithosphere greater than 180 km thick (Kennard et al., 1994; Kennett et al., 2013; Czarnota et al., 2014). This is confirmed for the eastern Canning Basin by the presence of 19–22 Ma diamond bearing lamproites intruded into the basin depocentre and along the north eastern margin (Evans et al., 2012). The entire subsidence history of the western Canning Basin is adequately explained by Ordovician rifting of approximately 120 km thick lithosphere followed by post-rift thermal subsidence as described by the established model, suggesting thin lithosphere in that region. In contrast, the architecture of the Fitzroy Trough reveals continuous rifting between Ordovician and Carboniferous periods followed by negligible post-rift thermal subsidence which cannot be accounted for by the established model. We attribute this difference in basin architecture to rifting of thick

lithosphere. In order to generate accommodation space for the deposition of approximately 15 km of sediments in the Fitzroy Trough and account for observed crustal thicknesses and densities, isostatically it necessary for the lithospheric mantle beneath the Fitzroy Trough to be depleted by 50–70 kg/m³ with respect to MORB source depleted mantle. The actual depletion of the lowermost lithospheric mantle can be constrained by modelling rare earth element (REE) concentrations of alkaline ultrapotassic rocks (including the 19–22 Ma lamproites) which intrude the basin and the Kimberley Craton to the north, following the method outlined by (Tainton and McKenzie, 1994). The result of this geochemical analysis reveals a minimum density depletion in the range of 40–70 kg/m³, agreeing with the results of the isostatic analysis.

Together, these results suggest that thinning of thick lithosphere to less than 120 km is thermally stable and is not accompanied by post-rift thermal subsidence driven by thermal rethickening of the lithospheric mantle because mantle that cooled in the Phanerozoic would have a much less depleted composition (Griffin et al., 2009). Furthermore, the subsidence data from the entire Canning Basin reveals that thick Kimberley Craton lithosphere extended beneath the Fitzroy Trough and along-strike Gregory Sub-Basin in the Ordovician. Wedge shaped basin depocentre geometries (de Vries et al., 2006) indicate that thinning of the lithosphere beneath Canning Basin, which began during the Ordovician, was controlled by dextral strike-slip motion on the Lasseter Shear zone which bounds the eastern side of the Kimberley Craton. Therefore, both the eastern and western margins of the Kimberley Craton were reactivated during the Ordovician, albeit under different tectonic modes. The apparent discrepancy between estimates of lithospheric thickness derived from subsidence data in the western Canning Basin and estimates derived from shear wave tomography suggests that current tomographic models of Western Australia cannot resolve lithospheric thickness variations on half wavelengths of less than 300 km. Interestingly, REE modelling of alkaline ultrapotassic rocks from Western Australia, following (Tainton and McKenzie, 1994), reveals that the lowermost sub-continental lithospheric mantle beneath the Kimberley Craton has

1 Geoscience Australia, GPO Box 378, Canberra, ACT, 2601, Australia
(karol.czarnota@ga.gov.au)

2 Bullard Laboratories, Madingley Rise, Madingley Road, Cambridge, CB30EZ, UK

been metasomatically enriched by 3–9% whereas the Yilgarn Craton has only been enriched by 1–3%. This difference suggests that the hypothesis that giant magma-related ore systems (including gold) are controlled by the degree of refertilisation (i.e. metasomatism) of the sub-continental lithospheric mantle put forward by (Griffin et al., 2013) may not be universally applicable.

References

- Crosby, AG, Fishwick, S and White, N 2010, Structure and evolution of the intracratonic Congo Basin: Geochemistry, Geophysics, Geosystems, v. 11, p. 1–20.
- Czarnota, K, Roberts, GG, White, NJ and Fishwick, S 2014, Spatial and temporal patterns of Australian dynamic topography from River Profile Modeling: Journal of Geophysical Research: Solid Earth, v. 119, no. 2, p. 1384–1424.
- de Vries, S, Fry, N, and Pryer, L 2006, OZ SEEBASE Proterozoic Basins: FrOG TEch, 80p. (unpublished).
- Evans, NJ, McInnes, BA, McDonald, B, Danisik, M, Jourdan, F, Myers, C, Thern, E and Corbett, D 2012, Emplacement age and thermal footprint of the diamondiferous Ellendale E9 lamproite pipe, Western Australia: Mineralium Deposita, v. 48, no. 3, p. 413–421.
- Griffin, WL, Begg, GC and O'Reilly, SY 2013, Continental-root control on the genesis of magmatic ore deposits: Nature Geoscience, v. 6, no. 11, p. 905–910.
- Griffin, WL, O'Reilly, SY, Afonso, JC and Begg, GC 2009, The composition and evolution of the lithospheric mantle: A re-evaluation and its tectonic implications: Journal of Petrology, v. 50, no. 7, p. 1185–1204.
- Kennard, JM, Jackson, MJ, Romine, KK, Shaw, RD and Southgate, PN 1994, Depositional sequences and associated petroleum systems of the Canning Basin, WA, in The Sedimentary Basins of Western Australia edited by PG Purcell and RR Purcell: Petroleum Exploration Society of Australia, Western Australian Branch, Perth, Western Australia, p. 657–676.
- Kennett, BLN, Fichtner, S, Fishwick, S and Yoshizawa, K 2013, Australian Seismological Reference Model (AuSREM): mantle component: Geophysical Journal International, v. 192, no. 2, p. 871–887.
- McKenzie, D 1978, Some remarks on the development of sedimentary basins: Earth and Planetary Science Letters, v. 40, no. 1, p. 25–32.
- Tainton, KM and McKenzie, D 1994, The generation of kimberlites, lamproites, and their source rocks: Journal of Petrology, v. 35, no. 3, p. 787–817.
- White, N 1993, Recovery of strain-rate variation from inversion of subsidence data: Nature, v. 366, p. 449–452.

Regolith landforms of the west Kimberley: distribution and composition

by

N de Souza Kovacs

The 1:100 000 scale west Kimberley interpretive regolith-landform map, covering an onshore area of 88 000 km² (Geological Survey of Western Australia, 2014) is a product of the Kimberley Science and Conservation Strategy (KSCS), a Western Australian State government initiative to provide a better understanding of the Kimberley region. The map shows the distribution of different regolith types in a landform context, and their relationship to bedrock.

The west Kimberley area is composed of Paleoproterozoic granitic and metamorphic rocks of the King Leopold Orogen and Paleoproterozoic to Mesoproterozoic igneous and sedimentary rocks forming the Kimberley Plateau (Tyler et al., 2012; Fig. 1). Interpretive regolith-landform mapping, using GSWA's regolith classification scheme and approach to regolith mapping (Geological Survey of Western Australia, 2013), was largely carried out using remotely-sensed data. Existing geological maps were used in conjunction with geophysical (radiometrics, aeromagnetism) and satellite (Landsat™, ASTER) imagery to identify bedrock and regolith composition, whereas digital elevation models, orthophotos, and Google Earth imagery were used to delineate landform types. Ground observations from the WAROX database and site observations made during three regolith sampling programs were used to refine interpretations.

Distribution and composition

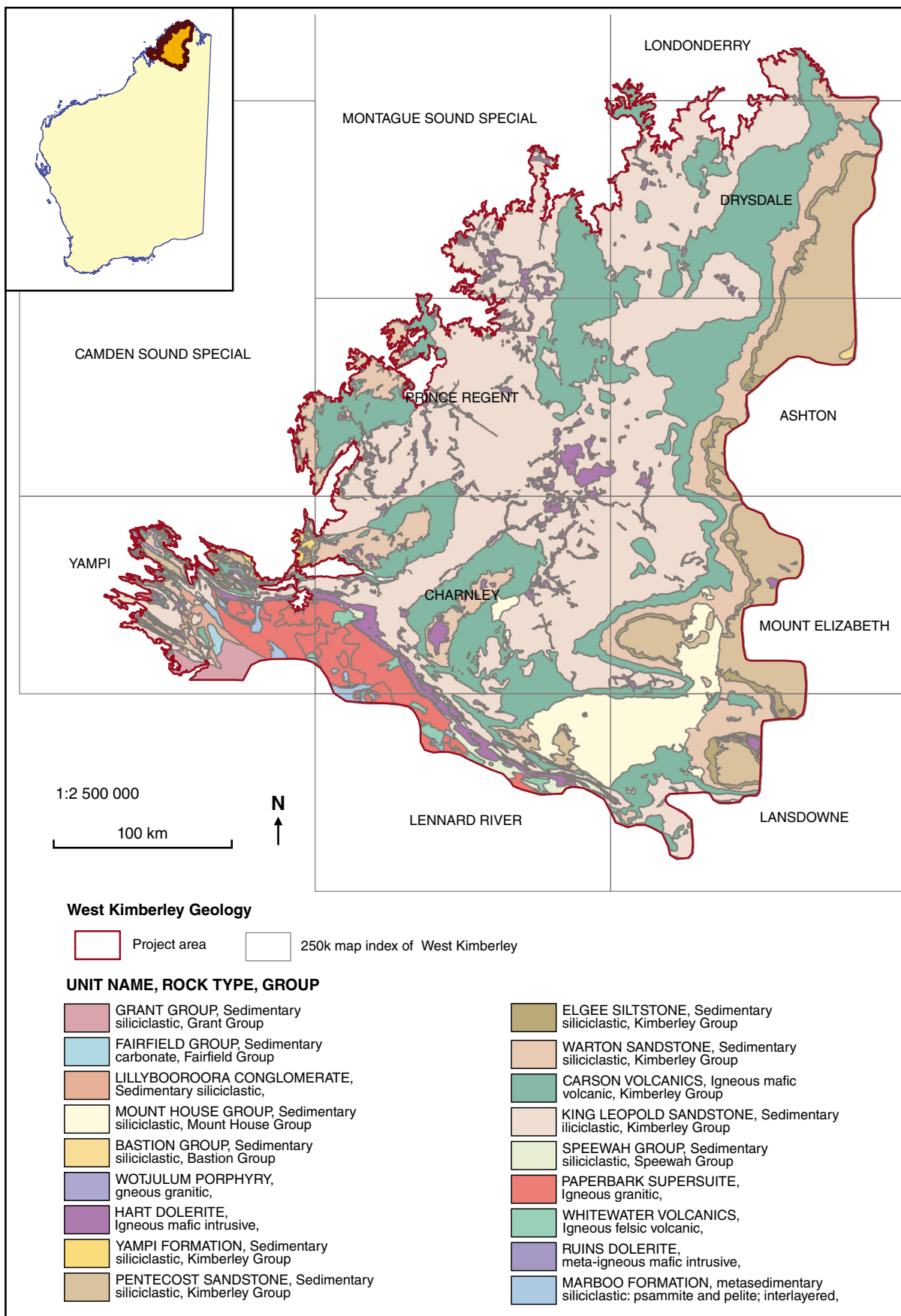
The distribution of different regolith-landform units reflects a combination of bedrock composition and structure, topography, and chemical and physical weathering. Generally the regolith is compositionally similar to the underlying bedrock, indicating largely in situ development of regolith and short transportation distances. Siliciclastic sedimentary, mafic and felsic igneous rocks are the most abundant lithologies in the mapped area (Fig. 1). The landscape is erosional and dominated by 68% exposed bedrock, with 32% regolith cover (Fig. 2, Table 1). Of the total area, 5% is residual/relict regolith, and 27% is depositional regolith, mostly colluvium and alluvium.

Excluding exposed regime material, the most abundant regolith type (12% by area) is that derived from siliciclastic sedimentary rocks, with 10% derived from mafic rocks (basalt and dolerite). About 3% of regolith is derived from felsic or quartzofeldspathic granitic rocks.

Siliciclastic sedimentary rocks such as the King Leopold, Pentecost and Warton sandstones are quartz-rich, whereas units such as the Elgee siltstone are composed of feldspathic and quartz-rich sandstone and micaceous siltstone. Quartz-rich sandstones are the least weathered rocks in the area, with thin and more homogeneous regolith profiles compared to the thicker and more compositionally diverse profiles developed on mafic rocks. The latter include ferruginous and less common aluminous duricrust on mesas and hilltops, whereas quartz-rich sedimentary rocks form more weakly dissected plateaus. Downslope, regolith derived from mafic igneous rocks consists of pisolite-rich colluvium occupying very low angle slopes and pediplains, and black soils on alluvial plains. Felsic or quartzofeldspathic granitic rocks weather to proximal colluvium, composed of white to pale-pink quartzofeldspathic coarse-grained sand. Few residual units are preserved.

Residual versus relict regolith

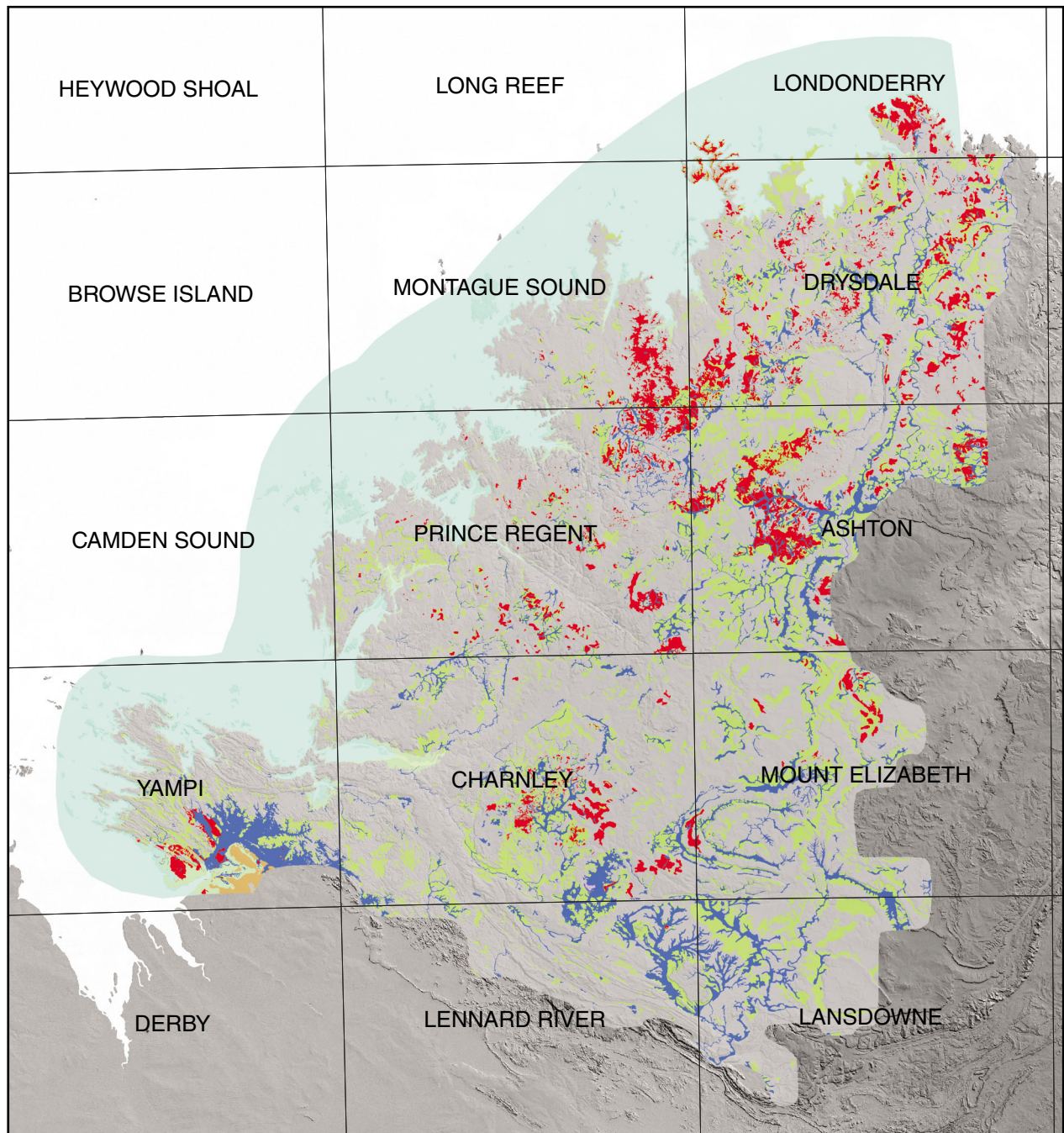
Residual-relict regolith has been divided into seven residual (i.e. in situ) units and one transported (i.e., relict) unit. Five of the residual units are found on mafic rocks and two on sedimentary siliciclastic rocks (Table 1). On mafic rocks (Carson Volcanics and Hart Dolerite) in situ regolith profiles have an upper part composed of pisolitic ferruginous and/or aluminous duricrust up to 3 m thick. Two residual units are developed on sandstone units, ferruginous duricrust and sand. Ferruginous duricrust, characterized by ferruginised sandstone in an Fe-rich matrix, is found on rounded hills. Residual sand is thin and unconsolidated, made up of quartz-rich sand, ferruginised granules and sandstone clasts.



NDSK1

11.12.14

Figure 1. Simplified geological map of the west Kimberley. Sedimentary siliciclastic and mafic rocks dominate the Kimberley Plateau, whereas granitic, sedimentary and mafic igneous rocks are found to the south, forming the King Leopold Orogen.



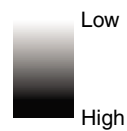
NDSK4

11.12.14

Primary Landform Code

- | | |
|--|--|
|  Alluvial/fluvial |  Coastal tide-dominated |
|  Coastal wave-dominated |  Sheetwash |
|  Colluvial |  Exposed Rock |
|  Marine | |
|  Residual/Relict | |
|  Sandplain | |

Digital Elevation Model NE hillshade Value



100 km

Figure 2. Simplified version of the west Kimberley regolith-landform map showing the primary regolith-landform units and major linear structures overlaid on digital elevation model.

Table 1. Summary of regolith-landform units of the west Kimberley area.

<i>Regolith units</i>	<i>Regolith code</i>	<i>Area (km²)</i>	<i>% of total area</i>
Residual-relict regime regolith			
Saprolite; in situ weathered basalt	Riwvb	56	0.1
Ferruginous duricrust derived from dolerite	Rrfpl	67	0.1
Ferruginous duricrust derived from siliciclastic sedimentary rocks	Rrfs	366	0.4
Ferruginous duricrust derived from basalt	Rrfvb	249	0.3
Aluminous duricrust derived from dolerite	Rrxapl	7	<0.1
Aluminous duricrust derived from basalt	Rrxavb	1 848	2
Residual sands	Rs	1 636	2
Ferricrete; ferruginous indurated gravels	Rtf	0.3	<0.1
Total		4 230	5
Exposed regime regolith (Bedrock)			
Quartzofeldspathic-rich felsic rocks; granophyre	Xgpf	29	<0.1
Quartzofeldspathic-rich felsic plutonic rocks; granite	Xgpg	2 349	3
Quartzofeldspathic-rich sedimentary rocks; sandstone and siltstone	Xgs	4 133	5
Quartzofeldspathic-rich felsic volcanic rocks; dacite	Xgvd	239	0.3
Carbonate-rich sedimentary rock; dolomite and limestone	Xkcd	880	1
Ferromagnesian mafic subvolcanic rock; dolerite	Xmpl	2 799	3
Ferromagnesian mafic rock; basalt	Xm vb	11 670	13
Quartz vein	Xq	7	<0.1
Quartz-rich sedimentary rock; sandstone	Xqss	38 987	43
Micaceous sedimentary and metasedimentary rock; siltstone and pelite	Xxis	1 610	2
Total		62 703	68
Depositional regime regolith			
<i>Colluvial</i>			
Ferromagnesian colluvium derived from weathered mafic rock	Cfw	354	0.4
Quartzofeldspathic colluvium derived from granite	Cgpg	647	1
Quartzofeldspathic colluvium derived from sedimentary rocks	Cgs	1 016	1
Quartzofeldspathic colluvium derived from felsic volcanic rocks	Cgvf	1	<0.1
Carbonate-rich colluvium derived from dolomite and limestone	Ckc	307	0.3
Ferromagnesian colluvium derived from dolerite	Cmpl	954	1
Ferromagnesian colluvium derived from basalt	Cm vb	4 216	5
Quartz-rich colluvium derived from sandstone	Cqs	6 875	8
Micaceous colluvium derived from sedimentary and metasedimentary rocks	Cxis	889	1
<i>Subtotal</i>		<i>15 259</i>	<i>17</i>
<i>Sheetwash</i>			
Sheetwash	W	30	<0.1
<i>Alluvial</i>			
Alluvium; undivided	A	5 393	6
Black soils; gilgai	Aacb	1 015	1
Floodplain	Af	31	<0.1
Meander plain	Am	19	<0.1
<i>Subtotal</i>		<i>6 458</i>	<i>7</i>

Table 1. continued

<i>Regolith units</i>	<i>Regolith code</i>	<i>Area (km²)</i>	<i>% of total area</i>
<i>Sandplain</i>			
Sandplain	S	200	0.2
<i>Coastal wave-dominated</i>			
Beach	Bb	45	<0.1
Foredune	Bd	3	<0.1
<i>Subtotal</i>		48	<0.1
<i>Coastal tide-dominated</i>			
Tidal bar, in channel	Tb	38	<0.1
Estuary	Te	329	0.4
Tidal flat	Tf	317	0.3
Mangrove flat	Tm	1 320	1%
Supratidal flat	Tu	322	0.4
<i>Subtotal</i>		2 326	3
<i>Marine</i>			
Marine reef	Mr	0.03	0.4
Total		24 320	27
TOTAL		91 253	100

Relict regolith is widespread in the west Kimberley, but occurrences are often too small to be shown at the map scale. This transported regolith is characterised by ferruginous indurated gravels often along drainage depressions. A more extensive unit is found adjacent to the Carson Volcanics over the King Leopold Sandstone, in the northwest of the mapped area. It may represent weathered Carson Volcanics which was subsequently transported and deposited on the sandstone.

Conclusion

The west Kimberley interpretive regolith-landform shows the distribution of different regolith types, and forms the basis for interpreting regolith geochemical data as well as providing a better understanding of the evolution of the Kimberley landscape.

References

- Geological Survey of Western Australia 2013, Revised classification system for regolith in Western Australia, and the recommended approach to regolith mapping: Geological Survey of Western Australia, Record 2013/7, 26p.
- Geological Survey of Western Australia 2014, Kimberley 2014 update: Geological Survey of Western Australia, Geological Information Series.
- Tyler, IM, Hocking, RM and Haines, PW 2012, Geological evolution of the Kimberley region of Western Australia: Episodes, v. 35, p. 298–306.

Bedrock–regolith relationships: examples from the Balangarra area, north Kimberley

by

PA Morris

As part of the State government’s Kimberley Science and Conservation Strategy, regolith samples have been collected from 407 sites at a nominal density of one sample per 25 km² in the Balangarra area of the north Kimberley. The <10 mm fraction of each sample has been analysed for 75 components, comprising major element oxides, trace and rare earth elements, ignition loss, pH, and total dissolved solids (Scheib et al., 2015). In conjunction with an interpretive regolith–landform map (GSWA, 2014), these data have been interpreted in terms of the relationship of regolith to bedrock, and the relative contribution of physical and chemical weathering in determining regolith composition. As regolith is thin and locally derived, regolith chemistry should be a good proxy for bedrock composition. This is illustrated by two examples using regolith chemistry from the Carson Volcanics.

Carson Volcanics

The Carson Volcanics covers an area of approximately 2900 km² in the Balangarra project area, from which 116 regolith samples have been collected. The unit is dominated by weakly porphyritic largely subaerial mafic volcanic rocks, although pillow lava, peperite, units of stromatolites and interbeds of quartz-rich siliciclastic rocks indicate localized submarine eruption.

The interpretive regolith–landform map shows a dominance of thin and patchy regolith over outcrop of the Carson Volcanics (66 % by area). A further 6 % comprises regolith developed by in situ weathering, represented by ferruginous and aluminous duricrust. Thus, over 70 % of regolith has developed in situ, so regolith chemistry should be a good proxy for bedrock if the effects of physical and chemical weathering can be understood.

Changes in flow chemistry with stratigraphic height

Box and whisker plots of regolith geochemical data for regolith from the Carson Volcanics show a wide range in chemistry for most elements. For some elements,

there is a change in element concentration throughout the unit. For example, chromium (Cr), which has a median concentration of 91 ppm (range 9 – 376 ppm; n = 116), is found in statistically anomalous concentrations (i.e. >210 ppm) in several regolith samples which plot on or near to the base of the lower contact of the Carson Volcanics with the King Leopold Sandstone. As very few of these samples are from areas of residual or relict regolith, elevated Cr does not reflect chemical weathering. When Cr is plotted against distance from the lower contact (after correcting the sample location for the strike and dip (5°) of the unit), there is a clear trend of decreasing Cr with increasing stratigraphic height (Fig. 1). Similar plots for MgO (wt%), As (ppm), and total dissolved solids (mg/kg) also show the same relationship, and three of the four samples with detectable Pt concentrations (ppb) are found within 900 m of the lower contact. These data indicate that less fractionated, chalcophile and PGE-rich lavas are found at the base of the Carson Volcanics, whereas elevated total dissolved solids could relate to more hydrothermal alteration lower in the succession.

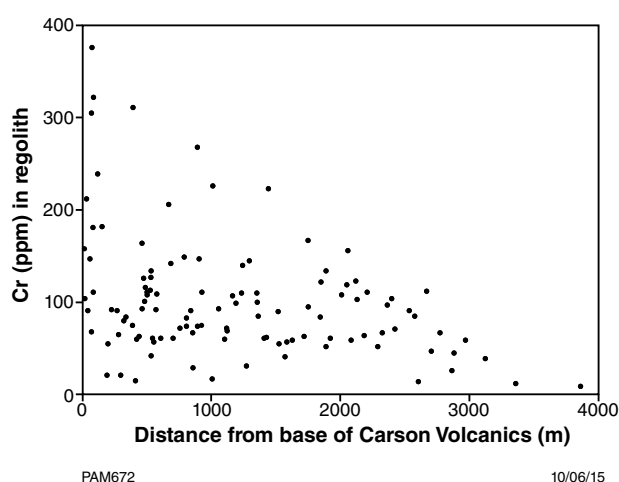


Figure 1. Variation in Cr (ppm) with stratigraphic height (metres) above the lower contact for regolith samples from the Carson Volcanics. The stratigraphic height has been estimated by correcting the sample location for the strike of the unit (estimated at 023) and a regional dip of 5° to the ESE.

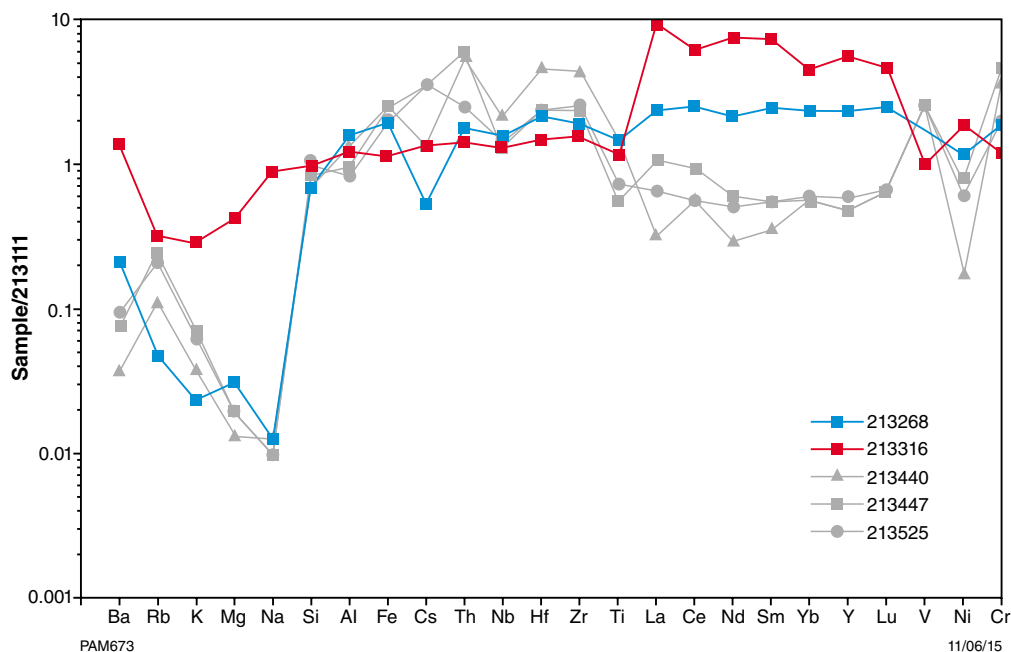


Figure 2. Multi-element plot of regolith samples from the Carson Volcanics normalised to fresh Carson Volcanics 213111. Samples 213440, 213447, and 213525 are typical examples of in situ weathered regolith, whereas 213316 and 213268 are unusually REE-enriched regolith from areas of outcrop. 213316 also has anomalous concentrations of Ni (94 ppm) and Zn (155 ppm).

Anomalous REE chemistry of Carson Volcanics regolith

Weathering of mafic volcanic rocks from the Carson Volcanics results in depletion of labile elements such as Ba, Rb, K, Mg, Na, Ni (typically found in ferromagnesian silicates and feldspars), and enrichment in Al, Fe, and Th, V and Cr, and the high field strength elements Nb, Hf, Zr and Ti (Fig. 2). The rare earth elements (REE: La – Lu) are also depleted. However, two regolith samples (213316 and 213268) have elevated REE concentrations relative to fresh Carson Volcanics, and the most REE-enriched sample (213316) shows only weak signs of weathering in terms of the Ba – Na interval. This sample also has anomalous concentrations of Ni and Zn. As these two samples are from areas of bedrock, and REE are enriched rather than depleted relative to fresh Carson Volcanics, their chemistry is more likely a reflection of the bedrock rather than the effects of weathering. One possibility is that these regolith samples represent unusually REE-enriched yet unfractionated magma. Examination of regional geophysics and structures show that both samples plot on or close to northeast-trending dikes, which could be lower volume partial melts of the Carson Volcanics, or intrusions related to the c. 500 Ma Kalkarindji LIP.

Conclusions

As the majority of regolith sampled from the Carson Volcanics is both thin, and on or near to areas of outcrop,

the effects of transport on the composition of regolith can be largely discounted. The regolith chemistry instead reflects that of the bedrock modified by physical and chemical weathering. Statistical analysis of regolith chemical data has identified samples with anomalous Cr concentrations, a high proportion of which are close to the base of the Carson Volcanics. Elevated concentrations of other elements show the preponderance of unfractionated and mineralized flow units near to the base of this unit, consistent with stratigraphic controls on mineralization in this unit (Marston, 1979). By evaluating the effects of chemical weathering, two samples with anomalous REE concentrations have been identified, both of which are found close to regional dikes. These dikes may represent small volume partial melts within the Carson Volcanics, or intrusive rocks related to a c. 500 Ma large igneous province.

References

- GSWA, 2014, Kimberley Geological Information Series 2014 update: Geological Survey of Western Australia, digital data.
- Marston, RJ 1979, Copper mineralization in Western Australia: Geological Survey of Western Australia, Mineral Resources Bulletin 13, 210p.
- Scheib AJ, Morris PA and de Souza Kovacs N 2015. The regolith sampling in the Kimberley: an overview: Geological Survey of Western Australia, Record 2015/6.

Overview of the REE mineralization in the East Kimberley – West Tanami region

by

S Morin-Ka and T Beardsmore

Rare earth elements (REE) are in high demand for use in advanced technologies, and supply of both light and heavy REE to the global market is dominated and tightly controlled by China. The supply of heavy REE is particularly critical, since these are currently produced from just one location in China, and manufacturers are seeking reliable alternative REE sources. The East Kimberley – West Tanami region of northern Western Australia is emerging as a potentially significant REE province, containing deposits of both light and heavy REE in a variety of mineralization styles (Fig. 1; Table 1). Cummins Range (Navigator Resources) is a predominantly light REE deposit in the central part of a c. 905 Ma carbonatite-pyroxenite plug emplaced into Paleoproterozoic metasediments of the Olympio Formation and granite gneiss of the Lamboo Complex. Monazite (LaPO_4) and bastnäsite ($\text{La}(\text{CO}_3)\text{F}$) are the dominant REE minerals, and weathering has been important for upgrading the mineralisation. At Hastings-Brockman (Hastings Rare Metals), REE-Nb-Ta-F mineralization is contained in gel-zircon and niobates stratabound within the relatively thin Niobium Tuff, the lowermost unit of a cogenetic suite of alkaline to

metaluminous trachytes comprising the c. 1870 Ma (or 1848 Ma) Butchers Gully Volcanic member of the Olympio Formation (locally named the Brockman Volcanics). The c. 1620 Ma John Galt (Northern Minerals) deposit comprises heavy REE-dominated xenotime (YPO_4) in siliceous hydrothermal breccias that cut a prominent quartz arenite unit of the Paleoproterozoic Red Rock Formation, close to the convergence of the NNE-trending Halls Creek Fault and the NE-trending Osmand Fault. REE mineralisation at Browns Range (Northern Minerals) occurs as xenotime and lesser florencite ($\text{CeAl}_3(\text{PO}_4)_2(\text{OH})_6$) in several c. 1650 Ma hydrothermal quartz vein and breccia deposits cutting tightly folded Paleoproterozoic meta-arkoses (Browns Range Metamorphics), that are unconformably overlain by the Paleoproterozoic Gardiner Sandstone (Birringudu Group). REE mineralisation at the Tanami West (Killi Killi) prospects (Orion Metals) comprises c. 1630 Ma hydrothermal or authigenic xenotime and subordinate florencite, largely dispersed in basal Birringudu Group conglomerates lying unconformably on tightly folded metasediments of the Paleoproterozoic Killi Killi Formation, but also locally extending into the basement rocks.

Table 1.

<i>Deposit</i>	<i>Mineralization style</i>	<i>Principal REE minerals</i>	<i>Production status</i>	<i>Age</i>	<i>References</i>
Cummins Range	Carbonatite-hosted	monazite, bastnäsite	Administration	905±2Ma Rb-Sr age of phlogopite-apatite separates	(Sun et al., 1986)
Hastings-Brockman	Alkaline volcanic-hosted	Gel-zircon, niobates	Pre-feasibility	1870±4Ma or 1848+3 Ma U-Pb SHRIMP age of magmatic zircon	(Taylor et al., 1995) (Blake et al., 1999)
Browns Range	Hydrothermal vein	xenotime	Pre-feasibility	1648±5Ma U-Pb SHRIMP age of xenotime	GSWA unpublished
John Galt	Hydrothermal vein	xenotime	Prospect	1619±9Ma U-Pb SHRIMP age of xenotime	GSWA unpublished
West Tanami (Killi Killi)	"Authigenic"	xenotime	Prospect	1632+3 Ma U-Pb SHRIMP age of 'authigenic' xenotime	(Vallini et al., 2007)

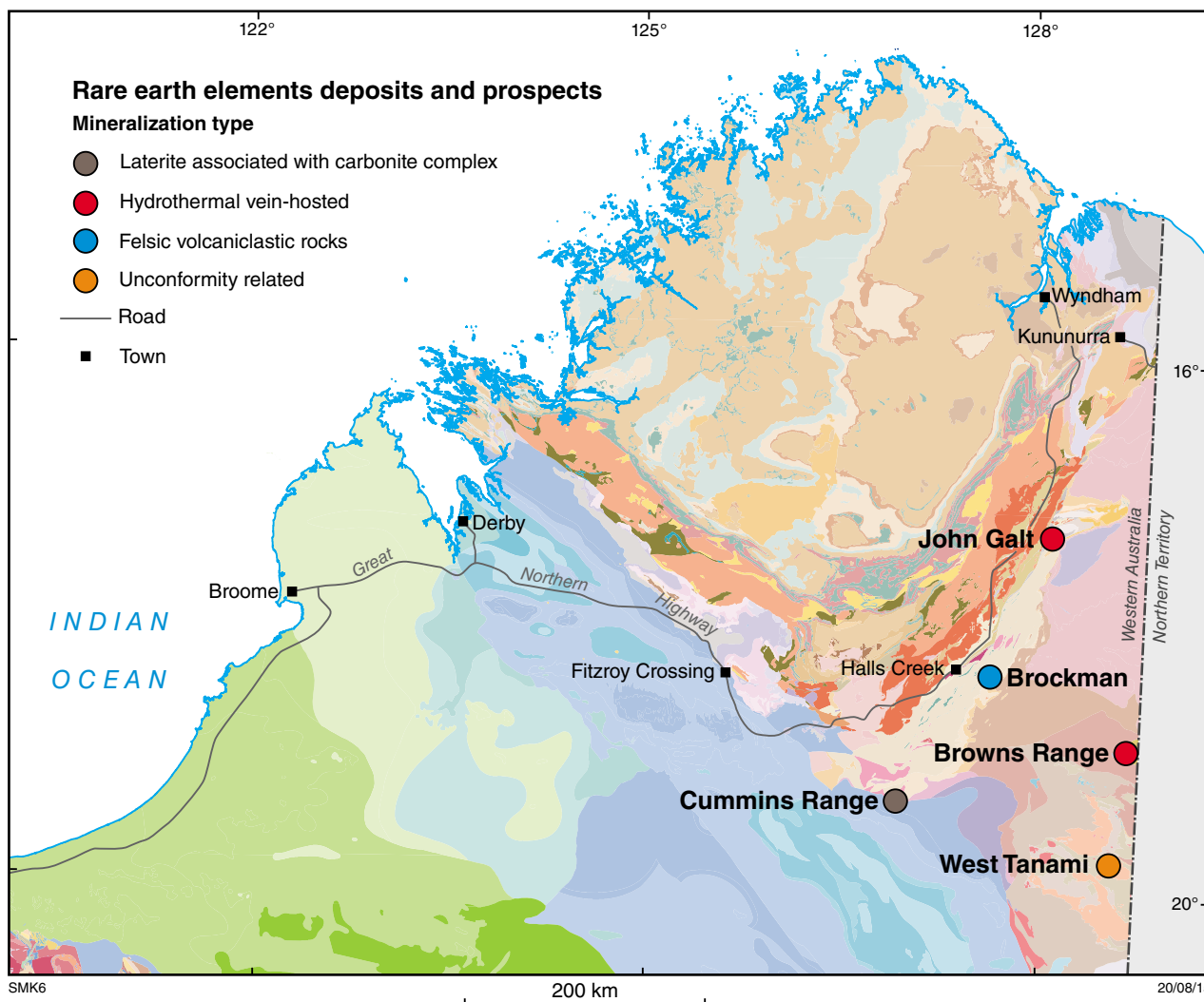


Figure 1. Geological map of the Kimberley region showing the location of rare earth elements prospects and deposits by mineralization type

The carbonatite-hosted Cummins Range and alkaline volcanic-hosted Hastings-Brockman REE deposits are the only known examples of their type in Northern Australia. They have widely disparate ages, subtle footprints, and poorly understood metallogenic controls, making it difficult to assess prospectivity or predict other locations for these deposits types. The metallogeny of the xenotime-dominant mineralisation is similarly poorly understood, but these deposits collectively appear to be similar to one another in geological setting, mineralogy and age, suggesting the occurrence of a widespread, long-lived hydrothermal event at c. 1620-1650 Ma (broadly contemporaneous with unconformity-related uranium mineralisation in the Pine Creek Orogen in the Northern Territory; Vallini et al., 2007). This enhances the potential for discovering other heavy REE mineralization in northern Australia.

References

- Blake, DH, Tyler, IM, Griffin, TJ, Sheppard, S, Thorne, AM and Warren, RG 1999, Geology of the Halls Creek 1:100 000 Sheet area (4461), Western Australia: Australian Geological Survey Organisation, Explanatory Notes, 36p.
- Sun, SS, Jaques, AL and McCulloch, MT 1986, Isotopic evolution of the Kimberley Block, Western Australia, in Abstracts 16: Geological Society of Australia; Fourth International Kimberlite Conference, Perth, WA, 11 August 1986, p. 346-348.
- Taylor, WR, Page, RW, Esslemont, G, Rock, NMS and Chalmers, DI 1995, Geology of the volcanic-hosted Brockman rare-metals deposit, Halls Creek Mobile Zone, northwest Australia. I. Volcanic environment, geochronology, and petrography of the Brockman volcanics: *Mineralogy and Petrology*, v. 52, p. 209-230.
- Vallini, AA, Groves, DI, McNaughton, NJ and Fletcher, IR 2007, Uraniferous diagenetic xenotime in northern Australia and its relationship to unconformity-associated uranium mineralisation: *Mineralium Deposita*, v. 42, p. 51-64.

The regolith sampling program in the Kimberley: an overview

by

AJ Scheib, PA Morris, and N de Souza Kovacs

Introduction

In June 2010, the Western Australian State government initiated the Kimberley Science and Conservation Strategy (KSCS), a five-year, multi-agency program aimed at providing a better understanding of the Kimberley region. A part of this program focused on evaluating the landscape evolution, and to improving knowledge on vegetation distribution, and how this affects the distribution of feral weeds and animals, and helps with fire management. A key factor in understanding vegetation distribution is the extent of different soil (regolith) types, and accordingly, the Geological Survey of Western Australia (GSWA),

a division of the Department of Mines and Petroleum (DMP), formulated a regolith sampling program. This regolith sampling program involved the collection and multi-element analysis of regolith from sites at a nominal density of one sample per twenty five square kilometres. With a size of about 88 000 km², this equates to 3500 samples across the KSCS. At the conclusion of the program in June 2014, samples from 1019 sites had been collected, equating to nearly 30% of the project area (Fig. 1). Complementing the sampling program, a 1:100 000 scale interpretive regolith-landform map has been compiled (De Souza Kovacs, this volume; Geological Survey of Western Australia, 2014).

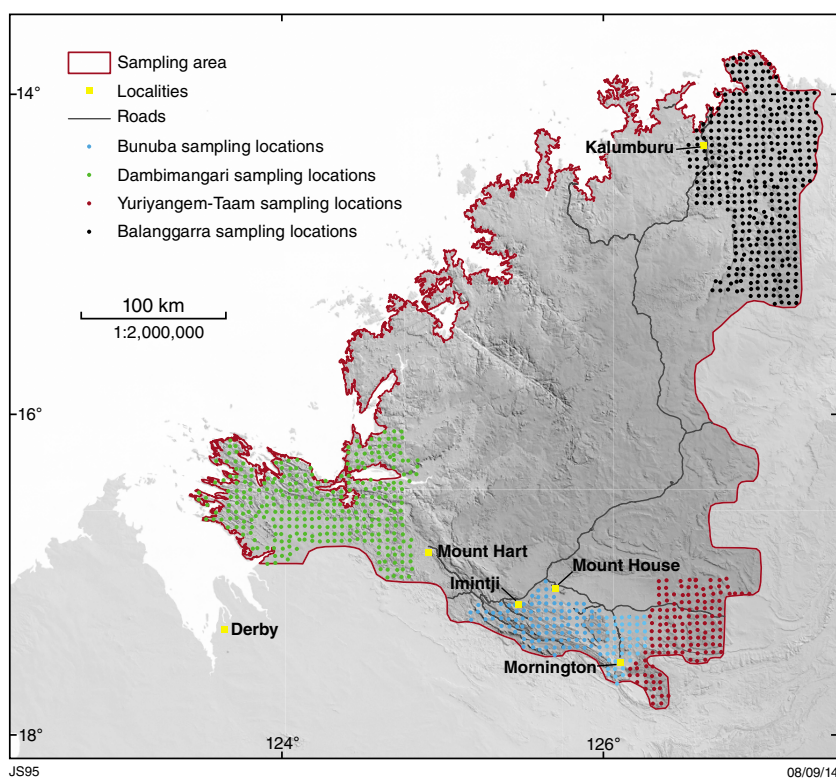


Figure 1. Distribution of sampling sites for the Balangarra (n=, Bunuba and Yuriyangem-Taam (n=, and Dambimangari (n= areas within the Kimberley Science and Conservation strategy area.

Sampling areas and methodology

Regolith sampling involved three separate sampling programs composed of 407 samples from the Balangarra area, 289 from Bunuba and Yuriyangem-Taam, and 323 from Dambimangari (Fig. 1). For all three programs, the sampling was carried out following consultation with traditional owners.

Due to the rugged and remote terrain, sampling of the three areas was carried out by helicopter (Fig. 2a). Each sampling team was composed of a geologist and field assistant, and followed a flight plan along a set of pre-defined sampling sites. At each location, the field assistant collected approximately 5–6 kg of material from a depth of up to 30 cm, whilst the geologist recorded the site location using a GPS, and made observations about surface and downhole regolith and bedrock geology on a sampling form. For most sites the regolith was very thin (<10 cm)

and the material generally coarse grained and poorly sorted, dry and unconsolidated (Fig. 2a–e).

Sample preparation and analysis

Due to the coarse grained nature of the regolith, a part of each sample was dry screened to <10 mm, and then crushed to <2 mm. Two hundred grams of the <2 mm was used for the determination of total dissolved solids (TDS) and pH. The remainder of the <2 mm material was pulverized in a low-Cr steel ring mill to a nominal 85% passing 75 μm . Approximately 150 g of this pulp was given a randomly-ordered GSWA number and submitted for multi-element analysis together with a series of control samples. For each batch of about 150 samples, control samples comprised 10% site duplicates, 10% sample duplicates as well as blanks and a series of in-house and certified reference materials.

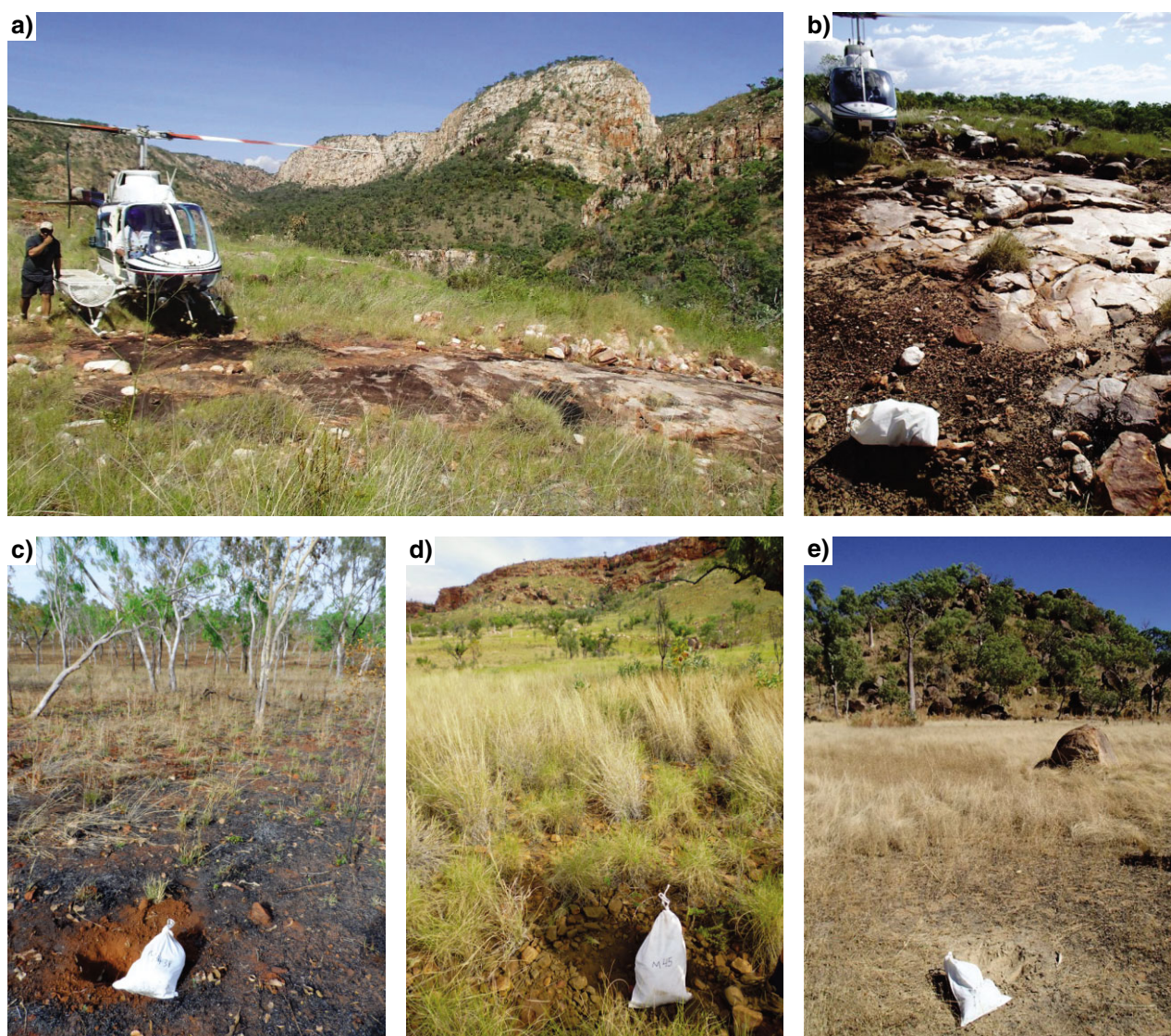


Figure 2. Photographs of: a) panoramic view of sampling site M1162 (GSWA 217990) with King Leopold Sandstone (KLS) exposure in the fore – and background (Dambimangari area); b) sample M1164 (GSWA 218272) of thin residual regolith at exposed KLS (Dambimangari area); c) sample M3438 (GSWA 213578) of ferromagnesian colluvium near exposed Carson Volcanics (Balangarra); d) sample M45 (GSWA 217466) of coarse, sandy colluvium with a cliff of KLS in the background (Bunuba and Yuriyangem-Taam area); e) sampling site M585 (GSWA 218133) of sheetwash near exposed granitic rocks (Dambimangari area).

Major element determinations were carried out on the <75 µm pulp using X-ray fluorescence spectrometry (XRF) of a fused glass disc. Trace element concentrations were determined by inductively coupled plasma (ICP) optical emission spectroscopy (OES) and (ICP-) mass spectrometry (MS) following fusion and acid digestion, or a four-acid digest. Gold and platinum group elements were determined by fire assay ICP-MS.

Outputs

Each regolith sample was analysed for 70 components, comprising 13 analytes as oxides, 54 analytes as trace elements, loss-on-ignition, pH and total dissolved solids (TDS). These data are freely available via the DMP's online data portal <www.dmp.wa.gov.au/geochem>.

References

- De Souza Kovacs, N 2105, The regolith-landform map of the KSCS, in GSWA Kimberley Workshop 2014: extended abstracts: Geological Survey of Western Australia, Record 2015/6.
- Geological Survey of Western Australia 2014, Kimberley Geological Information Series 2014 update: Geological Survey of Western Australia, Digital data.

This Record is published in digital format (PDF) and is available as a free download from the DMP website at www.dmp.wa.gov.au/GSWApublications.

Further details of geological products produced by the Geological Survey of Western Australia can be obtained by contacting:

Information Centre
Department of Mines and Petroleum
100 Plain Street
EAST PERTH WESTERN AUSTRALIA 6004
Phone: +61 8 9222 3459 Fax: +61 8 9222 3444
www.dmp.wa.gov.au/GSWApublications

